FLUVIAL-LACUSTRINE SEQUENCE STRATIGRAPHY, PROVENANCE, ICHNOLOGY, AND SANDSTONE RESERVOIR MODELING OF THE TERTIARY UINTA AND DUCHESNE RIVER FORMATION, NORTHERN UINTA BASIN, UTAH

by

Takashi Sato

A thesis submitted to the faculty of
The University of Utah
in partial fulfillment of the requirements for the degree of

Master of Science

in

Geology

Department of Geology and Geophysics

The University of Utah

May 2015

The University of Utah Graduate School

STATEMENT OF THESIS APPROVAL

The following faculty members served as the supervisory committee chair and members for the thesis of **Takashi Sato**.

Dates at right indicate the members' approval of the thesis.

Marjorie A. Chan, Chair	**Dec 12, 2014** Date Approved
Allan A. Ekdale, Member	**Dec 15, 2014** Date Approved
Lisa Stright, Member	**Dec 16, 2014** Date Approved

The thesis has also been approved by **John Bartley** Chair of the Department/School/College of **Geology and Geophysics**

and by David B. Kieda, Dean of The Graduate School.

ABSTRACT

The Tertiary Uinta and Duchesne River Formations exhibit spectacular outcrop exposures in the Uinta Basin, northeastern Utah. This paper documents four different geological topics/subjects resulting from field and laboratory studies: 1) fluvial-lacustrine sequence stratigraphy, 2) source-to-sink fluvial system, 3) ichnology and paleoenvironment implications, and 4) sandstone reservoir models and characterization.

Chapter 1 highlights a sequence stratigraphic framework and basin-scale facies architecture of the Duchesne River Formation. An upward-fining sequence of the lower three members was heavily influenced by uplift in the Uinta Mountains. Its internal fluvial-lacustrine deposits show marked contrasts between the western and eastern part of the basin due to irregular allogenic controls of tectonic subsidence and water discharge (climate and source terrain input controls).

Chapter 2 highlights a source-to-sink fluvial system of the basal member of the Duchesne River Formation, which preserves a high net-sand-to-gross-thickness ratio (NTG) system in the western sink (basin) and a low NTG system in the eastern sink. Petrographic data and drainage patterns indicate a high discharge from multiple source terrains with a long sediment transport along the E-W basin axis in the western part of the basin. These factors were important for development of large-volume and high-quality (porous) fluvial sandstone reservoirs in the sink.

Chapter 3 focuses on distinct trace fossil assemblages within the fluvial-lacustrine sequence of the uppermost Uinta and the overlying Duchesne River Formations. The study demonstrates the important relationships of depositional facies and trace fossils: 1) lacustrine deposits with the dominant horizontal grazing trace fossil assemblage, 2) fluvial deposits with the dominant insect trace fossil assemblage, and 3) transitional (wetland) deposits with

intermediate trace fossil assemblage.

Chapter 4 emphasizes the outcrop-based geological/reservoir modeling of fluvial and lacustrine deposits of the Uinta and Duchesne River Formations. The study provides statistical inputs of fluvial channel geometry for reservoir modeling applications, and demonstrates which stochastic modeling techniques best represent observed depositional patterns derived from outcrop data.

The Uinta and Duchesne River Formations exhibit the important aspects of coarse-grained deposits in the late-stage lacustrine basin fill.

TABLE OF CONTENTS

LIST OF TABLES

LIST OF FIGURES

ACKNOWLEDGEMENTS

This research project has been achieved through the support of many individuals. In particular, my heartfelt appreciation goes to my supervisory committee, Marjorie Chan, Allan Ekdale, and Lisa Stright, whose comments and suggestions were highly insightful and constructive. I express my gratitude to the geology faculty of the University of Utah, including Erich Petersen, Cari Johnson, and Lauren Birgenheier for their useful comments on this project. Stephen Hasiotis at the University of Kansas provided input on the continental trace fossils. Wil Mace and Quintin Sahratian provided technical help with thin section and QEMScan preparation. Douglas Sprinkel at the Utah Geological Survey was a great supporter and provided valuable insight on the Uinta Basin geology. I acknowledge the Ute Indian Tribe, the Bureau of Land Management in Vernal Ouray National Wildlife Refuge, Bill Barrett Corporation, and Owl and the Hawk who provided field permissions.

CHAPTER 1

FLUVIAL-LACUSTRINE FACIES ARCHITECTURE AND SEQUENCE STRATIGRAPHY OF THE TERTIARY DUCHESNE RIVER FORMATION, UINTA BASIN, UTAH

1.1 Abstract

Continental sequence stratigraphy in dynamic upstream environments can be complex due to the interplay of source tectonics, climate change (global and local), and topography. The Tertiary Duchesne River Formation represents the last stage of Lake Uinta intermontane basin fill, surrounded by sediment source mountain ranges of the Uinta Mountains to the north and Sevier Fold Thrust Belt (FTB) to the west. Excellent basin-scale exposures allow vertical and lateral characterization of facies architectures to interpret controlling mechanisms in the upstream environments.

The four members of the Duchesne River Formation are distinctive lithological units. The lower three members comprise a typical upward-fining fluvial sequence (unconformity-bounded) from the basal coarse-grained unit into overlying fine-grained units. The fourth (uppermost) coarse-grained member records the onset of another upward-fining cycle. The sequence stratigraphy at these member scales was primarily tectonic-driven, due to uplift of the Uinta Mountains, which was similar to, but smaller than the main Laramide events that produced the nearby series of Paleogene lacustrine basins.

Internally, the Duchesne River Formation records a distinct change in fluvial – lacustrine styles between the western and eastern part of the basin, demonstrating the variable allogenic controls of tectonics (subsidence) and discharge (local climate and source terrain input) within the basin. Specifically, the western high NTG (degradational) fluvial system of the basal member was controlled by high discharge due to a wet climate and two source terrain inputs

(Uinta Mountains and Sevier FTB), whereas the eastern low NTG (aggradational) fluvial system was controlled by low discharge due to a dry climate and single source terrain input (Uinta Mountains). The development of lacustrine environments of the third member in the west was controlled by differential tectonic subsidence in the basin. The Duchesne River Formation of the Uinta Basin preserves a valuable example of an upstream sequence, and demonstrates how internal facies architectures at the basin-scale evolved by allogenic controls.

1.2 Introduction

Concepts of continental sequence stratigraphy are important to aid in exploration of lacustrine basins that may have lacustrine source rocks and fluvial reservoir rocks. However, sequences and facies in dynamic upstream environments are controlled by complicated and interdependent allogenic factors such as tectonics, climate change (global and local), and topography. Early studies in fluvial sequence stratigraphy mainly emphasized sea level controls in marine - coastal systems (Posamentier and Vail 1988; Wright and Marriott 1993; Shanley and McCabe 1994). However, some workers downplayed the influence of sea level changes in upstream environments (e.g., Schumm 1993; Shanley and McCabe 1994; Dalrymple et al. 1998). Still others adopted different terminology for fluvial systems tracts on the basis of change in accommodation (Currie 1997) and stacking patterns (Legaretta and Uliana 1998), which provided a descriptive mechanism to apply the sequence stratigraphic concepts to fluvial deposits even if the driving mechanism is unclear. Fluvial sequence stratigraphy is commonly assessed and discussed by separating upstream controls and downstream controls (e.g., Blum and Tornqvist 2001; Catuneanu 2006; Holbrook et al. 2006). In upstream environments where sea or lake level fluctuations (i.e., downstream control) do not influence the sequence development, tectonics and climate change are interpreted as the main controlling factors on fluvial sequences (e.g., Catuneanu 2006). However, since both tectonics (accommodation control) and climate (discharge control) could be variable laterally within a continental basin, resulting large-scale fluvial-lacustrine facies and stacking patterns might significantly differ even within the coeval units.

The purpose of this paper is to: 1) document major lithological architecture and facies of the Duchesne River Formation in vertical and lateral extents across the Uinta Basin, 2) build the regional sequence stratigraphic framework, and 3) assess how tectonic (accommodation) and climatic and source terrain (discharge) controls are reflected in large-scale (>1,000 m) vertical successions and dramatic, basin-scale (>130 km) lateral facies changes. This is an unusual geological example with sufficient vertical and lateral exposures to demonstrate these scales of change. The sequence stratigraphic approach in this paper is based on the recognition of major sequence boundaries (unconformities). Although many different sequence stratigraphic models and systems tracts for alluvial strata have been proposed (summarized in Gibling et al. 2011), the sequence boundary is the only universal surface among these models. Classifications of systems tracts based on accommodation (e.g., low and high accommodation) or stacking patterns (e.g., degradation and aggradation) do not fit with the stratigraphic framework of the Duchesne River Formation, because differences in accommodation and stacking pattern occur even within one coeval unit. Although some measured sections do show individual parasequences (i.e., cyclicity at the scale of tens of meters), here we focus on the large-scale facies change that provides the basic sequence stratigraphic framework.

1.3 Geological Context and Previous Work

The Uinta Basin contains thick Paleogene continental deposits of the Wasatch, Green River, Uinta, and Duchesne River formations in ascending order (Fig. 1.1). The upper three of the formations comprise a typical upward-shallowing/coarsening lacustrine basin filling (Visher 1965; Picard and High 1972; Lambiase 1990) preserving the following generalized depositional environments: extensive basinal to marginal lacustrine (Green River Formation), lacustrine-deltaic and fluvial mixed/transitional (Uinta Formation), and fluvial (Duchesne River Formation) (Fig. 1.1). A series of lake basins emerged in the present central Rocky Mountain region in Montana, Wyoming, Utah, and Colorado during the Laramide orogeny in the latest Cretaceous to early Paleogene (Dickinson et al. 1988), including Lake Uinta (situated around the present Uinta Basin). The lacustrine organic-rich shale deposited in Lake Uinta (i.e., Green River

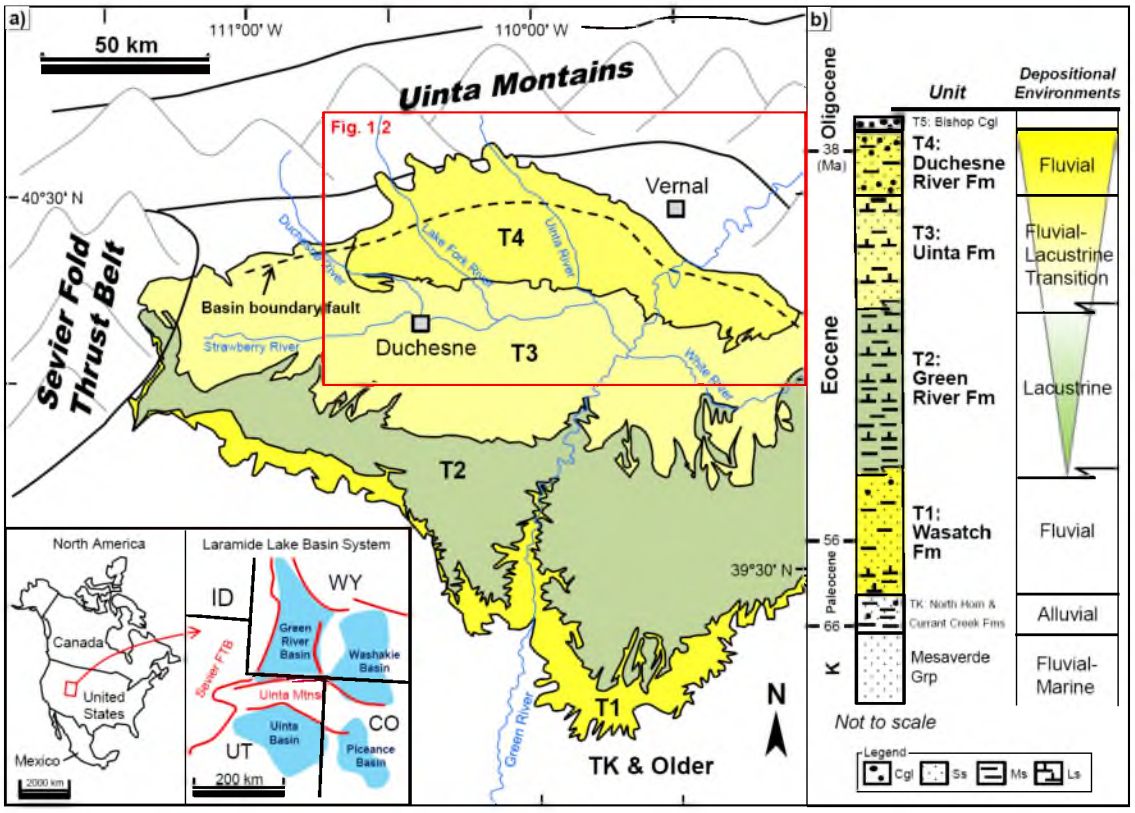

Figure 1.1. Geological map of the Uinta Basin. a) The generalized geological map, modified from Andersen and Picard (1974), Bryant et al. (1989), Bryant (1992), Hintze et al. (2000), and Sprinkel (2006 and 2007). Regional dip is to the north and formations get progressively younger toward the Uinta Mountains. The basin is surrounded by high mountain ranges of the Uinta Mountains to the north and the Sevier Fold Thrust Belt (FTB) to the west. The map of Laramide lake basin system is from Dickinson et al. (1988). b) A schematic geologic column shows the Paleogene sequence of the Uinta Basin (modified from Hintze et al. 2000). T2 to T4 exhibits a typical upward-coarsening/shallowing lacustrine basin-fill succession.

shales) is a renowned, world-class, hydrocarbon source rock. In this intermontane lacustrine basin, most regional stratigraphic studies focused on the Green River Formation (e.g., Keighley et al. 2003). In contrast, the overlying Uinta and Duchesne River Formations have received much less attention despite their good exposures, probably due to their lesser economic significance.

The Duchesne River Formation derived sediment from adjacent active source mountain range(s) of the Uinta Mountains in the north (Andersen and Picard 1974; Bruhn et al. 1986) and possibly the Sevier Fold Thrust Belt (FTB) in the west. The paleoenvironmental setting was very

far (700+ km) from any marine influence (e.g., Blakey 2011) and shows no evidence of large-scale terminal lake development during its history (e.g., Franczyk et al. 1992). The formation is comprised primarily of braided and meandering fluvial deposits, with some minor lacustrine deposits. It is subdivided into four members: Brennan Basin (Db), Dry Gulch Creek (Dd), Lapoint (Dl), and Starr Flat (Ds) members in ascending order (Andersen and Picard 1972) (Fig. 1.2). The lower three members generally comprise an upward-fining succession of sandstone-dominated Db to mudstone-dominated Dl. The uppermost member (Ds) is rich in sandstone and conglomerate. The mudstone-dominated Dl contains abundant tuff or tuffaceous beds, with K-Ar ages of ~40 Ma reported from tuffs at the base of this member (McDowell et al. 1973; Andersen and Picard 1974; Prothero and Swisher 1992; Kelly et al. 2012) (see the detailed nomenclatural history and the geological age of the Duchesne River Formation in Appendix A).

1.4 Methods

Field studies broadly examined the Duchesne River Formation throughout its E-W and N-S exposure in the Uinta Basin. Methodologies included basin-scale examinations from aerial imagery as well as specific field measured sections with tape, Jacob staff, and a laser range finder, as well as gigapan photography. A total of 35 locations of measured geological sections (labeled MS01 to MS35 in Fig. 1.2) covered a total of 2,750 m in stratified length (described at minimum resolution of 10-20 cm). The measured sections strategically covered major member boundaries and represent the regional facies architecture of the Duchesne River Formation. The sections were grouped along north-south trending composite sections lettered A to G (Fig. 1.2) to construct a regional stratigraphic framework. The member thickness and stratigraphic positions of acquired measured sections at each composite section were controlled by the modified geological map (Fig. 1.2) along with structural strikes and dips. A total of 441 paleocurrent measurements were acquired throughout all four members of the formation (all detailed measured sections with paleocurrent data are in Appendix B).

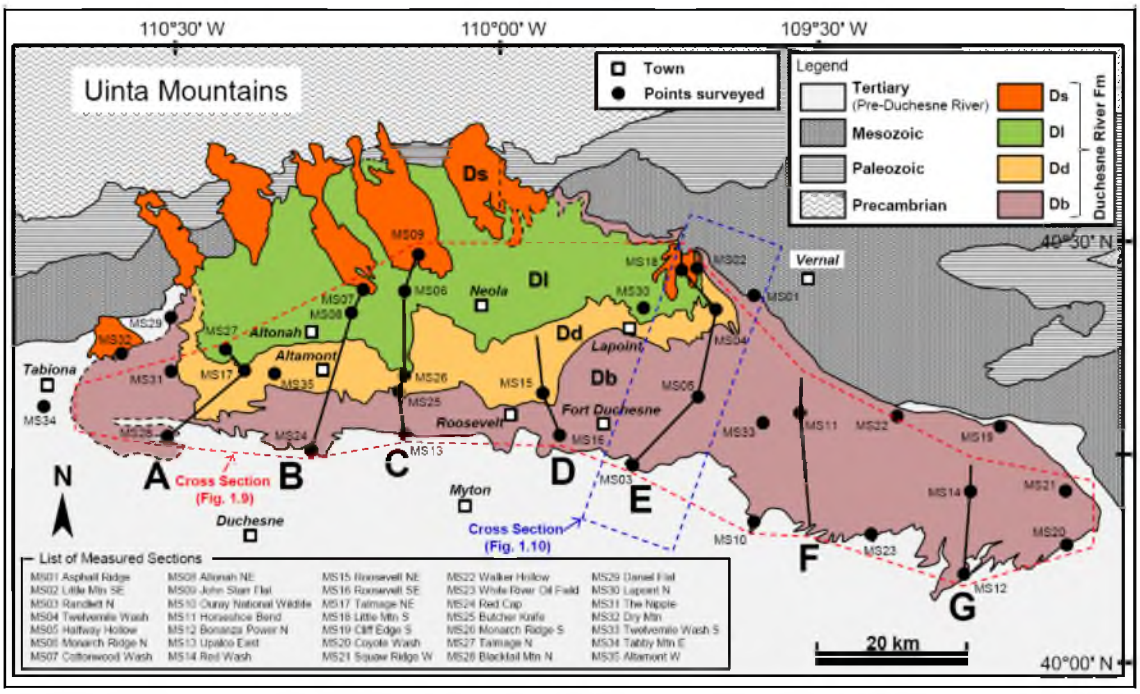

Figure 1.2. Geological map of the Duchesne River Formation and surrounding area. Regional dip is to the north and the Duchesne River members (Db: Brennan Basin Member, Dd: Dry Gulch Creek Member, Dl: Lapoint Member and Ds: Starr Flat Member) get progressively younger toward the Uinta Mountains. The location of 35 measured sections (MS) are marked by black circles and composite sections A to G (black lines) are shown on the map. The map is modified after Andersen and Picard (1974), Rowley et al. (1985), Bryant et al. (1989) and Sprinkel (2006 and 2007).

1.5 Lithofacies and Facies Associations

Twelve lithofacies and six facies associations that characterize the Duchesne River Formation are described and interpreted in this section. A typical facies association is usually a group of associated sedimentary facies at scales of tens of meters representing a specific depositional environment or a related succession (e.g., Allen and Johnson 2010; Aswasereelert et al. 2012; Kukulski et al. 2013). The facies associations in this study are nearly an order of magnitude greater in vertical thickness (e.g., hundreds of meters), and thus these are more akin to “large-scale facies associations”, which are used to express the basin-scale facies architecture.

1.5.1 Lithofacies

Twelve basic lithofacies fall into broad categories of a conglomerate, five sandstone, four mudstone, a limestone, and a tuff lithofacies (detailed in Table 1.1, arranged in order of approximate decreasing grain size). Each lithofacies is distinguished with a combination code of lithology and key features as described below. The first capitalized letter of lithofacies code represents a primary lithology (i.e., C = conglomerate, S = sandstone, M = mudstone, L = limestone, T = tuff/tuffaceous clastics). The second lower-case letter(s) represents key features for the later environmental interpretations such as geometries or body shapes for sandstones and conglomerates (i.e., c = channelized, ta = tabular, th = thin-layered) and colors for mudstones (i.e., r = red, y = yellow, g = green/gray). In addition, numerical characters are added to lithofacies Sc to distinguish different connected sandbody dimension/size (largest Sc1 to smallest Sc3) and Mg to distinguish different internal sedimentary structures (i.e., Mg1: mottled, Mg2: massive or laminated). These subcategories are helpful to distinguish six facies associations described in the following section. Although these twelve lithofacies are individually distinctive (Table 1.1), because of the large-scale emphasis of the fluvial-lacustrine facies architecture, this paper herein focuses on the facies associations.

1.5.2 Facies Association 1 (FA1): Amalgamated Braided Fluvial Channels

1.5.2.1 Description

FA1 is dominated by strongly amalgamated channelized sandstones of Sc1, which exhibits a high net-sandstone-to-gross-thickness ratio (NTG) (0.75 at MS28). FA1 is composed of three lithofacies (Table 1.2, Fig. 1.3): a) Sc1, fine- to coarse-grained, yellowish and reddish gray, poor- to well-sorted, channelized, and trough cross-stratified sandstones with strongly amalgamated bodies (with apparent connected bodies over lateral distances of >1,000 m); b) Mr, clay- to silt-sized, red, massive or mottled mudstone with common vertical and semivertical burrows; and c) Sth, poor- to well-sorted, thin-layered (commonly < 1m), massive or trough cross-stratified (occasionally indistinct) sandstone and siltstone with common intensive bioturbation. Trace fossils are common in FA1 although less abundant than in FA2 and FA5.

Table 1.1. Summary of Duchesne River Lithofacies

Lithofacies Name	Code	Grain Size	Color	Sorting	Shape	Sedimentary Structures	Other Features
Upward-fining package of conglomerate-sandstone	Cc (Cgl)	Granule to boulder (max >1 m)	Varicolored	Very poor	Channelized (max 10 m thick) or lenticular	Structureless or imbricate structures	Clast-supported, well-rounded to sub-angular clasts
	Cc (Ss)	Very fine to very coarse, occasionally silty	Yellowish white, yellowish gray	Poor to moderate	Channelized or lenticular	Commonly trough cross-stratified	Occasionally calcareous
Amalgamated channelized sandstones	Sc1	Fine to coarse, occasionally very fine, partly angular granules	Yellowish gray, reddish gray	Poor to well	Channelized, strongly amalgamated (>1,000 m lateral apparent connected bodies)	Trough cross-stratified, rip-up clasts	Noncalcareous to slightly calcareous, common iron concretions
Stacked broad channelized sandstones	Sc2	Fine to coarse, occasionally very fine, partly angular granules	Light gray, yellowish gray	Poor to moderate	Channelized, stacked/ amalgamated (>100 m lateral apparent connected bodies)	Trough cross-stratified, rip-up clasts	Commonly calcareous, uncommon lateral accretion features
Isolated and narrow channelized sandstones	Sc3	Fine to coarse, partly angular granules	Light gray, grayish white, yellowish white	Poor to well	Channelized, isolated (<100 m lateral apparent connected bodies)	Trough cross-stratified	Commonly calcareous
Thin-layered sandstone and siltstone	Sth	Silt, fine to medium, occasionally coarse	Red, grayish white, greenish gray, light gray, yellowish gray	Poor to well	Thin-layered (<1 m thick)	Massive or trough cross-stratified (occasionally indistinct), occasional rip-up clasts	Commonly calcareous, common intensive bioturbation
Tabular sandstone	Sta	Very fine to medium, occasionally silty	Light gray, yellowish gray, red	Well	Tabular (>1,000 m lateral apparent connected bodies (maximum))	Massive, rippled, parallel and wavy laminated, planar and trough cross-stratified	Calcareous or noncalcareous, common bioturbation, common carbonaceous materials
Red mudstone/silty mudstone	Mr	Clay to silt	Red	N/A	N/A	Massive or mottled	Occasional slickensides, common vertical and semi-vertical burrows (filled with white, calcareous siltstones)
Yellow mudstone	My	Clay to silt	Yellow, brown	N/A	N/A	Mottled, common relict bedding	
Green/gray mudstone	Mg1	Clay to silt	Dominantly green and gray, partly yellow, purple and red	N/A	N/A	Mottled	Occasional thin carbonaceous mudstones/materials, occasional intensive horizontal to oblique gypsum veins
Green, gray, and dark gray mudstone	Mg2	Clay to silt	Dominantly green, gray and dark gray	N/A	N/A	Massive or laminated	Occasional thin siltstone and carbonaceous mudstone layers
Limestone	Lth	Clay (calcilutite)	Tan, brownish gray and gray	N/A	Thin-layered (<40 cm thick)	Massive	Commonly fossiliferous (gastropods and bivalves)
Tuff and tuffaceous bed	T	Clay to silt, partly sandy	White, light gray	N/A	Tabular, channelized, lenticular	Massive	Occasionally rich in biotite

Table 1.2. Summary of Duchesne River Facies Associations

FA #	Facies Association	Member Occurrence	Facies Components		Trace Fossils				Ss/Ms Ratio	Apparent Sandbody Dimensions
			Lithofacies Code	Interpretation	Rare	Sparse	Common	Abundant		
FA 1	Amalgamated Braided Fluvial Channels	Db (western part of basin), Ds	Sc1	Amalgamated braided fluvial channels					75/25 (MS28)	> 1,000 m (MS28)
			Sth	Overbank deposit, typically pedogenically-altered						
			Mr	Well-drained flood plain paleosol						
FA 2	Extensive Flood Plain and Stacked Broad Fluvial Channels	Db, Dd and Dl (central-eastern part of basin)	Sc2	Braided and sinuous fluvial channels					50/50 (MS33)	> 100 m (MS33)
			Sc3	Isolated small stream channel						
			Sth	Overbank deposit, typically pedogenically-altered						
			Mr	Well-drained flood plain paleosol						
			My	Moderately-drained flood plain paleosol						
FA 3	Extensive Flood Plain and Isolated Small Steams	Db (eastern part of basin)	Sc3	Isolated small stream channel					15/85 (MS14)	< 100 m (MS14)
			Sth	Overbank deposit, typically pedogenically-altered						
			Mr	Well-drained flood plain paleosol						
			My	Moderately-drained flood plain paleosol						
FA 4	Alluvial Fan Complex	All members (northern margin of basin)	Cc	Alluvial fan channel/lobe					70/30 (cgl+ss/ms) (MS01)	n/a
			Mr	Well-drained flood plain (interchannel) paleosol						
			Mg1	Playa or wetland deposit in the distal fan						
FA 5	Dry and Wet Flood Plains and Fluvial Channels	Dd (western part of basin)	Sc2	Braided and sinuous fluvial channels					27/73 (MS15)	> 100 m (Sc2), > 1,000m (Sta)
			Sta	Marginal lacustrine deltaic deposit						
			Sth	Overbank deposit, typically pedogenically-altered						
			Mr	Well-drained flood plain paleosol						
			My	Moderately-drained flood plain paleosol						
			Mg1	Poorly-drained wetland or shallow lacustrine deposit						
FA 6	Extensive Lacustrine Deposits	Dl (western part of basin)	Sc3	Isolated small stream channel					5/95 (MS06)	n/a
			Sta	Marginal lacustrine deltaic deposit						
			Mr	Well-drained paleosol						
			Mg2	Lacustrine deposit						
			Lth	Lacustrine deposit						
			T	Ash fall and reworked deposit						

Abbreviations: FA = Facies Association, MS = Measured Section

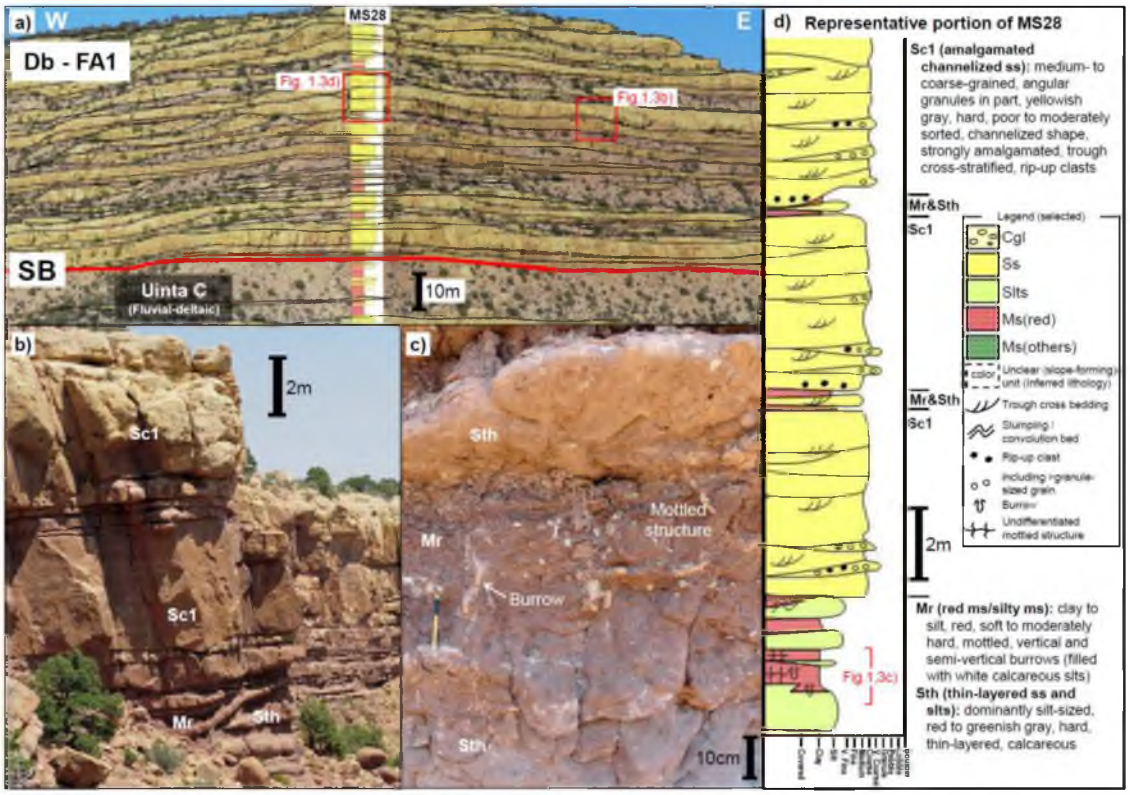

Figure 1.3. Facies association FA1 at MS28. a) Outcrop interpretation shows amalgamated channelized sandstone bodies (Sc1) highlighted in yellow. b) Lithofacies Sc1 and underlying Mr and Sth. c) Mottled and burrowed structures of lithofacies Mr and adjacent Sth (massive). d) Representative portion of MS28 shows the detailed descriptions of lithofacies Sc1, Mr, and Sth. Lithofacies descriptions (generalized) and codes are in Table 1.1.

1.5.2.2 Interpretation

FA1 represents a fluvial style of widespread multiple interweaving fluvial channels (i.e., braided channels of Sc1), punctuated by dry flood plain environments (Sth and Mr). Lithofacies Sc1 (amalgamated channelized sandstones) indicates traction transport mainly in the upper part of the lower flow regime. Lithofacies Mr (red mudstone/silty mudstone) indicates suspension deposition followed by pedogenic alterations with well-drained conditions (e.g., Kraus 2002; Atchley et al. 2004; Kraus and Hasiotis 2006). Lithofacies Sth (thin-layered sandstone and siltstone) indicates traction transport usually followed by pedogenic alterations. The lower abundance of trace fossils than FA2 and FA5 might reflect frequent destruction of traces due to repetitive cut-and-fill patterns of the amalgamated fluvial channels (Sc1).

1.5.3 Facies Association 2 (FA2): Extensive Flood Plain and Stacked Broad Fluvial Channels

1.5.3.1 Description

FA2 is dominated by stacked channelized sandstones of Sc2 and red-colored mudstones of Mr, which exhibits a moderate NTG (0.5 at MS33). Overall these channelized sandstones (Sc2) are less connected than strongly amalgamated channelized sandstones (Sc1) of FA1. FA2 is composed of five lithofacies (Table 1.2, Fig. 1.4): a) Sc2, fine- to coarse-grained, light and yellowish gray, channelized, and trough cross-stratified sandstones with stacked/amalgamated bodies (with apparent connected bodies over lateral distances of >100 m) and uncommon lateral accretion features; b) Sc3, fine- to coarse-grained, light gray and grayish/yellowish white, channelized, and trough cross-stratified sandstones with isolated narrow bodies (with apparent connected bodies under lateral distances of <100 m); c) Sth; d) Mr; and e) My, clay- to silt-sized, yellow to brown, mottled mudstone with common relict bedding. FA2 has abundant trace fossils such as root structures (rhizoliths) in mudstones and a variety of meniscate backfill burrows and nesting structures both in mudstones and sandstones.

1.5.3.2 Interpretation

FA2 represents a depositional environment of extensive dry flood plains (Mr, My, and Sth) with mixed braided, meandering, and isolated small river systems (Sc2 and Sc3). Lithofacies Sc2 (stacked broad channelized sandstones) and Sc3 (isolated and narrow channelized sandstones) both indicate traction transport mainly in the upper part of the lower flow regime. Uncommon lateral bar accretion features of Sc2 indicate some rivers were at least more sinuous than those of FA1. Lithofacies My (yellow mudstone) indicates suspension deposition followed by pedogenic alterations with moderately-drained conditions (e.g., Atchley et al. 2004; Kraus and Hasiotis 2006). The abundance of trace fossils in this facies association indicates prosperous organic communities under moderately prolonged stable conditions and high preservation potential of organic traces due to the aggradational stacking pattern (i.e., episodic burial without destroying traces).

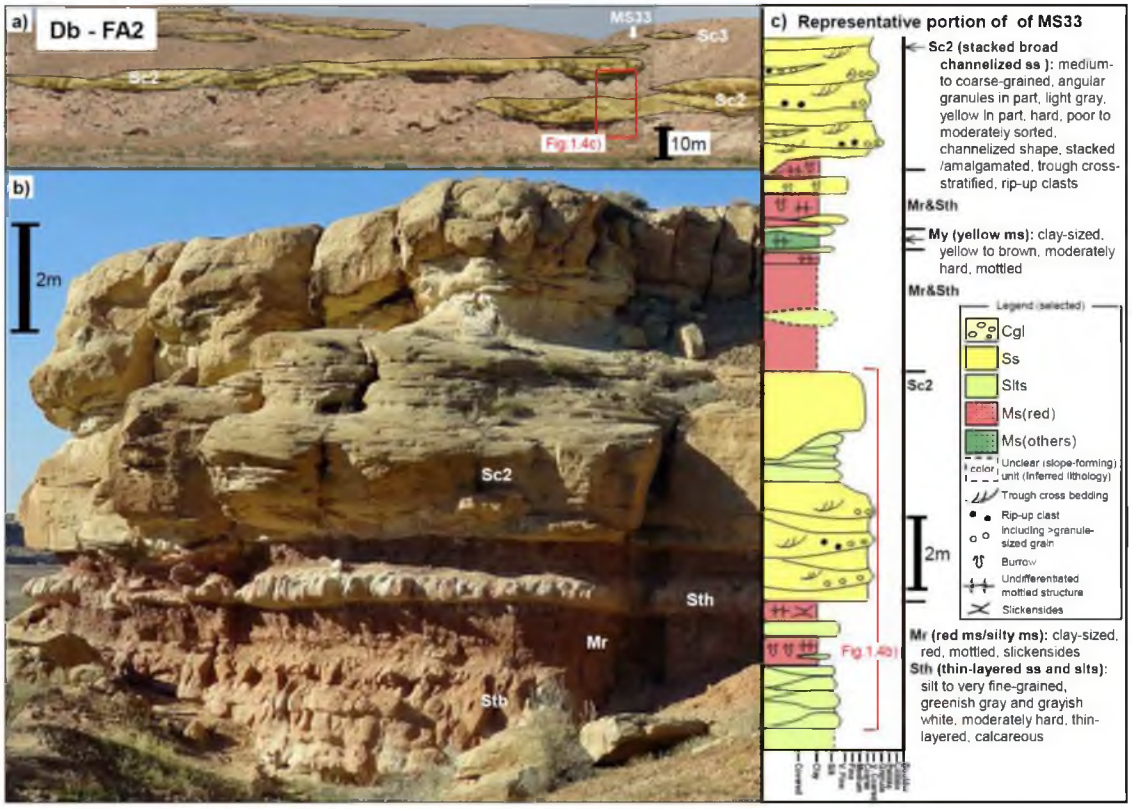

Figure 1.4. Facies association FA2 at MS33. a) Outcrop interpretation shows stacked broad channelized sandstones (Sc2) and isolated and narrow channelized sandstones (Sc3) highlighted in yellow. b) Lithofacies Sc2 and underlying Mr, and Sth. c) Representative portion of MS33 shows the detailed descriptions of lithofacies Sc2, Mr, and Sth. Lithofacies descriptions (generalized) and codes are in Table 1.1.

1.5.4 Facies Association 3 (FA3): Extensive Flood Plain and Isolated Small Streams

1.5.4.1 Description

FA3 is dominated by red-colored mudstones of Mr, which exhibits a low NTG (0.15 at MS14). FA3 is composed of four lithofacies (Table 1.2, Fig. 1.5): a) Sc3; b) Sth; c) Mr; and d) My. The difference between FA2 and FA3 is the absence of board channelized sandstones of Sc2 (i.e., only small and isolated channelized sandstones of Sc3 occur in FA3). This facies association tends to form very muddy, poorly exposed, slope-forming “badlands” outcrops. FA3 has moderate amounts (lesser amounts than FA2 and FA5) of trace fossils.

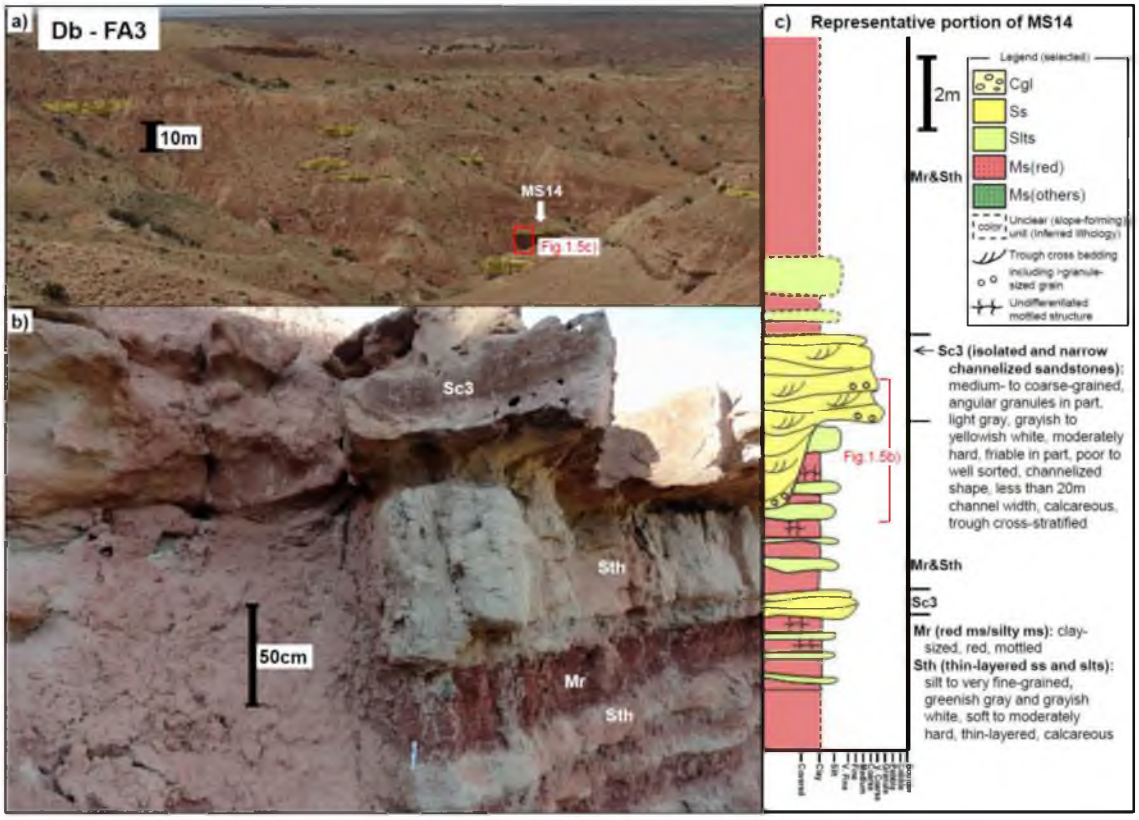

Figure 1.5. Facies association FA3 at MS14. a) Outcrop interpretation shows isolated and narrow channelized sandstones (Sc3) highlighted in yellow. b) Lithofacies Sc3 and underlying Mr and Sth. c) Representative portion of MS14 shows the detailed descriptions of lithofacies Sc3, Mr, and Sth. Lithofacies descriptions (generalized) and codes are in Table 1.1.

1.5.4.2 Interpretation

The absence of Sc2 (stacked broad channelized sandstones) and the dominance of mudstones (Mr) indicates a depositional environment of extensive dry flood plains (Mr, My, and Sth) with only isolated small streams (Sc3). The low abundance of trace fossils in FA3 compared to FA2 an FA5 could be resulted from a sampling (data collection) bias due to poorly exposed conditions of this muddy facies association.

1.5.5 Facies Association 4 (FA4): Alluvial Fan Complex

1.5.5.1 Description

FA4 is dominated by the conglomeratic lithofacies Cc, which exhibits a high percentage of coarse-grained deposits (e.g., the ratio of conglomerate/sandstone and mudstone is 70:30 at MS01). FA4 is composed of three lithofacies (Table 1.2, Fig. 1.6): a) Cc (thick upward-fining package of mixed conglomerate-sandstone), poor-sorted, granule- to boulder-size (max 1 m), structureless or imbricate conglomerates with channelized or lenticular shaped bodies (max 10 m thick), and very fine- to very coarse-grained, trough cross-stratified sandstones with channelized or lenticular shaped bodies; b) Mr; and c) Mg1, clay- to silt-sized, dominantly green and gray to partly yellow, purple and red, mottled mudstone with thin carbonaceous (e.g., fossil plants/woods) mudstone layers, and intensive gypsum veins. Trace fossils are scarce in this facies association, although there are large rhizocretes at one locality (MS01).

1.5.5.1 Interpretation

FA4 is interpreted to represent an alluvial fan (Cc) with relatively narrow interchannel (Mr) and playa/wetland environments (Mg1). Structureless conglomerates in the lower portion of lithofacies Cc indicate debris flows. These vertically transition to imbricated conglomerates and trough-cross stratified sandstones in the upper portion indicating traction transport (Nemec and Steel 1984), with considerable variations in paleocurrent directions (e.g., NW to E paleoflow at MS01 and MS22). The mixed transportation mechanisms and radial paleocurrent indicators suggest very high-energy seasonal to perennial gravel-bed river processes, and episodic and repetitive avulsions and lobe switching (e.g., Crews and Ethridge 1993). Mg1 (green/gray mudstone) indicates suspension deposition followed by pedogenic modifications under poorly-drained (wet) conditions (e.g., Kraus 2002; Atchley et al. 2004; Kraus and Hasiotis 2006).

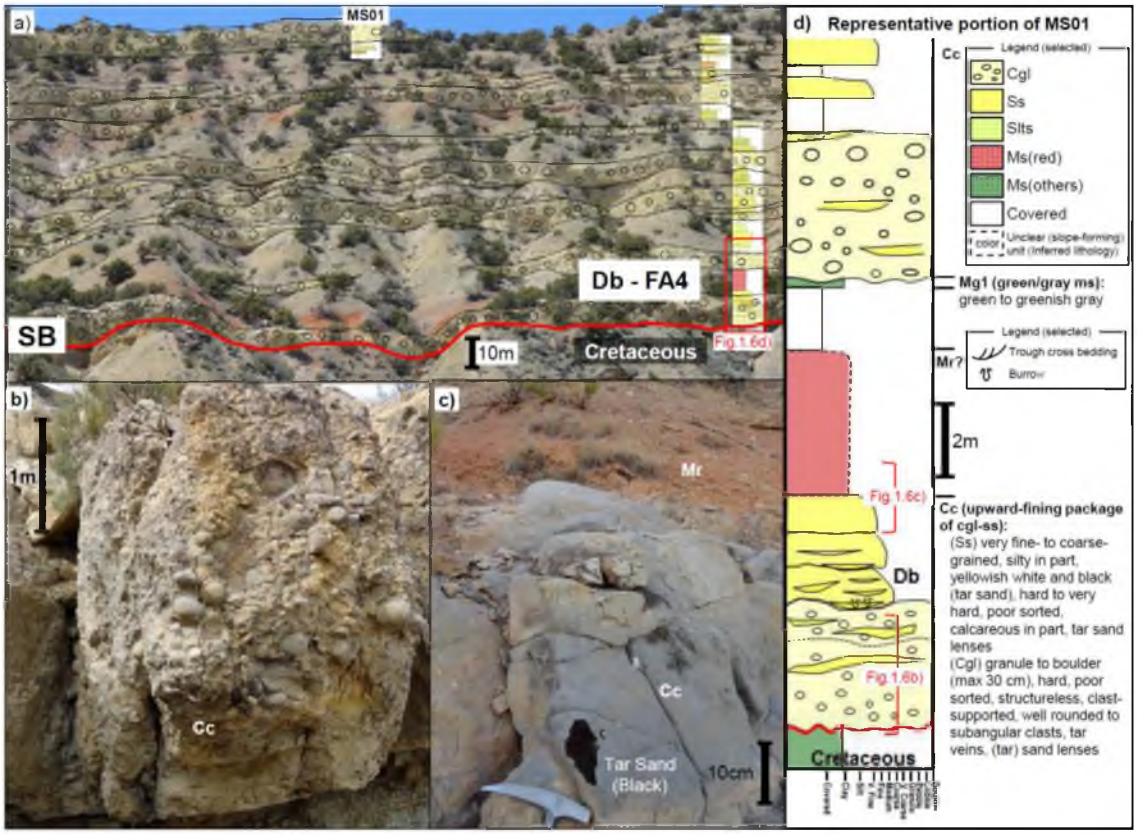

Figure 1.6. Facies association FA4 at MS01. a) Outcrop interpretation shows distinctive conglomerates and sandstones (Cc) highlighted in yellow. b) Granule- to boulder-size conglomerate of lithofacies Cc. c) Sandstone (including tar) of lithofacies Cc and overlying Mr (mostly covered). d) Representative portion of MS01 shows the detailed descriptions of lithofacies Cc. Lithofacies descriptions (generalized) and codes are in Table 1.1.

1.5.6 Facies Association 5 (FA5): Dry and Wet Flood Plains and Fluvial Channels

1.5.6.1 Description

FA5 is dominated by red-colored mudstones of Mr and green/gray-colored mudstones of Mg1 with scattered stacked channelized sandstones of Sc2, which exhibits a moderate NTG (0.27 at MS15). FA5 is composed of six lithofacies (Table 1.2, Fig. 1.7). In this facies association, lithofacies Sc2, Sta, Mr, and My, which are constituents of FA2, coincide with lithofacies Mg1 and minor Sta (tabular sandstone). Lithofacies Sta is characterized by very fine- to medium-grained, well-sorted, tabularly bedded (50 to 200 cm thick), massive, rippled (wave and current) or trough cross-stratified sandstones with common bioturbation and

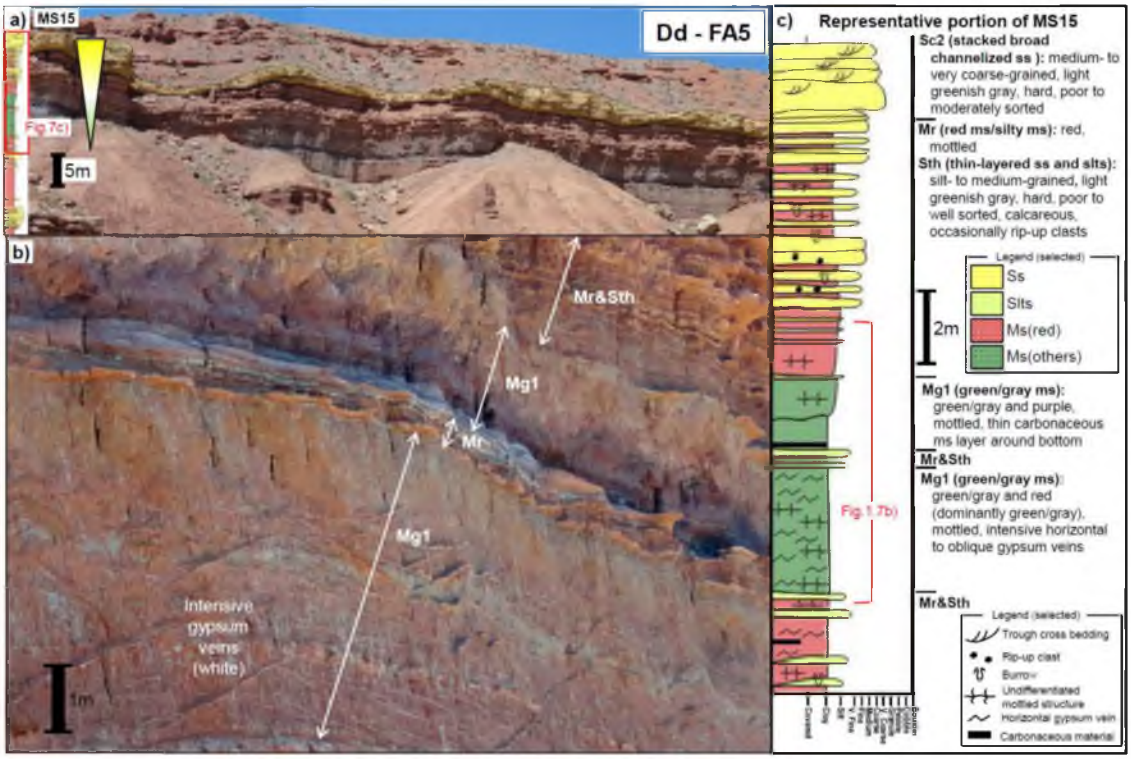

Figure 1.7. Facies association FA5 at MS15. a) Outcrop interpretation shows an upward-coarsening succession of FA5 with stacked broad channelized sandstones (Sc2) highlighted in yellow. b) The lower part of an upward-coarsening succession comprised of lithofacies Mg1 and Mr. c) Representative portion of MS15 shows the detailed descriptions of lithofacies Sc2, Sth, Mr, and Mg1. Lithofacies descriptions (generalized) and codes are in Table 1.1.

carbonaceous/woody materials. Some thick sandstones of Sta are traceable laterally at scales of thousands of meters. Trace fossils including rhizoliths and meniscate backfill burrows are abundant in this facies association.

1.5.6.2 Interpretation

FA5 represents a depositional environment of extensive alluvial plains accompanying wetland and shallow lacustrine conditions. In this facies association, there is a common challenge in interpreting continental depositional environments due to extensive post-depositional pedogenic processes that modify or destroy indications of the original depositional environments (Hasiotis 2000; Retallack 2001). Mg1 generally exhibits mottled structures, indicating pedogenic alterations. Nevertheless, upward-coarsening successions, which are

comprised of basal gypsiferous and partly carbonaceous green/gray mudstones (Mg1), alternating red mudstones (Mr) and thin-layered sandstones (Sth), and capped channelized sandstones (Sc2), can represent shallow lacustrine-fill succession (Fig. 1.7). Lithofacies Sta (tabular sandstone) indicates several sedimentation processes (e.g., oscillatory flow, sandy gravity flow). Minor occurrences of this lithofacies also suggest some short-lived lacustrine conditions.

1.5.7 Facies Association 6 (FA6): Extensive Lacustrine Deposits

1.5.7.1 Description

FA6 is composed of four fine-grained and two coarse-grained lithofacies (Table 1.2, Fig. 1.8), and is dominated by green/gray-colored mudstones of Mg2. FA6 exhibits an extremely low NTG (0.05 at MS06). The four fine-grained lithofacies are: a) Mr, red mudstone; b) Mg2, clay-sized, dominantly green, gray and dark gray, massive or laminated mudstone occasionally including thin siltstones and carbonaceous mudstones; c) Lth, clay-sized (calcilutite), tan, very hard, thin-layered limestone including gastropods and bivalves; and d) T, clay- to silt-sized, occasionally sandy, white to light gray, soft, massive, tabular or lenticular tuff or tuffaceous mudstone/siltstone occasionally rich in biotite. The two sandstone lithofacies are: a) Sc3, isolated small channelized sandstones; and b) Sta, tabular sandstones. Trace fossils are sparse in this facies association, although some U-shaped burrows and horizontal traces occur in lithofacies Sta (tabular sandstone).

1.5.7.2 Interpretation

FA6 represents extensive lacustrine environments indicated by dominant Mg2 (green, gray and dark gray mudstone) and occurrences of Sta (tabular sandstone) and Lth (limestone) (Fig. 1.8). Lithofacies Mg2 indicates suspension deposition (lacking any pedogenesis feature such as mottled and slickenside structures). Lithofacies Lth suggests deposition in shallow and quiet (sediment-starved) water. Lithofacies T indicates ash fall or reworked ash fall deposits. Common occurrences of red mudstones (Mr) indicate oxidizing conditions of exposure, thus the

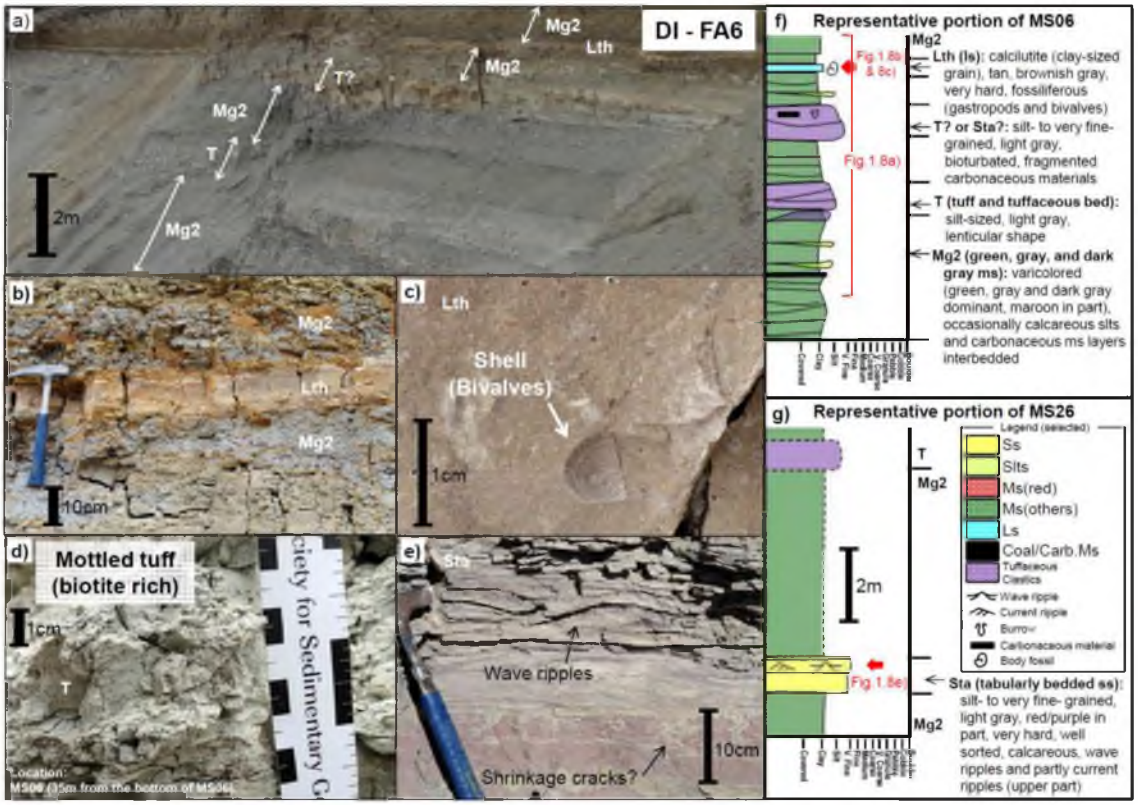

Figure 1.8. Facies association FA6 at MS06 and MS26. a) Outcrop photo shows a typical FA6 succession at MS06. b) Lithofacies Mg2 and Lth. c) Lithofacies Lth including a shell of bivalves at MS06. d) Lithofacies T (biotite-rich tuff) at MS06. e) Lithofacies Sta with wave ripples at MS26. f) Representative portion of MS06 shows the detailed descriptions of lithofacies Mg2, Lth, and T. g) Representative portion of MS26 shows the detailed descriptions of lithofacies Sta. Lithofacies descriptions (generalized) and codes are in Table 1.1.

lacustrine environments were relatively shallow, as well as periodic and not long-lived.

1.6 Regional Facies Architecture and Paleocurrent

1.6.1 Regional Facies Architecture

E-W basin-wide regional correlations of composite sections are presented in Figure 1.9. Distinct sequence boundaries are recognized at the bases of members Db and Ds. This section describes and interprets boundaries, internal facies (facies association) architectures, and thickness changes of the Duchesne River members.

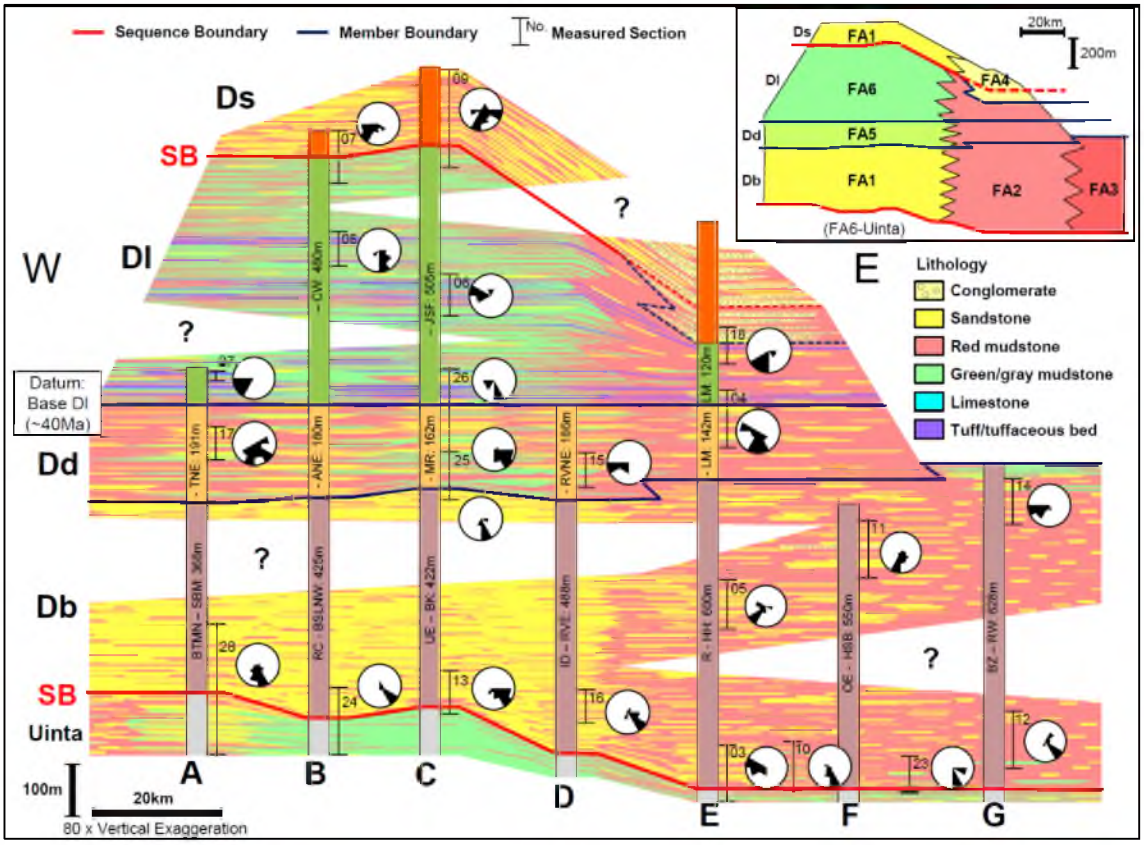

Figure 1.9. E-W regional correlations of composite sections A to G (location of cross section in Fig. 1.2). Paleocurrent data at measured section locations (vertical bars with numbers) are shown as rose diagrams. The stratigraphic datum is set at the base of Dl, which can be regarded as a nearly isochronous boundary (~40Ma). Lithology classifications represent the dominant or representative lithology and are generalized for this scale of correlation. Lithological interpretations between measured sections (detailed sections in the Appendix 2) are schematic. The architecture of facies associations (FA1-FA6) is shown in the upper-right inset panel. Note the significant contrast of facies (facies association) between the western and eastern portion. Composite section abbreviations: BTMN; Blacktail Mountain North, SBM; Steamboat Mountain, TNE; Talmage NE, RC; Red Cap, BSLNW; Big Sand Lake NW, ANE; Altonah NE, CW; Cottonwood Wash, UE; Upalco E, BK; Bucher Knife, MR; Monarch Ridge, JSF; John Starr Flat, ID; Independence, RVE; Roosevelt E, RVNE; Roosevelt NE, R; Randlett, HH; Halfway Hollow, LM; Little Mountain, OE; Ouray E, HSB; Horseshoe Bend, BZ; Bonanza, RW: Red Wash.

1.6.1.1 Brennan Basin Member (Db)

The basal Brennan Basin Member (Db) of the Duchesne River Formation is characterized by channelized sandstones interbedded with red fine-grained rocks (Andersen and Picard 1972). It consists of fluvial facies associations of FA1, FA2, and FA3 in the E-W regional section (Fig. 1.9). This member has a sharp contact with the underlying Uinta Formation, particularly at several locations (e.g., MS13, MS24) in the mid-western part of the basin. In these locations, dominant green mudstones and conspicuous stromatolitic limestones of the Uinta Formation that clearly indicate a lacustrine environment are overlain by amalgamated channelized sandstones (lithofacies Sc1) of the Db fluvial environment (FA1). Thus, the base of Db marks a sequence boundary that represents an abrupt basinward shift of facies. This sequence boundary becomes gradually obscure to the west (MS28) where both Db and the Uinta Formation are dominated by sandstones, and to the east (MS03, MS10, and MS23) where both Db and the Uinta Formation are dominated by mudstones (Fig. 1.9). Mudstone colors are important to help trace the contact (i.e., sequence boundary) of Db (red) with the Uinta Formation (green/gray) at these locations. This sequence boundary forms an angular unconformity in the northern margin of the basin, where Db overlies the older rocks (Anderson and Picard 1972; Campbell and Ritzma 1979). For example, the FA4 (alluvial fan complex) of Db unconformably overlies the Cretaceous Mesaverde Group along Asphalt Ridge (see N-S regional section of Fig. 1.10). Db exhibits a significant contrast of facies; sandy FA1 in the west and muddy FA2 and FA3 in the east. The difference in the total thickness between the west (~400 m) and east (~600 m) indicates a lower aggradation rate (i.e., more bypassing and/or degradation) of FA1 in the west and a higher aggradation rate of FA2 and FA3 in the east, even though the E-W cross section shows some exaggeration due to the intertonguing relationship at the upper member boundary (Fig. 1.9).

1.6.1.2 Dry Gulch Creek Member (Dd)

The second Dry Gulch Creek Member (Dd) of the Duchesne River Formation is characterized by red and green/gray fine-grained rocks with interbedded sandstones (Andersen

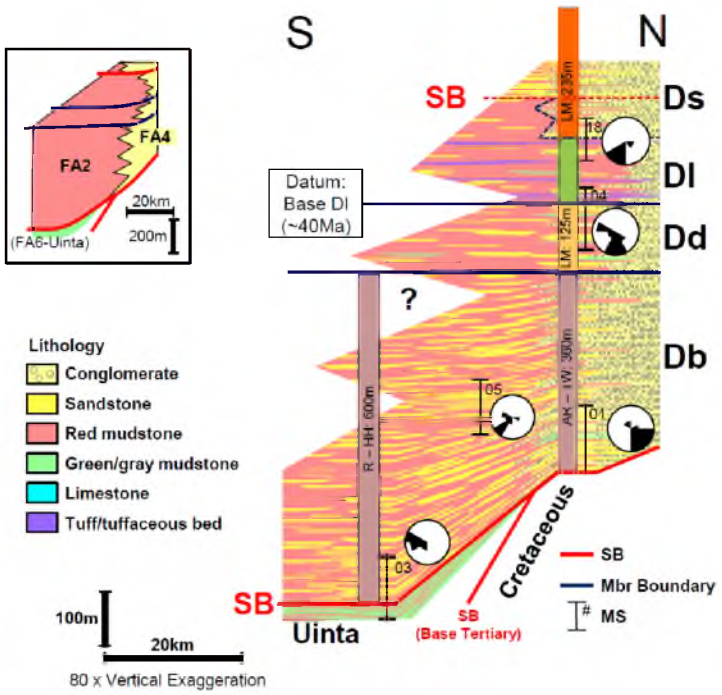

Figure 1.10. N-S geological cross section along MS01 - MS05 - MS03 (location of cross section in Fig. 1.2). Paleocurrent data at measured section locations are shown as rose diagrams. The architecture of facies associations is shown in the upper-left inset panel. FA4 (alluvial fan complex) commonly occurs throughout all the members in the north (i.e., foothills of the Uinta Mountains). Note that Db is juxtaposed with the Cretaceous Mesaverde Group in the north where the Tertiary Uinta and Green River formations are completely eroded out. Composite section abbreviation: AR; Asphalt Ridge, TW; Twelvemiles Wash, LM; Little Mountain, R; Randlett, HH; Halfway Hollow.

and Picard 1972). It is composed of fluvial - lacustrine facies associations of FA5 and FA2 in the E-W regional section (Fig. 1.9). It has a conformable contact with the underlying Db, and the basal beds interfinger upsection to the east of Roosevelt (Bryant et al. 1989). The contacts are nearly isochronous to the west of MS15 near Roosevelt as the basal green/gray mudstones (lithofacies Mg1) are widely traceable. Although Dd exhibits a significant contrast of facies, red and green/gray mudstones with interbedded sandstones of FA5 (wetland) in the west and red mudstones with interbedded sandstones of FA2 (dry alluvial plain) in the east, there is no significant difference in formation thickness between the west and east.

1.6.1.3 Lapoint Member (Dl)

The third Lapoint Member (Dl) of the Duchesne River Formation is characterized by dominant green/gray mudstones and minor red fine-grained and coarse-grained rocks (Andersen and Picard 1972). It is composed of facies associations of FA6 and FA2 in the E-W regional section (Fig. 1.9). The base of this member is defined by the occurrence of extensive bentonitic fine-grained beds (lithofacies T), and thus is regarded as a nearly isochronous boundary (Andersen and Picard 1972). Tuffs were presumably sourced from volcanoes in the Wasatch Range, East Tintic Mountains, and Oquirrh Mountains to the west (Bryant et al. 1989). Dl shows contrasting facies associations that are green/gray mudstone-dominated FA6 (lacustrine) in the west and red mudstone-dominated FA2 (dry alluvial plain) in the east (Fig. 1.9). Correspondingly, there is also a remarkable difference in the total thickness where the west is several hundred meters thicker than the east (Fig. 1.9).

1.6.1.4 Starr Flat Member (Ds)

The uppermost Starr Flat Member (Ds) of the Duchesne River Formation is characterized by dominant conglomerates and sandstones with lesser amounts of fine-grained rocks (Andersen and Picard 1972). It is composed of facies associations FA1 and FA4. It has a sharp contact with the underlying Dl at the type locality (MS09) where sandstone-dominated FA1 of Ds overlies green/gray mudstone-dominated FA6 (lacustrine) of Dl (Fig. 1.9). This basal contact indicates an abrupt basinward shift of facies (i.e., sequence boundary). In some other areas to the west (e.g., MS32) and east (e.g., MS02, MS18), sporadic conglomeratic FA4 (alluvial fan) of Ds are observed. Bryant et al. (1989) noticed that conglomeratic facies of Ds unconformably overlie the underlying Duchesne River members in some areas. However, it is difficult to assign these outcrops to Ds and make basin-scale correlations with confidence because of their patchy distribution caused by modern erosion, limited exposure by vegetation, and lithological similarities to the overlying Bishop Conglomerate.

1.6.2 Paleocurrent and Fluvial Style

Newly acquired paleocurrent measurements show dominant southerly transport that confirms earlier reports by Warner (1965, 1966) and Andersen and Picard (1974). However, examination of paleocurrents of the fluvial channel dominated member Db shows significant features that assist in interpreting the paleodrainage patterns (Fig. 1.11). The western half of the basin tends to have more east or southeast directed flows, whereas the central-eastern part of the basin shows more south to southwest directed flows. Flow directions in the eastern part of the basin are more variable. Correspondingly, there is a remarkable contrast of fluvial styles between the western and eastern portions of the basin (Fig. 1.11): a high NTG amalgamated channel system of FA1 in the western part and a lower NTG isolated channel system of FA2 and FA3 in the eastern part. A possible scenario is that in the western part of the basin, more confined and packed eastward axial drainage systems developed, while the east had less confined and relatively isolated drainage patterns. Notably well-sorted and quartz-rich sandstones in the eastern part of Db-FA1 (e.g., MS24, MS13) suggest their long transport from the west and support this scenario.

1.7 Proposed Scenario of Duchesne River Sequence

The basin-scale stratigraphic architecture (Fig. 1.9) shows distinct vertical and lateral (west to east) facies changes. A tectonic-driven sequence development scenario can explain the evolution of the Duchesne River late basin-fill (Fig. 1.12, Fig. 1.13). Although a tectonic force (uplift) is the ultimate control on the large-scale sedimentary packages, irregular accommodation and discharge controls within the basin (both caused in response to a tectonic uplift event) and resultant lateral facies changes are discernable. This section presents a three-staged evolutionary scenario (Fig. 1.12, Fig. 1.13) for the upward-fining sequence of members Db (stage 1), Dd (stage 2), and Dl (stage 3). A traditional terminology scheme of sequence stratigraphy for these stages (i.e., LST: lowstand systems tract for stage 1, TST/HST: transgressive/highstand systems tract for the combined stages 2 and 3) is adopted in this study. The systems tracts here are based on the relative position of water table depth (Fig. 1.12). Thus,

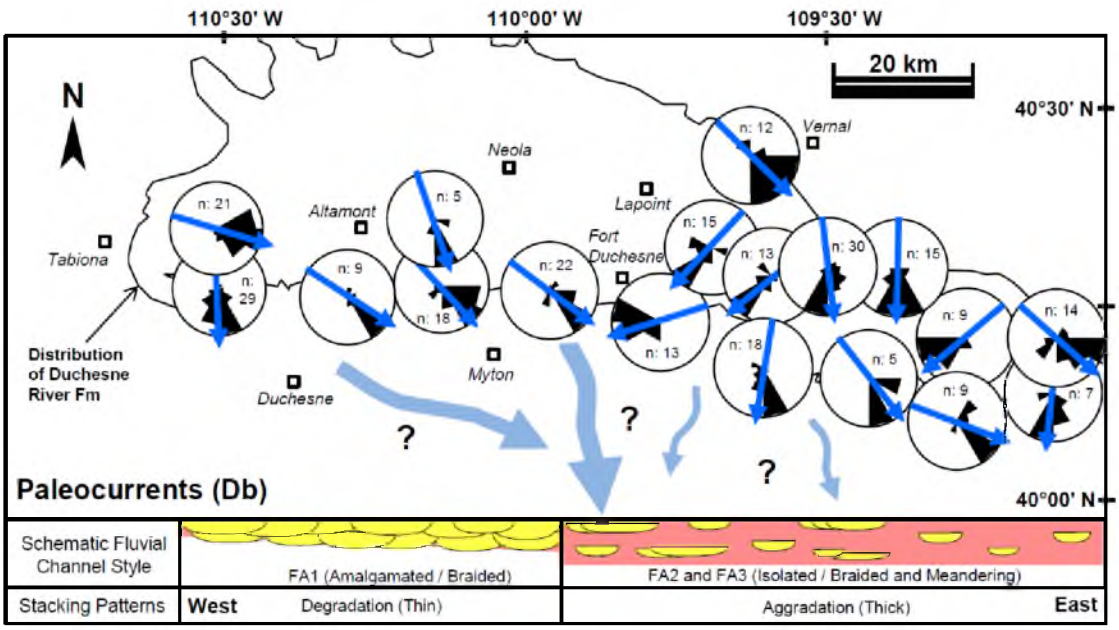

Figure 1.11. Paleocurrent data (total 264 measurements, magnetic declination: +11° used for corrections) plotted as rose diagrams with average directions (blue arrows), schematic fluvial channel styles, and stacking patterns of Db. More east and southeast flows in the western portion are possibly indicative of a confined eastward axial drainage system, while the eastern portion suggests an isolated and unconfined southward drainage system. These two systems possibly met near around the south of Roosevelt - Fort Duchesne and flowed south along the present-day basin axis.

LST represents the dominant fluvial environment where the water table is low, and TST/HST marks dominant wetland to lacustrine settings where the water table is rising or high. The term “base level” is not used in this study, since the definition of base level at fluvial environments is debatable (Schumm 1993; Dalrymple et al. 1998; Catuneanu 2006). The base-level or a graded equilibrium profile in upstream environments are the result of complex allogenic controls such as 1) tectonics (uplift and subsidence), 2) flow energy/slope, and 3) discharge (e.g., Holbrook et al. 2006). Therefore, the relative water table level change in this paper is also a consequence of these allogenic controls.

1.7.1 Stage 1 - Db

The first stage (Db) is marked by a basal sequence boundary and initial deposits comprising an upward-fining sequence (Fig. 1.12). There is a clear indication of the Uinta

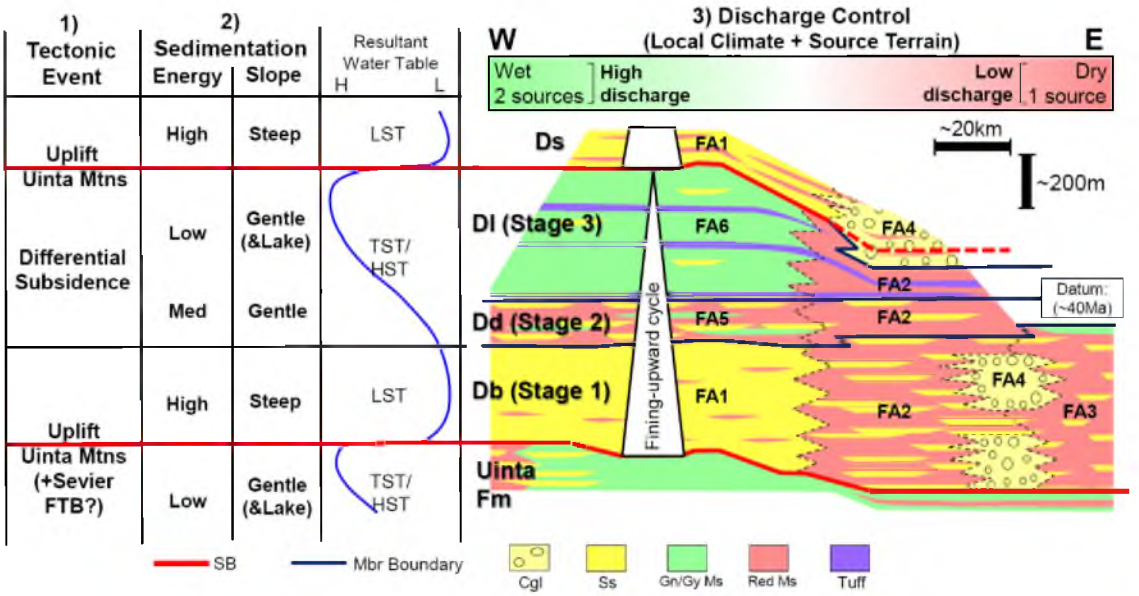

Figure 1.12. Proposed tectonic-driven sequence stratigraphic framework for the Duchesne River Formation. The Duchesne River sequence development is primarily triggered by uplift(s) in the Uinta Mountains and possibly in the Sevier FTB. The upward-fining sequence in the western part of the basin started with high energy sedimentation on the steep slope (stage 1), followed by a lower energy fluvial system accompanying wetland conditions on the gentle slope (stage 2). Then an extensive lake system emerged as a result of differential subsidence (stage 3). In contrast, the eastern part of the basin predominantly exhibits mixed braided, meandering, and isolated fluvial channel systems with gradually decreasing coarse-grained deposits upward (stage 1 to stage 3). Here, the relative water table level change is a consequence of three major allogenic controls of tectonics, flow energy/slope, and discharge (see text).

Mountains uplift because of an angular unconformity in the northern margin of the basin at the beginning of this stage (Fig. 1.10). Correspondingly, the southern part of basin also exhibits a distinct basinward shift of facies (i.e., sequence boundary) shown by the lacustrine deposits of the Uinta Formation overlain by the fluvial deposits of Db. There is a possibility that the Sevier FTB also activated at the same time (as discussed in the later section). These Uinta and Sevier FTB uplifts would induce the following environmental changes: 1) destruction of accommodation space in the proximal part of the basin, 2) higher discharge and sediment influx from uplifted mountain range(s), and 3) formation of steep and unstable slopes around the basin boundary fault. These changes are reflected in the deposition (progradation) of the fluvial facies associations (FA1, FA2, FA3) of Db and the cessation of lake deposition (Fig. 1.12).

The internal difference in basin-wide facies association between the west (FA1) and the

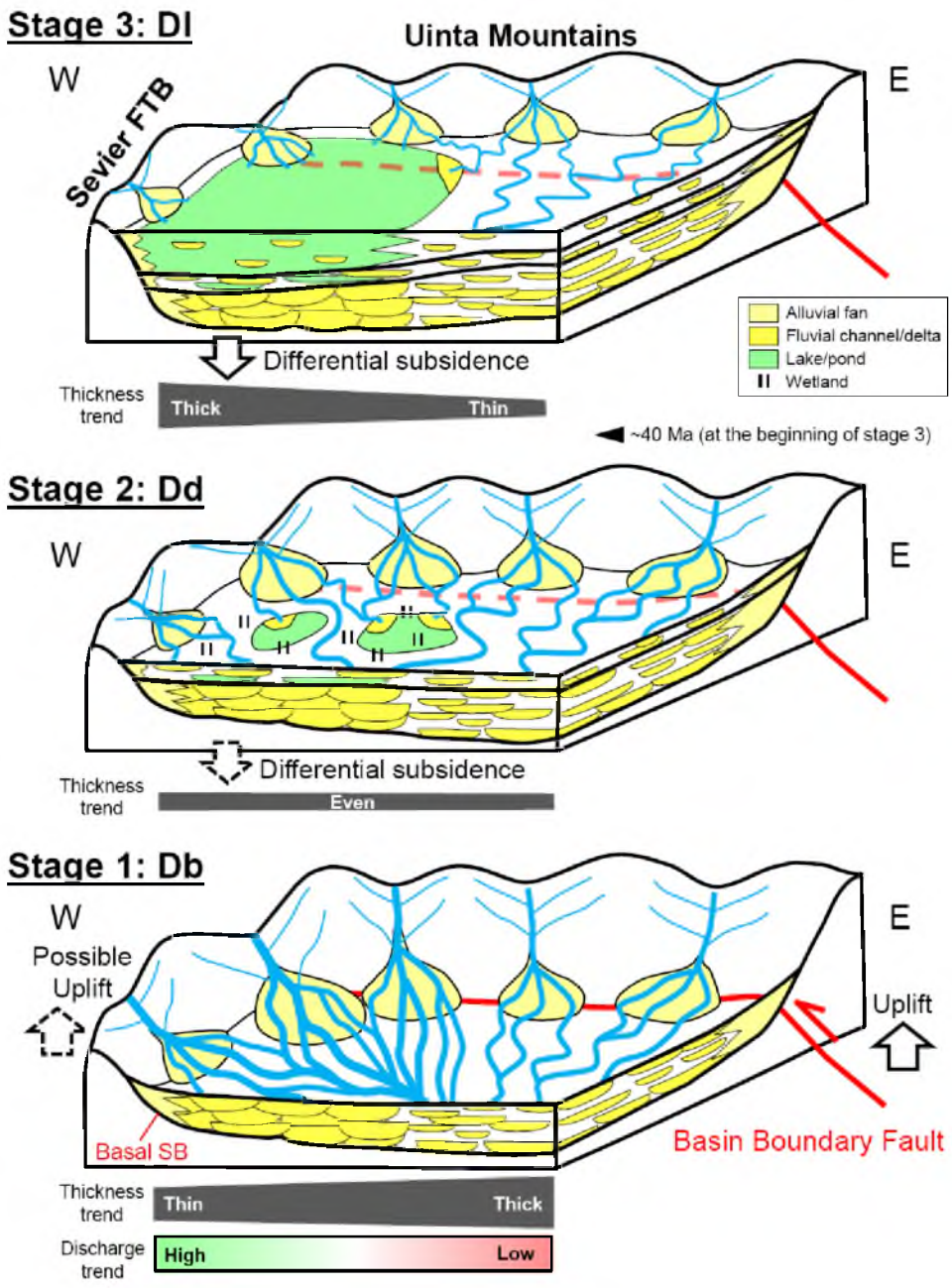

Figure 1.13. Three-staged evolutionary paleogeographic scenario of the upward-fining sequence of the Duchesne River Formation. Stage 1 is characterized by: uplift(s) possible in two source terrains; formation of an angular unconformity (SB); and development of a confined, high NTG braided fluvial system in the western part of the basin due to a high discharge from two source terrains (Uinta Mountains and Sevier FTB). In stage 2, retreat of sediment entry points in the alluvial fan facies, a decrease in discharge and sediment influx, and a possible differential subsidence caused development of low NTG fluvial systems on wet (west) and dry (east) alluvial plains. In stage 3, further retreat of sediment entry points and differential subsidence allowed development of an extensive lake system in the western part of the basin. Note the significant difference in facies, thickness, and stacking pattern between the west and east due to irregular allogenic controls (discharge and tectonic subsidence) within the basin.

east (FA2 and FA3) can be explained by local topographic and climatic factors. Specifically, the two clastic source terrains (Uinta Mountains and Sevier FTB) in the west could have caused a higher discharge (Fig. 1.13). The channel systems might have been confined (topographically controlled) along the east-west trending basin-axis in the western part of the basin. These controls resulted in the western high NTG braided river system (FA1) with repetitive cut-and-fill (degradational) patterns and frequent avulsions. Concurrently, the eastern part of the basin probably received a lower discharge due to a single source terrain (Uinta Mountains) and low channel confinement (resulting in lower NTG aggradational stacking patterns) (Fig. 1.13). It should be noted that there is a climatic contrast even in the present, modern-day Uinta Basin and surrounding ranges. The western area currently has a wetter climate and higher precipitation because it is surrounded by higher ranges of the Uinta and Wasatch Mountains, while the eastern area has a drier climate and lower precipitation (Greer 1981; Jensen et al. 1990; Gillies and Ramsey 2009). Although the modern Green River flowing across the eastern Uinta Mountains gives a significant amount of discharge into the eastern dry Uinta Basin (Fig. 1.1), this large drainage system opened in the late Miocene or early Pliocene time (Hansen 1986) and did not exist in the Late Eocene. Thus, the Db climatic contrast discussed here was probably strongly affected by local tectonics (i.e., climatic feedback mechanism by mountain range formation) rather than global climatic dynamics. The name of systems tract LST was adopted for this stage on the basis of the relative low water table level that is recorded in the dominance of fluvial environments.

1.7.2 Stage 2 - Dd

The second stage (Dd) is the transitional phase between stage 1 (Db) and stage 3 (Dl). A lower energy (relatively sinuous) fluvial system developed on the gentle slopes due to retreat of sediment entry points in the alluvial fan facies and a decrease in discharge and sediment influx as a result of erosional lowering of the source mountain ranges. The internal lateral facies change of Dd between the west (FA5) and east (FA2) probably reflects tectonic and/or climatic controls (Fig. 1.12). The wetter facies of FA5 in the west could be a response to 1) differential

tectonic subsidence and formation of a depression area in the west, and/or 2) continuous high discharge from multiple source terrains to the west. Total sediment package during this transitional stage is thinner than other stages, and thus the time period of this phase might be shorter than other stages. This is a possible reason why there is no distinct difference in thickness between the western and eastern part of the basin. The name of systems tract TST/HST was adopted for this stage on the basis of the relatively higher water table level.

1.7.3 Stage 3 - DI

The third and youngest phase of the upward-fining sequence is characterized by fine-grained sediments (Fig. 1.12). The dominance of fine-grained deposits suggests a further retreat of sediment entry points and alluvial fan facies due to the possible lowering of source mountain ranges. The lateral facies change from wetter/lacustrine FA6 in the west to drier/fluvial FA2 in the east reflects continuous tectonic and climatic controls from stage 2. The development of a more extensive lake system of FA6 in the west is largely due to differential subsidence (i.e., faster accommodation space development). A significant thickness difference between the west (thick) and the east (thin) within DI (Fig. 1.9) could be caused by a thrust-loading mechanism, which is a classic subsidence concept in Laramide basins (Beck et al. 1988). The uplift(s) of the Uinta Mountains (i.e., reactivation of the basin boundary fault) to the north and possibly the Sevier FTB to the west could produce higher subsidence in the western part of the basin due to a higher thrust-loading in the west (Fig. 1.13). In the Uinta Basin, numerous tuff/tuffaceous beds in this stage suggest contemporaneous volcanic activity presumably in the mountain ranges (Wasatch Range, East Tintic Mountains, and Oquirrh Mountains) to the west (Bryant et al. 1989). Although this volcanic activity might have occurred far away from the Uinta Basin and the tectonic impact on the basin is unrecognizable, there was surely some change in clastic source materials. The high water table position of the lacustrine system suggests a TST/HST for this final and last stage in the upward-fining sequence.

1.8 Discussion

1.8.1 Upward-fining Succession and Tectonics along the Sevier FTB

The Eocene intermontane system in central Utah shows a common pattern of upward-fining succession that suggests a strong relationship to a regional tectono-sedimentary regime (i.e., uplift in the Sevier FTB). Lake Flagstaff is another Eocene lake system/basin that developed in the present central Utah along the Sevier FTB (e.g., Stanley and Collinson 1979; Zawiskie et al. 1982; Davis et al. 2009). The Eocene Crazy Hollow Formation consists of fluvial channel and flood plain deposits (Willis 1994; Weiss and Warner 2001), and unconformably overlies lacustrine deposits of the Green River Formation in the Flagstaff Basin (Weiss 1982). The Crazy Hollow Formation is in turn conformably overlain by the Aurora (Bald Knoll) Formation, which is more lacustrine dominated (McGookey 1960; Williams and Hackman 1971). Willis (1988) acquired biotite K-Ar ages of 38.4±1.5 to 40.5±1.7 Ma from the upper part of the Aurora Formation, which is similar and correlatable to the K-Ar ages of ~40 Ma (by several researchers as noted above) from the tuff at the base of Dl. Collectively, this upward-fining succession has a very similar profile (i.e., distinct sequence boundary at base and gradual change from fluvial to shallow lacustrine upwards), with a similar age to the upward-fining Duchesne River sequence. Thus, it is possible that the Sevier FTB activated contemporaneously with the Uinta Mountains at the beginning of the Duchesne River deposition, and it simultaneously triggered the development of the upward-fining Crazy Hollow – Aurora sequence as well as the Duchesne River sequence.

1.8.2 Controlling Factors on the Duchesne River Sequence

In proximal continental environments, it is broadly accepted that an upward-fining sequence is controlled by source uplift that initially brings in coarse-grained sediments on steep slopes and the fine-grained sediments ensue later due to source area retreat and relief decline (e.g., Mack and Ramussen 1984; Catuneanu and Elango 2001). Here, we examine three major controlling factors, 1) tectonics (accommodation), 2) flow energy/slope, and 3) discharge, on the three-staged Duchesne River sequence (Db, Dd, Dl) and fluvial - lacustrine styles (Fig. 1.12, Fig.

1.13). The relative water table level curve in Figure 1.12 is the result of these three allogenic controls, and thus represents dominant depositional environments (i.e., LST: fluvial, TST/HST: wetland to lacustrine settings). All three major controlling factors were in response to the initial tectonic pulse (uplifts) in the Uinta Mountains and possibly in the Sevier FTB (see descriptions for each factor below). Other major allogenic contributions (i.e., global climate changes) would likely be completely masked or overpowered by the strong, local tectonic driving force in the Uinta Basin.

1.8.2.1 Tectonics

Initial source uplift(s) in the Uinta Mountains to the north and possibly the Sevier FTB to the west caused a low accommodation space in the proximal part of the basin and induced the progradation of fluvial environments (cessation of the lake environment of the Uinta Formation) in stage 1 (Db). The late-stage thrust-loading (i.e., differential subsidence) caused a high accommodation space in the western part of the basin and induced development of lacustrine environment in stage 3 (Dl).

1.8.2.2 Flow Energy/Slope

Initial high flow energy from uplifted mountain range(s) gradually decreased over time due to reduced relief and source area retreat (following models by Mack and Ramussen 1984; Catuneanu and Elango 2001). This trend resulted in the overall member-scale, upward-fining sequence from stage 1 (Db) to stage 3 (Dl).

1.8.2.3 Discharge

The geographical difference in discharge (high discharge in the west and low discharge in the east) was attributed to local climate (climatic feedback mechanisms from mountain range uplifts) and source terrain input. This difference induced contrasting fluvial styles and stacking patterns of high NTG / degradation in the west and low NTG / aggradation in the east, during stage 1 (Db) (Fig. 1.13).

1.8.3 Comparison with Fluvial-Lacustrine Sequence Stratigraphic Models

The upward-fining sequence within the Duchesne River Formation is similar to the fluvial sequence stratigraphic models by Wright and Marriot (1993), Shanley and McCabe (1994), Currie (1997), and Legaretta and Uliana (1998). Their models commonly show a vertical profile with facies change from basal confined amalgamated channels (degradation) into upper unconfined isolated channels (aggradation). However, the Duchesne River example shows gradation from an amalgamated channel (degradational) system (FA1) into an isolated/unconfined channel (aggradational) system (FA2, FA3, and FA5), not only in the vertical succession, but also in the lateral and coeval successions. Thus, this Duchesne River study provides a comprehensive three-dimensional picture of how irregular allogenic controls such as tectonics (differential subsidence) and discharge (different local climate and source terrain input) within a continental basin can affect the resultant basin-scale lateral facies variations of fluvial – lacustrine deposits.

The western portion of fluvial-lacustrine architecture of the Duchesne River Formation can also be explained by a lacustrine sequence stratigraphic model of Carroll and Bohacs (1999). Their lake-basin type classification system is based on the interaction of the rates of sediment and water supply (mostly climatic) with potential accommodation (mostly tectonic). Potential accommodation space was overwhelmed by sediment and water supplies during the stage 1 (Db) of the Duchesne River sequence, resulting in fluvial sedimentation. By contrast, these factors of accommodation and sedimentation were more equal or balanced due to an increase in potential accommodation where the differential subsidence led to the lake development in the western part of the basin during the stage 3 (Dl).

1.9 Conclusions

This outcrop-based sequence stratigraphic study of the Tertiary Duchesne River Formation of the Uinta Basin reveals the basin-scale (>130 km) architecture of fluvial - lacustrine facies associations: FA1- amalgamated braided fluvial channels, FA2- extensive flood plain and stacked broad fluvial channels, FA3- extensive flood plain and isolated small streams,

FA4- alluvial fan complex, FA5- dry and wet flood plains and fluvial channels, and FA6- extensive lacustrine deposits.

The member-scale upward-fining sequence (unconformity-bounded) was likely triggered by the uplift(s) of the Uinta Mountains and possibly the Sevier FTB. A tectonic-driven sequence stratigraphic scenario with three stages (stage 1: Db, stage 2: Dd, stage 3: Dl) is proposed to decipher the evolution of the Duchesne River late basin-fill.

The significant facies and thickness variations between the western and eastern part of the basin record irregular allogenic controls of tectonics and discharge within the basin. Specifically, a high NTG (degradational) fluvial system (FA1) in the west in stage 1 reflects a higher discharge due to a wet climate and two source terrain inputs (Uinta Mountains and Sevier FTB), whereas a low NTG (aggradational) fluvial system (FA2 and FA3) in the east reflects a lower discharge due to a dry climate and single source terrain input (Uinta Mountains). The development of thick lacustrine deposits (FA6) in the west during final stage 3 reflects differential tectonic subsidence in the Uinta Basin.

The Duchesne River example provides a comprehensive picture of the complex sequence stratigraphic framework of upstream environments, and demonstrates how internal facies architectures at the basin-scale evolve by allogenic controls stemming from tectonic uplifts. These kinds of remarkable outcrop field exposures are valuable for testing and refining models of continental sequence stratigraphy, with applications to explorations in similar fluvial - lacustrine systems in continental basins.

1.10 References

Allen, J.L., and Johnson, C.L, 2010, Facies control on sandstone composition (and influence of statistical methods on interpretations) in the John Henry Member, Straight Cliffs Formation, Southern Utah, USA: Sedimentary Geology, v. 230, p. 60-76.

Andersen, D.W., and Picard, M.D., 1972, Stratigraphy of the Duchesne River Formation (Eocene-Oligocene?), northern Uinta basin, northeastern Utah: Utah Geological and Mineral Survey Bulletin, v. 97, 29 p.

Andersen, D.W., and Picard, M.D., I974, Evolution of synorogenic clastic deposits in the intermontane Uinta Basin of Utah, in Dickinson, W.R., ed., Tectonics and Sedimentation: SEPM Special Publication, v. 22, p. 167-189.

Aswasereelert, W., Meyers, S.R., Carroll, A.R., Peters, S.E., Smith, M.E. and Feigl, K.L., 2013, Basin-scale cyclostratigraphy of the Green River Formation, Wyoming: Geological Society of America Bulletin, v. 125, p. 216-228.

Atchley, S.C., Nordt, L.C., and Dworkin, S.I., 2004, Eustatic control on alluvial sequence stratigraphy: A possible example from the Cretaceous-Tertiary transition of the Tornillo Basin, Big Bend National Park, West Texas, U.S.A.: Journal of Sedimentary Research, v. 74, p. 391-404.

Beck, R.A., Vondra C.F., Filkins, J.E., and Olander, J.D., 1988, Syntectonic sedimentation and Laramide basement thrusting, Cordilleran foreland; Timing of deformation: Geological Society of America Memoirs, v. 171, p. 465-488.

Blakey, R., 2011, North American paleogeographic maps, Northern Arizona State University, Flagstaff.

Blum, M.D., and Tornqvist, T.E., 2000, Fluvial responses to climate and sea-level change: a review and look forward: Sedimentology, v. 47, p. 2–48.

Bruhn, R.L., Picard, M.D., and Isby, J.S., 1986, Tectonics and sedimentation of Uinta arch, western Uinta Mountains and Uinta Basin, in Peterson. J.A., ed., Paleotectonics and sedimentation in Rocky Mountain region, United States: American Association of Petroleum Geologists Memoir 41, p. 333-352.

Bryant, B., 1992, Geologic and structure maps of the Salt Lake City 1 degree x 2 degrees quadrangle, Utah and Wyoming: U.S. Geological Survey Miscellaneous Investigations Series Map I-1997.

Bryant, B., Naeser, C.W., Marvin, R.F., and Mehnert, H.H., 1989, Upper Cretaceous and Paleogene sedimentary rocks and isotopic ages of Paleogene tuffs, Uinta Basin, Utah: U.S. Geological Survey Bulletin 1787-J, 22 p.

Campbell, J.A., and Ritzma, H.R., 1979, Geology and petroleum resources of the major oil-impregnated sandstone deposits of Utah: Utah Geological and Mineral Survey Special Studies, v. 50, 24 p.

Carroll, A.R., and Bohacs, A.M., 1999, Stratigraphic classification of ancient lakes: Balancing tectonic and climatic controls: Geology, v. 27; p. 99-102.

Catuneanu, O., 2006, Principles of Sequence Stratigraphy: Amsterdam, Elsevier, 375 p.

Catuneanu, O., and Elango, H.N., 2001, Tectonic control on fluvial styles: the Balfour Formation of the Karoo Basin, South Africa: Sedimentary Geology, v. 140, p. 291-313.

Crews, S.G., and Ethridge, F.G., 1993, Laramide tectonics and humid alluvial fan sedimentation: NE Uinta Uplift, Utah and Wyoming: Journal of Sedimentary Petrology, v. 63, p. 420-436.

Currie, B.S., 1997, Sequence stratigraphy of nonmarine Jurassic–Cretaceous rocks, central Cordilleran foreland-basin system: Geological Society of America Bulletin, v. 109, p. 1206-1222.

Dalrymple, M., Prosser, J., and Williams, B., 1998, A dynamic systems approach to the regional controls on deposition and architecture of alluvial sequences, illustrated in the Stratfjord Formation (United Kingdom, northern North Sea), in Shanley, K.W., and McCabe, P.J., eds., Relative Role of Eustasy, Climate, and Tectonism in Continental Rocks: SEPM Special Publication, v. 59, p. 65-81.

Davis, S.J., Mulch, A., Carroll, A.R., Horton T.W., and Chamberlain, C.P., 2009, Paleogene landscape evolution of the central North American Cordillera: Developing topography and hydrology in the Laramide Foreland: Geological Society of America Bulletin, v. 121, p. 100-116.

Dickinson, W.R., Klute, M.A., Hayes, M.J., Janecke, S.U., Lundin, E.R., McKittrick, M.A., and Olivares, M.D., 1988, Paleogeographic and paleotectonic setting of Laramide sedimentary basins in the central Rocky Mountain region: Geological Society of America Bulletin, v.100, p. 1023-1039.

Franczyk, K.J., Fouch, T.D., Johnson, R.C., Molenaar, C.M., Cobban, W.A., 1992, Cretaceous and Tertiary paleogeographic reconstructions for the Uinta-Piceance Basin Study Area, Colorado and Utah: U.S. Geological Survey Bulletin 1787-Q, 37 p.

Gibling, M.R., Fielding, C.R., and Sinha, R., 2011, Alluvial valleys and alluvial sequences: towards a geomorphic assessment, in Davidson, S.K., Leleu, S., and North, C.P., eds., From River to Rock Record: The Preservation of Fluvial Sediments and Their Subsequent Interpretation: SEPM Special Publication, v. 97, p. 423–447.

Gillies, R.R., and Ramsey, R.D., 2009, Climate of Utah, in Banner, R.E., Baldwin, B.D., and McGinty, E.L., eds., Rangeland Resources of Utah (revised): Utah State University, Cooperative Extension Service, p. 39-45.

Greer, D.C., Director, 1981, Atlas of Utah: Provo, Utah, Brigham Young University Press, 300 p.

Hansen, W.R., 1986, Neogene tectonics and geomorphology of the eastern Uinta Mountains in Utah, Colorado, and Wyoming: U.S. Geological Survey Professional Paper 1356, 78 p.

Hasiotis, S.T., 2000, The invertebrate invasion and evolution of Mesozoic soil ecosystems: the ichnofossil record of ecological innovations, in Gastaldo, R., and DiMichele, W., eds., Phanerozoic Terrestrial Ecosystems: Paleontological Society Short Course 6, p. 141-169.

Hintze, L.F, Willis, G.C., Laes, D.Y.M., Sprinkel, D.A., and Brown, K.D., 2000, Digital geologic map of Utah 1:500000: Utah Geological Survey.

Holbrook, J.M., Scott, R.W., and Oboh-ikuenobe, F.E., 2006, Base-level buffers and buttresses: a model for upstream versus downstream control on fluvial geometry and architecture within sequences: Journal of Sedimentary Research, v. 76, p. 162–174.

Jensen, D.T., Bingham, G.E., Ashcroft, G.L., Malek, E., McCurdy G.D., and McDougal, W.K., 1990, Precipitation pattern analysis Uinta Basin-Wasatch Front, Report to Division of Water Resources, State of Utah under Contract Number 90-3078: Office of the State Climatologist, Utah State University, Logan, Utah, 41 p.

Keighley, D., Flint, S., Howell, J., and Moscariello, A., 2003, Sequence stratigraphy in lacustrine basins: a model for part of the Green River Formation (Eocene), southwest Uinta Basin, Utah: Journal of Sedimentary Research, v. 73, p. 987-1006.

Kelly, T.S., Murphey, P.C., and Walsh, S.L., 2012, New records of small mammals from the middle Eocene Duchesne River Formation, Utah, and their implications for the Uintan-Duchesnean North American Land Mammal Age transition; Paludicola, v. 8, p. 208-251.

Kraus, M.J., 2002, Basin-scale change in flood plain paleosols: Implications for interpreting alluvial architecture: Journal of Sedimentary Research, v. 72, p. 500-509.

Kraus, M.J., and Hasiotis, S.T., 2006, Significance of different modes of rhizolith preservation to interpreting paleoenvironmental and paleohydrologic settings: Example from Paleogene paleosols, Bighorn Basin, Wyoming, U.S.A.: Journal of Sedimentary Research, v. 76, p. 633–646.

Kukulski, R.B., Hubbard, S.M., Moslow, T.F., and Raines, M.K., 2013, Basin-scale stratigraphic architecture of upstream fluvial deposits: Jurassic–Cretaceous foredeep, Alberta Basin, Canada: Journal of Sedimentary Research, v. 83, p. 704–722.

Lambiase, J.J., 1990, A model for tectonic control of lacustrine stratigraphic sequences in continental rift basins, in Katz, B.J., ed., Lacustrine Basin Exploration—Case Studies and Modern Analogs: American Association of Petroleum Geologists Memoir 50, p. 265–276.

Legaretta, L., and Uliana, M.A., 1998, Anatomy of hinterland depositional sequences: Upper Cretaceous fluvial strata, Nequen Basin, west-central Argentina, in Shanley, K.W., and McCabe, P.J., eds., Relative Role of Eustasy, Climate and Tectonism in Continental Rocks: SEPM Special Publication, v. 59, p. 83-92.

Mack, G.H., and Rasmussen, K.A., 1984, Alluvial-fan sedimentation of the Cutler Formation (Permo-Pennsylvanian) near Gateway, Colorado: Geological Society of America Bulletin, v. 95, p. 109-116.

McDowell, F.W., Wilson, J.A., and Clark, J., 1973, K-Ar dates for biotite from two paleontologically significant localities: Duchesne River Formation, Utah, and Chadron Formation, South Dakota: Isochron/West, v. 7, p. 11-12.

McGookey, D.P., 1960, Early Tertiary stratigraphy of part of central Utah: American Association of Petroleum Geologists Bulletin, v. 44, p. 589-615.

Nemec, W., and Steel, R.J., 1984, Alluvial and coastal conglomerates: their significant features and some comments on gravelly mass-flow deposits, in Koster, E.H., and Steel, R.J., eds., Sedimentology of Gravels and Conglomerates: Canadian Society of Petroleum Geologists Memoir 10, p. 1-31.

Picard, M.D., and High, L.R., 1972, Criteria for recognizing lacustrine rocks, in Rigby, J.K., and Hamblin, W.K., eds., Recognition of ancient sedimentary environments: SEPM Special Publication, v. 16, p. 108-145.

Posamentier, H.W., and Vail, P.R., 1988, Eustatic controls on clastic deposition II–sequence and systems tract models, in Wilgus, C.K., Hastings, B.S., Kendall, C.G.St.C., Posamentier, H.W., Ross, C.A., Van Wagoner, J.C., eds., Sea Level Changes—An Integrated Approach: SEPM Special Publication, v. 42, p. 125-154.

Prothero, D.R. and Swisher, C.C., 1992, Magnetostratigraphy and geochronology of the terrestrial Eocene-Oligocene transition in North America, in Prothero, D.R., and Berggren, W.A., eds., Eocene-Oligocene climatic and biotic evolution: Princeton University Press, p. 46-74.

Retallack, G.J., 2001, Soils of the past, 2nd edition, Blackwell Science, Oxford, 404 p.

Rowley, P.D., Hansen, W.R., Tweto, O., and Carrara, P.E., 1985, Geologic map of the Vernal 1ø x 2ø quadrangle, Colorado, Utah, and Wyoming: U.S. Geological Survey Miscellaneous Investigations Series I-1526.

Schumm, S.A., 1993, River response to baselevel change: Implications for sequence stratigraphy: The Journal of Geology, v. 101, p. 279-294.

Shanley, K.W., and McCabe, P.J., 1994, Perspectives on the sequence stratigraphy of continental strata: American Association of Petroleum Geologists Bulletin, v. 78, p. 544-568.

Sprinkel, D.A., 2006, Interim geologic map of the Dutch John 30' x 60' quadrangle, Daggett and Uintah Counties Utah, Moffat County, Colorado, and Sweetwater County, Wyoming: Utah Geological Survey.

Sprinkel, D.A., 2007, Interim geologic map of the Vernal 30' x 60' quadrangle, Uintah and Duchesne Counties, Utah, and Moffat and Rio Blanco Counties, Colorado: Utah Geological Survey.

Stanley, K.O., and Collinson, J.W., 1979, Depositional history of Paleocene–lower Eocene Flagstaff Limestone and coeval rocks, Central Utah: American Association of Petroleum Geologists Bulletin, v. 63, p. 311–323.

Visher, G.S., 1965, Use of vertical profile in environmental reconstruction: American Association of Petroleum Geologists Bulletin, v. 49, p. 41-61.

Warner, M.M., 1965, Cementation as a clue to structure, drainage patterns, permeability, and other factors: Journal of Sedimentary Petrology, v. 35, p. 797-804.

Warner, M.M., 1966, Sedimentational analysis of the Duchesne River Formation, Uinta Basin, Utah: Geological Society of America Bulletin v. 77, p. 945-957.

Weiss, M.P., 1982, Relation of the Crazy Hollow Formation to the Green River Formation, Central Utah, Overthrust Belt of Utah: Utah Geological Association Publication, v. 10, p. 285–289.

Weiss, M.P., and Warner, K.N., 2001, The Crazy Hollow Formation (Eocene) of central Utah: Brigham Young University Geology Studies, v. 46, p. 143-161.

Williams, P.L., and Hackman, R.J., 1971, Geology, structure, and uranium deposits of the Salina Quadrangle, Utah: U.S. Geological Survey IMAP 591.

Willis, G.C., 1988, Geologic map of the Aurora quadrangle, Sevier County, Utah: Utah Geological and Mineral Survey, Map 112, 21 p.

Willis, G.C., 1994, Interim geologic map of the Richfield quadrangle, Sevier County, Utah: Utah Geological Survey Open-file Report 309, 73 p.

Wright, V.P., and Marriott, S.B., 1993, The sequence stratigraphy of fluvial depositional systems: the role of floodplain sediment storage: Sedimentary Geology, v. 86, p. 203-210.

Zawiskie, J., Champman, D., and Alley, R., 1982, Depositional history of the Paleocene–Eocene Colton Formation, north-central Utah, in Nielson, D.L., ed., Overthrust Belt of Utah: Utah Geological Association Publication, v. 10, p. 273–284.

CHAPTER 2

SOURCE-TO-SINK FLUVIAL SYSTEMS FOR SANDSTONE RESERVOIR EXPLORATION: EXAMPLE FROM THE BASAL BRENNAN BASIN MEMBER OF TERTIARY DUCHESNE RIVER FORMATION, NORTHERN UINTA BASIN, UTAH

2.1 Abstract

The Tertiary Duchesne River Formation represents the late-stage fill of the Uinta Basin, which preserves an upward-fining fluvial sequence. Extensive outcrop exposures of the Tertiary Duchesne River Formation can be traced from source to sink, and comprise a valuable example of basin-scale facies architectures to evaluate controlling factors on the depositional history. Distinct basin-scale facies change of the sandstone-dominated basal member of the Duchesne River Formation exhibits a high net-sandstone-to-gross-thickness (NTG) braided river system in the western and a low NTG braided, meandering, and isolated small river system in the eastern portion of the basin. Extensive paleocurrent data show overall southerly transport largely derived from the Uinta Mountains in the north. However, many southeastward flows and texturally and compositionally mature (quartz-rich) sandstones in the western part of the basin suggest the influence of long transportation from a different source terrain, specifically the Sevier Fold Thrust Belt to the west. The multiple transport patterns and petrographic data indicate that the high-discharge drainage system along the E-W basin axis in the western part of the basin was important for development of a large-volume and high-quality (porous) reservoir system. This example demonstrates the importance of deciphering the complex input of multiple source terrains for exploration of fluvial sandstone reservoirs in the sink.

2.2 Introduction

The Uinta Basin, a Laramide intermontane lake basin, is a prolific hydrocarbon province containing a world-class lacustrine source rock (i.e., Green River shale). The lacustrine basin-fill sequence has very good exposures at the basin margins, and thus comprises a valuable field analog for growing exploration efforts in more challenging lacustrine basins (e.g., deep-seated lacustrine basins on Atlantic margins, intracratonic rift basins in Africa). The Duchesne River Formation is an uppermost unit of the Lake Uinta basin-fill sequence that reveals detailed basin-scale fluvial – lacustrine facies architectures. There is a remarkable difference in fluvial sandstone reservoir facies and property between the western and eastern part of the basin within the basal member (Db). The purpose of this chapter is to document the multiple fluvial sedimentary processes from source terrains to the basin (sink). Two approaches, basin-scale field surveys and petrographic studies, are taken to decipher the mechanism of development of suitable fluvial sandstone reservoir facies in the sink.

2.3 Geological Context

2.3.1 Geological Setting

The Uinta Basin, situated in northeastern Utah (Fig. 2.1), is a part of the Laramide basin system that emerged during the latest Cretaceous to early Paleogene (Dickinson et al. 1988). After the Cretaceous Western Interior Seaway receded, Laramide basement-involved uplifts caused several segmented intermontane lake basins in the present Rocky Mountain region covering Montana, Wyoming, Colorado, and Utah (e.g., Dickinson et al. 1986, 1988). The Uinta Basin is surrounded by the Uinta Mountains to the north, the Sevier Fold Thrust Belt (FTB) to the west, Douglas Creek arch to the east, and the Uncompahgre uplift and San Rafael Swell to the south. The basin shows an asymmetric basin shape that is northerly bounded by a high-angle reverse fault at the foothills of Uinta Mountains (e.g., Fouch 1975; Bruhn et al. 1983, 1986).

The Paleocene-Eocene lacustrine basin-fill sequence is comprised of the Wasatch (fluvial), Green River (lacustrine), Uinta (fluvial-lacustrine), and Duchesne River (fluvial)

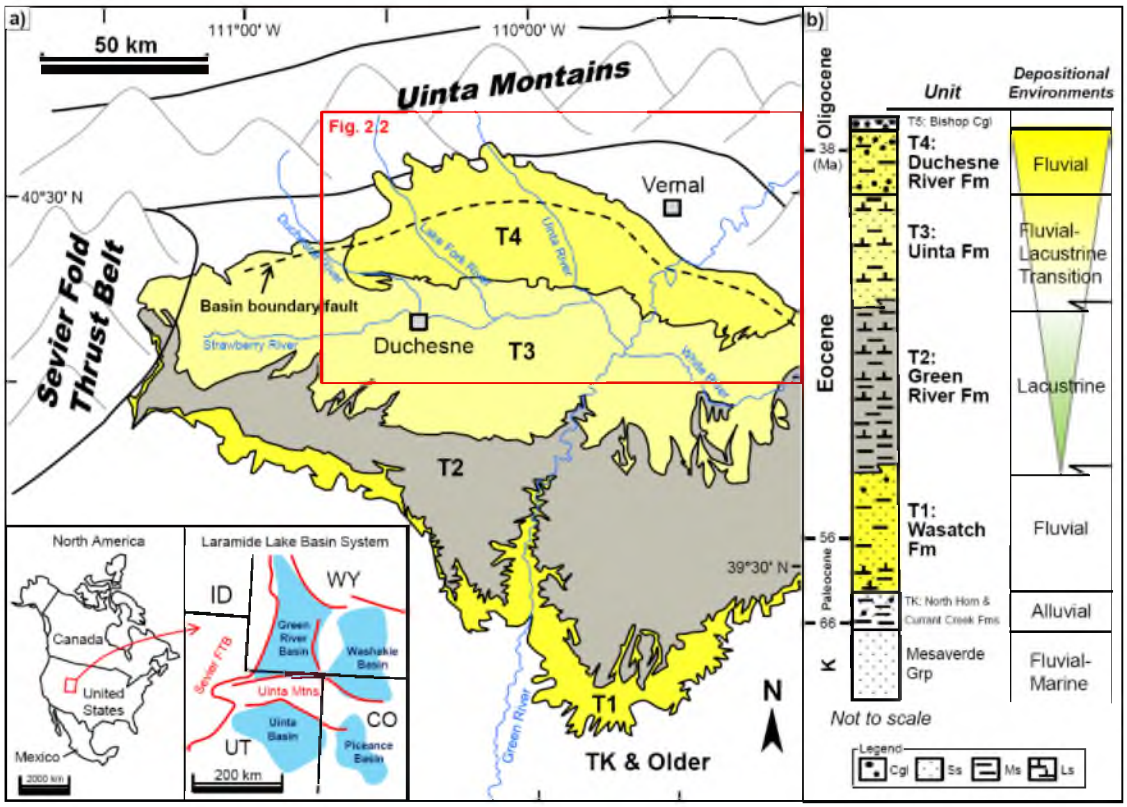

Figure 2.1. Geological map and geologic column of the Uinta Basin. a) Geological map of the Uinta Basin. Regional dip is to the north and formations get progressively younger toward the Uinta Mountains. The basin is surrounded by high mountain ranges of the Uinta Mountains and Sevier Fold Thrust Belt (FTB). The map of Laramide lake basin system is from Dickinson et al. (1988). The geological map is modified from Andersen and Picard (1974), Bryant et al. (1989), Bryant (1992), Hintze et al. (2000), and Sprinkel (2006 and 2007). b) Schematic geologic column showing the Paleogene sequence of the Uinta Basin (modified from Hintze et al. 2000). T2 to T4 exhibits a typical upward-coarsening/shallowing lacustrine basin-fill succession.

formations (Fig. 2.1) in ascending order. The upper three of these formations exhibit a typical upward shallowing or coarsening succession commonly observed in lacustrine basin-fill settings (Visher 1965; Picard and High 1972; Lambiase 1990). This basin-fill sequence is unconformably overlain by the Oligocene Bishop Conglomerate (Fig. 2.1).

The Duchesne River Formation is exposed in the northern part of the Uinta Basin (Fig. 2.1). It consists of four members, the Brennan Basin (Db), Dry Gulch Creek (Dd), Lapoint (Dl), and Starr Flat (Ds) members in ascending order (Fig. 2.2). The lower three members comprise an upward-fining sequence with a sandstone-dominated basal member (Db), a transitional second member (Dd), and a mudstone-dominated third member (Dl). It is noted that Dl is rich in

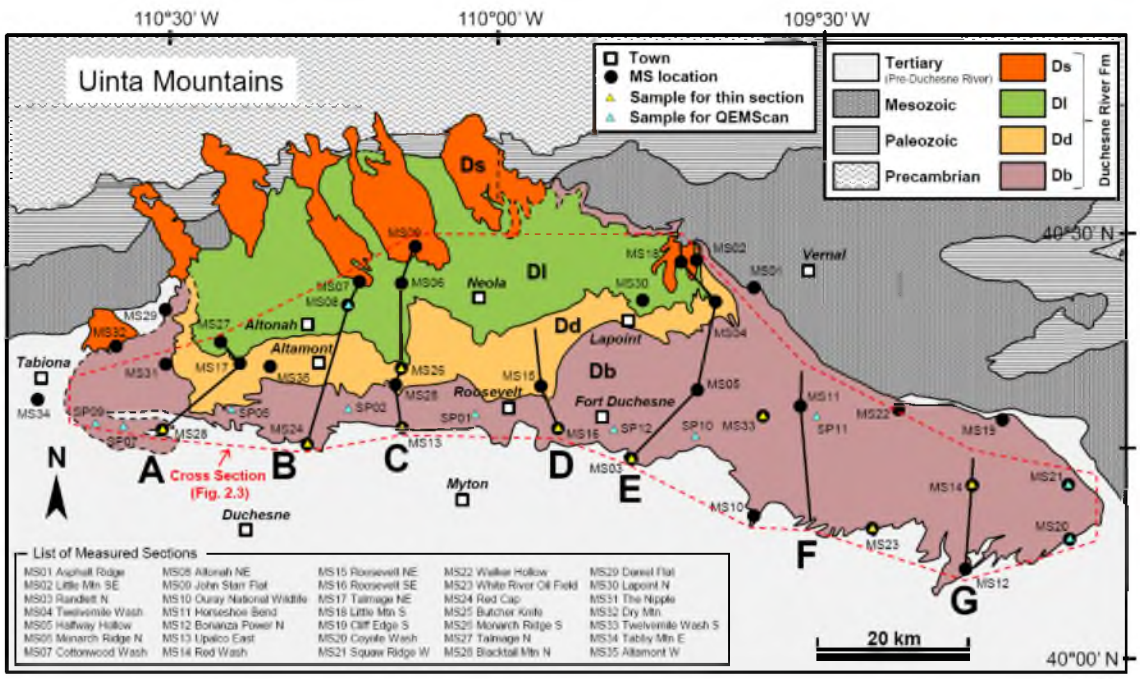

Figure 2.2. Geological map of the Duchesne River Formation and surrounding area. Regional dip is to the north and the Duchesne River members (Db: Brennan Basin Member, Dd: Dry Gulch Creek Member, Dl: Lapoint Member, and Ds: Starr Flat Member) get progressively younger toward the Uinta Mountains. The locations of 35 measured sections (MS), sandstone samples for thin section (yellow triangles) and for QEMScan (light blue triangles), and composite sections A to G (black lines) are shown on the map. The map is modified after Andersen and Picard (1974), Rowley et al. (1985), Bryant et al. (1989), and Sprinkel (2006 and 2007).

tuff/tuffaceous beds throughout the basin, and a basal tuff of this member is a good stratigraphic time-marker (K-Ar ages of ~40 Ma reported by several researchers, McDowell et al. 1973; Andersen and Picard 1974; Prothero and Swisher 1992; Kelly et al. 2012) (see the detailed discussion on the geological age in Appendix A). The uppermost member (Ds) consists mainly of coarse-grained rocks (e.g., sandstones and conglomerates), indicating the onset of another upward-fining fluvial cycle.

The Uinta Basin contains not only conventional hydrocarbon resources but also significant unconventional resources such as oil shales (e.g., Cashion 1964; Vanden Berg 2008), tar sands (e.g., Campbell and Ritzma 1979; Ritzma 1979; Blackett 1996), and gilsonites (e.g., Cashion 1967; Boden and Tripp 2012). In particular, the Duchesne River Formation contains significant amounts of tar sands at Asphalt Ridge situated in the eastern margin of the

basin (Fig. 2.2), as first studied in detail by Spieker (1931). This oil is sourced from the underlying Green River Formation (Covington 1957, 1963, 1964; Kayser 1966; Thomas et al. 1977; Hatcher et al. 1992).

2.3.2 Previous Studies

There are not many stratigraphic and sedimentological studies of the Duchesne River Formation compared with the well-studied underlying Green River Formation, which attracts more researchers due to its economic significance. The latest stratigraphic nomenclature for the four members of the Duchesne River Formation was defined by Andersen and Picard (1972) (detailed nomenclatural history in Appendix A). Rowley et al. (1985) and Bryant et al. (1989) were the first to regionally map the four members defined by Andersen and Picard (1972).

Andersen and Picard (1974) is the only study which examined sandstone compositions of the Duchesne River Formation. They noticed a geographical difference in sandstone compositions (i.e., rich in quartz in the western part of basin and rich in rock fragments in the eastern part of the basin). This chapter presents additional petrographic analyses focusing on the sandstone-dominated basal member of the Duchesne River Formation in order to recognize the mechanism of this geographical difference in sandstone compositions and also to examine the relationship with sandstone properties (porosity).

2.4 Methods

Two approaches were taken to decipher the source-to-sink fluvial depositional system of the Duchesne River Formation. Basin-wide field surveys contributed to the construction of the regional stratigraphic framework along with detailed internal facies architectures and interpretation of paleodrainage patterns. Petrographic studies on representative sandstone samples from all over the basin provided supportive data for sediment sources, transportation distance, and sandstone property as described in detail below.

2.4.1 Regional Stratigraphic Study

Thirty-five measured sections (MS01 to MS35) covering the distribution of the Duchesne River Formation (a total of 2,970 m, which includes the uppermost part of the Uinta Formation) and 441 paleocurrent measurements (264 measurements from the basal member) were acquired (Fig. 2.2). Then N-S trending composite sections A to G are correlated by referring to several geological maps and structural dips and strikes. It should be noted that the geological map is modified after Andersen and Picard (1974), Rowley et al. (1985), Bryant et al. (1989), and Sprinkel (2006, 2007). Although the latest regional 1° x 2° geological map of the Salt Lake City quadrangle (Bryant 1992) shows the "Undivided Duchesne River Formation" covering the broad area of the western part of the basin, this division obviously includes older units that are equivalent to the Uinta and Green River formations. For this region (to the west of Duchesne, UT), this study adopt the outline of the Duchesne River Formation by Andersen and Picard (1974), which is more suitable for sequence stratigraphic interpretation. E-W regional correlations of composite sections A to G are shown in Figure 2.3. The stratigraphic datum is set at the base of Dl (K-Ar ages of ~40 Ma from basal Dl tuffs as noted above). Lithological classifications presented in this correlation are the dominant or representative lithology. For the broad correlation, each lithology is generalized (e.g., a sandstone lithology mostly represents thicker channel type sandstone). Lithological interpretations between measured sections (MS locations on Figure 2.2 and detailed sections in Appendix B) are schematic. Nevertheless, expansive outcrops greatly support the interpretations presented here.

2.4.2 Petrographic Study

Twenty fine- to medium-grained sandstone samples were collected over the basin in this study (Appendix C, Fig. 2.2) to supplement the large amounts of data (79 sandstone composition data) in the previous work by Andersen and Picard (1974). Nine thin sections (8 samples from Db, 1 sample from Dd) were studied in detail. We followed the Gazzi-Dickinson approach (Gazzi 1966; Dickinson 1970; Ingersoll et al. 1984) for these nine thin sections, counting a total of 500 grain counts per section. In this method, any mineral >0.0625 mm is

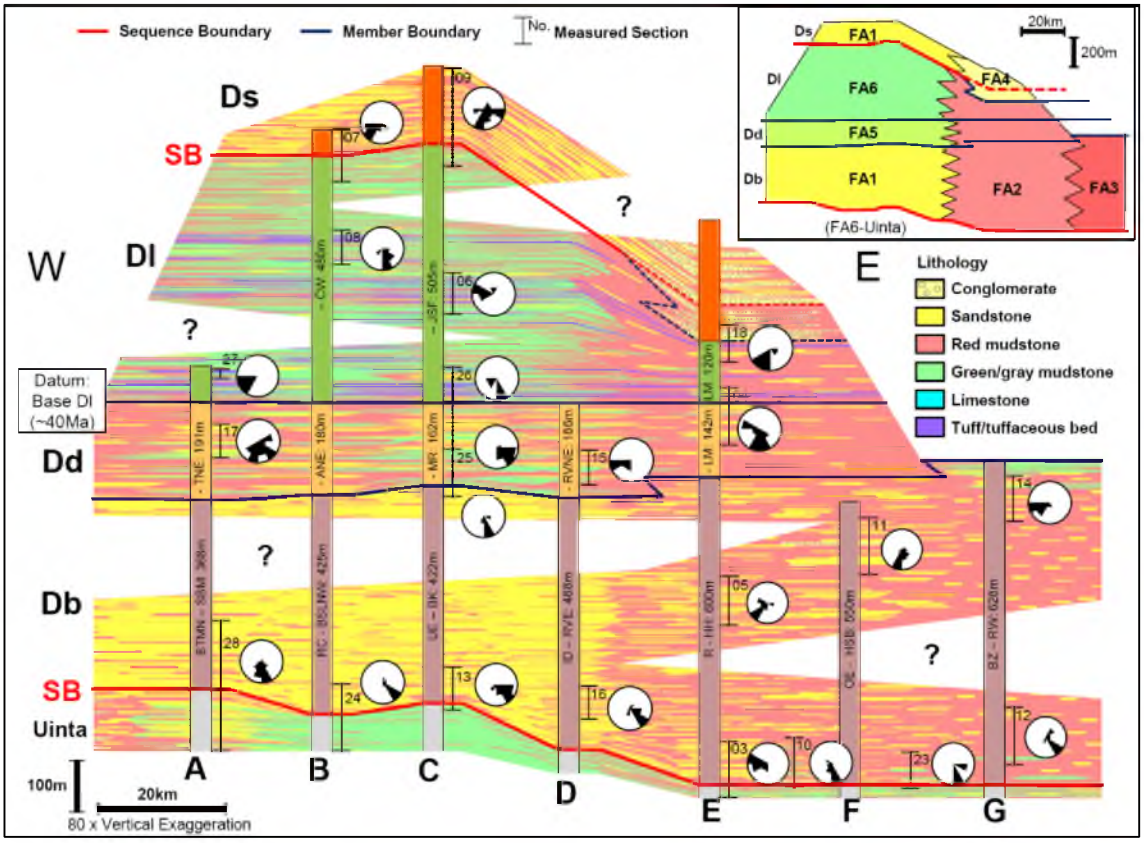

Figure 2.3. E-W regional correlations of composite sections A to G (location of cross section in Fig. 2.2). Paleocurrent data (magnetic declination: +11° used for corrections) at measured section locations (vertical bars with numbers) are shown as rose diagrams. The stratigraphic datum is set at the base of Dl (~40Ma). The thickness at each composite section is estimated by the modified geological map and structural dips. Lithology classifications represent the dominant or representative lithology and are generalized for this scale of correlation. Lithological interpretations between measured sections (detailed sections in the Appendix B) are somewhat schematic. The architecture of facies associations on this section is shown in the upper-right panel. Note that the significant contrast of facies (facies association) between the eastern and western portion. Abbreviation: BTMN; Blacktail Mountain North, SBM; Steamboat Mountain, TNE; Talmage NE, RC; Red Cap, BSLNW; Big Sand Lake NW, ANE; Altonah NE, CW; Cottonwood Wash, UE; Upalco E, BK; Bucher Knife, MR; Monarch Ridge, JSF; John Starr Flat, ID; Independence, RVE; Roosevelt E, RVNE; Roosevelt NE, R; Randlett, HH; Halfway Hollow, LM; Little Mountain, OE; Ouray E, HSB; Horseshoe Bend, BZ; Bonanza, RW: Red Wash.

counted as an individual grain component such as quartz and feldspar, even if this mineral forms a part of volcanic or sedimentary rock fragments. On the other hand, previous petrographic work by Andersen and Picard (1974) followed the classification of sandstone framework constituents of Folk (1968). However, there is no significant difference in the resultant compositions between the two approaches in sandstone samples of this study because rock fragments with such large (> 0.0625 mm) minerals/grains are quite minor and the majority of the fragments are composed of carbonates and cherts, as described in detail below.

In addition, QEMScan automated disaggregated counts (e.g., method described in Allen et al. 2012) were conducted for 20 sandstone samples to supplement the thin section data. Nine of the 20 samples were the same as those used for the above-mentioned thin section analysis (Appendix C), which were included to ensure the consistency of the results between the QEMSCan and petrographic point counting methods. Thus, 11 of 20 samples (10 samples from Db, 1 sample from Dl) are used to supplement or fill in gaps between thin section data points. The biggest advantage of QEMScan automated disaggregated count is to shorten the analytical time, although the duration depends on the resolution and the number of particles to be counted. The detailed procedure of the QEMScan automated disaggregated count is summarized in Appendix D.

2.5 Results and Interpretations

2.5.1 Basin-scale Facies Architectures

Chapter 1 of this thesis presented a detailed facies analysis and defined six facies associations, FA1 to FA6, in the Duchesne River Formation (Fig. 2.3, Table 2.1). Here, we present an abbreviated description of the Duchesne River members for presenting the context of depositional style and petrographic analysis.

2.5.1.1 Brennan Basin Member (Db)

The basal Brennan Basin Member (Db) of the Duchesne River Formation is characterized by channelized sandstones interbedded with red fine-grained rocks (Andersen

Table 2.1. Duchesne River Facies Associations

FA #	Facies Association	Member Occurrence	Facies Components			Trace Fossils				Ss/Ms Ratio	Apparent Sandbody Dimensions
			Lithology	Sedimentary Structure	Interpretation	Rare	Sparse	Common	Abundant		
FA 1	Amalgamated Braided Fluvial Channels	Db (western part of basin), Ds	Amalgamated channelized ss	Trough cross-stratified	Amalgamated multiple interweaving fluvial channels					75/25 (MS28)	> 1,000 m (MS28)
			Red ms/silty ms	Massive or mottled, usually in discontinuous/lenticular shape	Well-drained flood plain paleosol						
			Thin-layered ss and slts	Massive or trough cross-stratified (sometimes indistinct)	Overbank deposit, often pedogenically-altered						
FA 2	Extensive Flood Plain and Stacked Broad Fluvial Channels	Db, Dd and Dl (central-eastern part of basin)	Red ms/silty ms	Massive or mottled, usually in continuous shape	Well-drained flood plain paleosol					50/50 (MS33)	> 100 m (MS33)
			Yellow ms	Mottled, often relict bedding	Moderately-drained flood plain paleosol						
			Stacked broad channelized ss	Trough cross-stratified, occasionally lateral accretion	Braided and sinuous fluvial channels						
			Isolated and narrow channelized ss	Trough cross-stratified	Isolated small stream						
			Thin-layered ss and sits	Massive or trough cross-stratified (sometimes indistinct)	Overbank deposit, often pedogenically-altered						
FA 3	Extensive Flood Plain and Isolated Small Steams	Db (eastern part of basin)	Red ms/silty ms	Massive or mottled, usually in continuous shape	Well-drained flood plain paleosol					15/85 (MS14)	< 100 m (MS14)
			Yellow ms	Mottled, often relict bedding	Moderately-drained flood plain / levee paleosol						
			Isolated and narrow channelized ss	Trough cross-stratified	Isolated small stream						
			Thin-layered ss and slts	Massive or trough cross-stratified (sometimes indistinct)	Overbank deposit, often pedogenically-altered						
FA 4	Alluvial Fan Complex	All members (northern margin of basin)	Upward-fining package of cgl-ss	Structureless or imbrication (cgl), often trough cross-stratified (ss)	Alluvial fan channel/lobe					45/35/20 (cgl/ss/ms) (MS01)	n/a
			Red ms/silty ms	Massive or mottled	Well-drained flood plain (interchannel) paleosol						
			Green ms/silty ms	Mottled, thin-layered/veined gypsums, carbonaceous materials	Playa or wetland deposit in the distal fan						
FA 5	Dry and Wet Flood Plains and Fluvial Channels	Dd (western part of basin)	Red ms/silty ms	Mottled, usually in continuous shape	Well-drained flood plain paleosol					27/73 (MS15)	> 100 m (stacked fluvial channels), > 1,000m (deltaic ss)
			Green ms/silty ms	Mottled, thin-layered/veined gypsums, carbonaceous materials	Poorly-drained wetland or shallow lacustrine deposit						
			Stacked broad channelized ss	Trough cross-stratified, occasionally lateral accretion	Braided and sinuous fluvial channels						
			Tabularly and continuously bedded ss	Massive or wave rippled, carbonaceous materials	Marginal lacustrine deltaic deposit						
			Yellow ms	Mottled, often relict bedding	Moderately-drained flood plain / levee paleosol						
			Thin-layered ss and slts	Massive or trough cross-stratified (sometimes indistinct)	Overbank deposit, often pedogenically-altered						
FA 6	Extensive Lacustrine Deposits	Dl (western part of basin)	Green, gray, and dark gray ms	Massive or laminated	Lacustrine deposit					5/95 (MS06)	n/a
			Tuff and tuffaceous bed	Massive or trough cross-stratified	Ash fall and reworked deposit						
			Channelized ss	Trough cross-stratified	Relatively small and isolated fluvial channel						
			Tabularly bedded ss	Massive or wave rippled, carbonaceous materials	Marginal lacustrine deltaic deposit						
			Red and maroon ms	Massive, mottled or thin-layered	Well-drained paleosol						
			Ls	Fossiliferous	Lacustrine deposit						

Abbreviations: Cgl = Conglomerate, Ss = Sandstone, Slts = Siltstone, Ms = Mudstone, Ls = Limestone, FA = Facies Association, MS = Measured Section

and Picard 1972). It consists of three fluvial facies associations of FA1 (amalgamated braided fluvial channels), FA2 (extensive flood plain and stacked broad fluvial channels), and FA3 (extensive flood plain and isolated small steams) in the E-W cross section of Fig. 2.3 (see the detailed descriptions and interpretations of facies associations in Table 2.1). This member has relatively distinct contacts with the underlying Uinta Formation, particularly at several locations (e.g., MS13, MS24) in the mid-western part of the basin. In these locations, dominant green mudstones and conspicuous stromatolitic limestones of the Uinta Formation that clearly indicate a lacustrine environment are overlain by amalgamated channelized sandstones of Db (FA1). Thus, the base of Db marks a sequence boundary that represents an abrupt basinward shift of facies. This sequence boundary becomes gradually obscure to the west (MS28) where both Db and the Uinta Formation are dominated by sandstones, and to the east (MS03, MS10, and MS23) where both Db and the Uinta Formation are dominated by mudstones (Fig. 2.3). This sequence boundary forms an angular unconformity in the northern margin of the basin, where Db overlies the older rocks (Anderson and Picard 1972), and clearly marks the uplift of Uinta Mountains at the beginning of deposition of the Duchesne River Formation.

There is a significant contrast in fluvial styles between the west and east in this basal member (Fig. 2.3). The west is characterized by FA1 of a braided river system with a high net-sandstone-to-gross-thickness ratio (NTG), while the east has FA2 and FA3 of a braided, meandering and isolated river system with a low NTG. Correspondingly, there is a change in the total thickness of Db between the east and west; the western part of the basin is a few hundred meters thinner than the east (Fig. 2.3). This thickness change indicates the western part of the basin had repetitive channel cut-and-fills resulting in less aggradation, while the east had more stable aggradation.

2.5.1.2 Dry Gulch Creek Member (Dd)

The second Dry Gulch Creek Member (Dd) of the Duchesne River Formation is characterized by red and green/gray fine-grained rocks with interbedded sandstones (Andersen and Picard 1972). It consists of two fluvial-lacustrine facies associations of FA5 (dry and wet

flood plains and fluvial channels) and FA2 in the E-W cross section of Fig. 2.3 (detailed descriptions and interpretations of facies associations in Table 2.1). This member has a conformable contact with the underlying Db, and the basal beds interfinger upsection to the east of Roosevelt (Bryant 1989) (Fig. 2.3). The contacts are nearly isochronous to the west of MS15 near Roosevelt as the basal green/gray mudstones are widely traceable. Although there is a significant contrast in fluvial-lacustrine styles between the west (FA5) and east (FA2) in this second member, the basin-wide thickness change is subtle for this member, compared with the underlying Db and overlying Dl (Fig. 2.3).

2.5.1.3 Lapoint Member (Dl)

The third Lapoint Member (Dl) of the Duchesne River Formation is characterized by dominant green/gray mudstones and minor red fine-grained and coarse-grained rocks (Andersen and Picard 1972). It consists of two fluvial-lacustrine facies associations of FA6 (extensive lacustrine deposits) and FA2 in the E-W cross section of Fig. 2.3 (detailed descriptions and interpretations of facies associations in Table 2.1). The basal contacts are characterized by the near isochronous occurrence of tuff/tuffaceous beds (K-Ar ages of ~40 Ma reported by several researchers as mentioned above) and therefore, the base of this member is used for a time-marker/datum for regional correlations (Fig. 2.3). There is a significant contrast in fluvial-lacustrine styles between the west (FA6) and east (FA2) in this third member. Correspondingly, there is a huge basin-wide thickness change recognized in this member (the west is several hundred meters thicker than the east). The thickness change was likely caused by a differential subsidence during the deposition of Dl, as an extensive and thick lacustrine facies in the west indicates accommodation space was created at higher rates than in the east.

2.5.1.4 Starr Flat Member (Ds)

The uppermost Starr Flat Member (Ds) of the Duchesne River Formation is characterized by dominant conglomerates and sandstones with lesser amounts of fine-grained rocks (Andersen and Picard 1972). It consists of two fluvial facies associations of FA1 and FA4

in the E-W cross section of Fig. 2.3. The basal contacts are sharp at its type locality (MS09 John Starr Flat), where amalgamated channelized sandstones of FA1 overlie green/gray mudstones (FA6) of Dl, indicating an abrupt basinward shift of facies (i.e., sequence boundary). In some other areas, unconformable relationships have been reported (Rowley et al. 1985; Bryant et al. 1989) where conglomeratic facies of Ds overlie mudstone-dominated Dl or older deposits. This member has patchy distributions in the northern margin of the basin, and is sometimes hard to distinguish confidently from the overlying Oligocene Bishop conglomerates.

2.5.2 Sandstone Compositions and Provenances

This section focuses on the sandstone compositions and textures of the fluvial-dominated basal member (Db) in order to understand provenances and drainage systems/patterns. As described in the previous section, Db has significant differences in fluvial styles and net-sandstone-to-gross-thickness ratio (NTG): high NTG in the western part and low NTG in the eastern part of the basin as shown in Fig. 2.4. The sandstone compositions and textures in combination with paleocurrent data provide clues for deciphering mechanisms of these contrasting facies architectures.

2.5.2.1 Sandstone Compositions

Sandstones of the Duchesne River Formation are quartzose, sublithic, and lithic (Folk 1968 classification) (Fig. 2.5a), indicating feldspar is a very minor component of sandstones over the basin. In a QFL diagram with field dimensions (Dickinson et al. 1983), sandstones are mostly plotted in the petrofacies area of recycled orogenic (Fig. 2.5b). The breakdown of lithic grains from sublithic and lithic sandstones is shown in Figure 2.5c. Although the data in the plots are very scattered, carbonate grains are the most common and clastics are relatively minor.

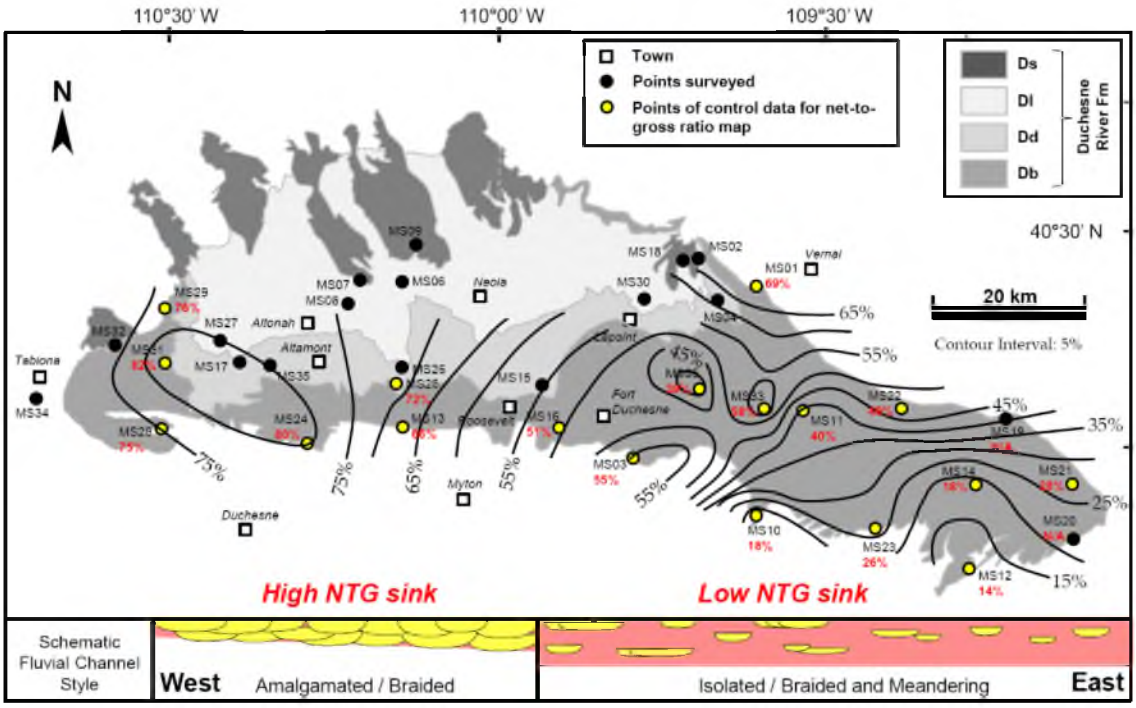

Figure 2.4. Net-sandstone-to-gross-thickness ratio (NTG) map and schematic fluvial styles of Db. Points of control data for NTG map are highlighted by yellow circles (accompanied with red text numbers of NTG used for contouring). The western part of the basin (from Tabiona to Roosevelt) exhibits a high net-to-gross ratio (over 60%), whereas the eastern part of the basin (Roosevelt to the eastern margin of Db distribution) shows a gradual decrease in NTG (60 to 14%).

2.5.2.2 Regional Trends and Provenances

In order to examine the geographical difference of sandstone compositions, a cross plot of longitude versus percent rock fragments of grains was created and juxtaposed along with a paleocurrent map (Fig. 2.6). Paleocurrents of the Duchesne River Formation indicate overall southerly sediment transport from the Uinta Mountains, as noticed by Andersen and Picard (1974). However, by closely looking at flow patterns of the basal member, the western part of the basin shows more eastward and southeastward flows. In contrast, the central-eastern and eastern parts of the basin have respectively south-southwestward flows and randomly directed flows. The plot of percent rock fragments indicates relative richness of quartz grains because feldspar is a minor component for all sandstones. Newly acquired data on this plot (Fig. 2.6) show the richness in rock fragments in the east (6-37%) relative to the west (1-7%).

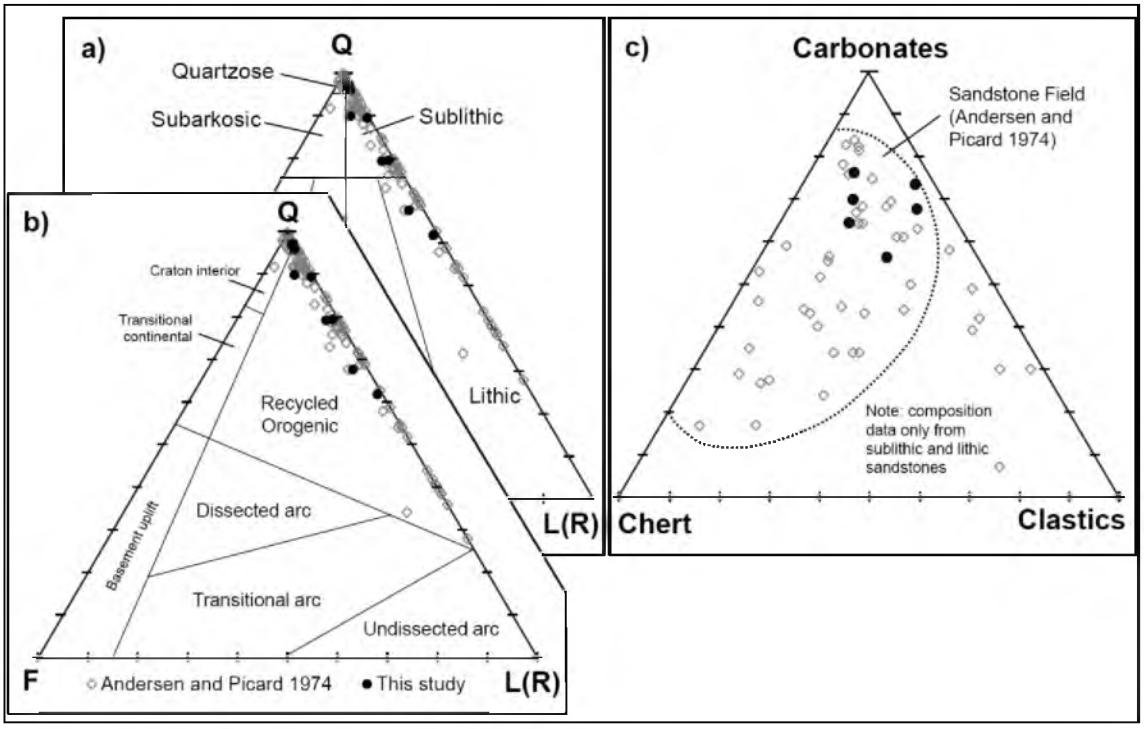

Figure 2.5. Ternary QFL(R) plots showing sandstone compositions of the Duchesne River Formation (data from Andersen and Picard (1974) and this study). Plots a) Folk's (1968) classification and b) Dickinson et al. (1983) classification indicates that feldspar is a very minor component of sandstones over the basin. Plot c) shows the breakdown of lithic grains that indicates that carbonate grains are the most common and clastics are relatively minor.

Thin section petrography, which provides visual information on sandstone textures and properties (i.e., porosity), also supports a distinct compositional difference between the eastern and western portions of the basin. The sandstones from the west (samples 1, 2, and 4) are richer in quartz (over 90% of total normalized grains), more porous (point count porosities ranging from 14.7% to 17.6%), and less matrix and/or cement materials (1.9% to 5.3% of total counts) than those from the east (samples 5, 6, 7, 8, and 9) (Fig. 2.7). It is likely that lithic-sublithic sandstones of the eastern part of the basin have lower porosity (6.1% to 12.3%) and a higher percentage of matrix and/or cement materials (10.4% to 25.0%), because some lithic grains were deformed or dissolved and migrated or precipitated into the original pore space during diagenesis. Compositionally mature quartz-rich sandstones in the west were favorable to keep the original pore space from destructions by cementations or grain deformations.

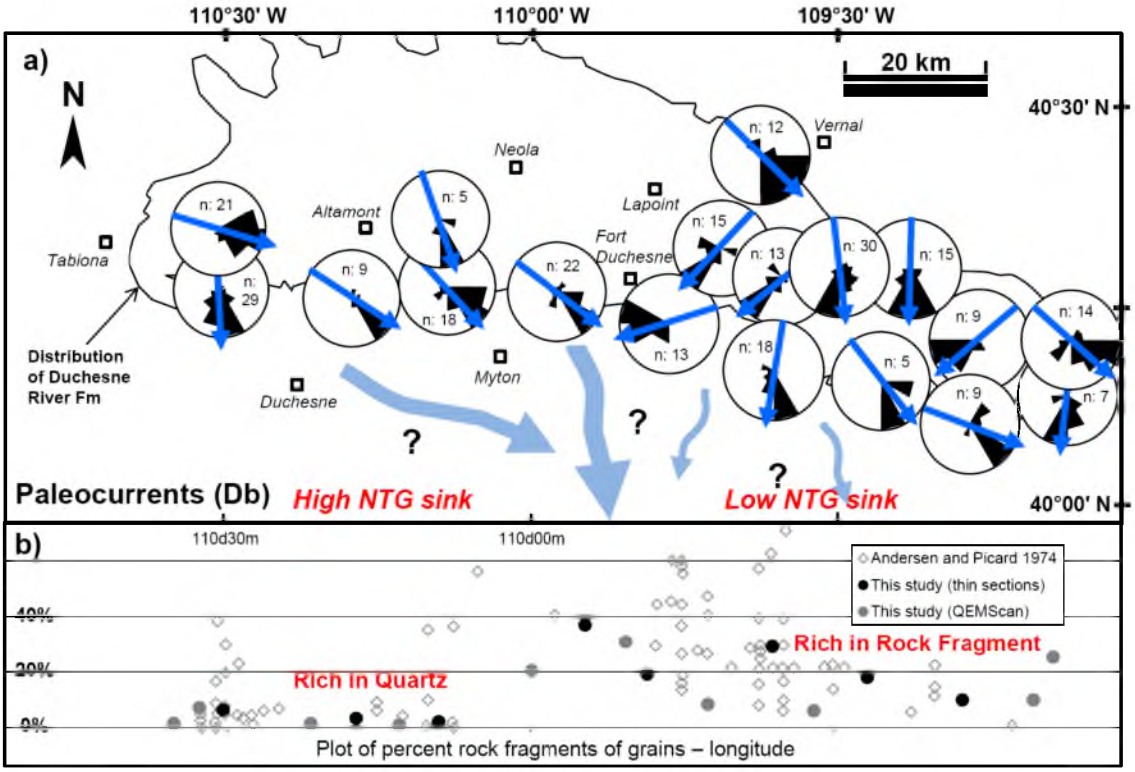

Figure 2.6. Paleocurrent data from Db (plot a) and longitude versus percent rock fragments of grains (plot b). a) Paleocurrents basically show overall southerly transports from the Uinta Mountains. Nevertheless, by closely looking at flow patterns, the western part of the basin shows more eastward and southeastward flows, whereas the eastern part of the basin has respectively south-southwestward or randomly directed flows. Correspondingly, the plot of percent rock fragments (i.e., indication of relative richness of quartz grain because feldspar is a minor component for all sandstones) shows the relative richness in quartz in the west and richness in rock fragments in the east.

Focusing on sandstone samples in the western part of the basin, samples 2 (MS24) and 4 (MS13) are remarkably better-sorted, more porous, and richer in quartz than sample 1 (MS28), which was taken from the western margin of the Db distribution (Fig. 2.7). This trend suggests MS28 was located in the upstream part, and MS24 and MS13, which contain more texturally and compositionally mature sediments, were located in the downstream part of the high NTG braided river system in the western part of the basin. Collectively, in combination with paleocurrent data, these texturally matured and porous sandstones in the central-eastern part of the basin are interpreted to reflect a long transport distance from the source terrains of the Uinta Mountains to the north and probably the Sevier FTB to the west.

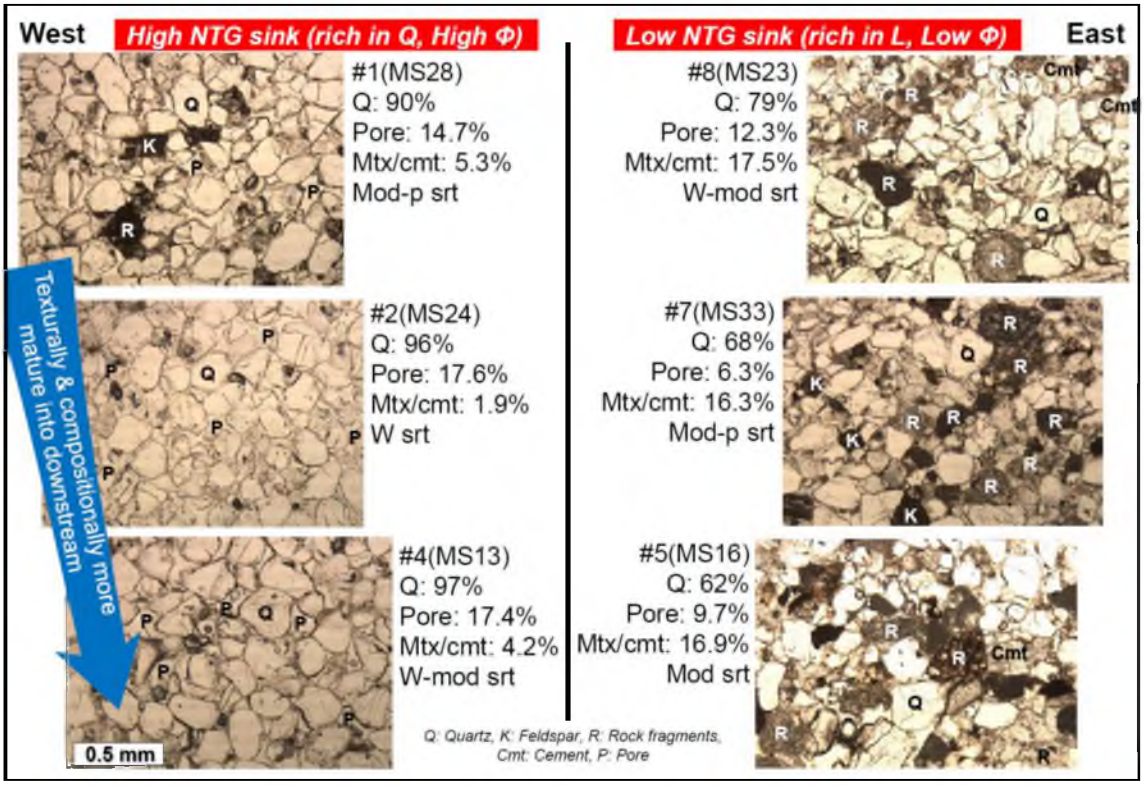

Figure 2.7. Thin section petrography of sandstone samples from Db. Note there are distinct compositional and porosity differences between the east (rich in rock fragments, lower porosity) and west (rich in quartz, higher porosity). A trend observed in sample 1 (moderately-sorted sandstone with 90% of quartz) to 4 (well- to moderately-sorted sandstone with 97% of quartz) indicates sandstones become texturally more mature downstream. All thin section figures are in the same scale.

2.6 Synthesis

2.6.1 Source-to-Sink Fluvial Systems and Controlling Factors

This section synthesizes a source-to-sink fluvial system, a basin-scale facies change, and controlling factors for member Db (Fig. 2.8), building upon the previous sections of the sediment provenances, flow directions, and patterns of the basin. The basal unconformity (i.e., sequence boundary) clearly indicates uplift in the source terrain(s) of the Uinta Mountains and possibly the Sevier FTB at the same time. This suggests that the tectonic event had a primary influence on the following three major controlling factors affecting the contrasting basinal facies of Db (i.e., the high NTG system with high-quality reservoirs in the western sink and the lower NTG system with low-quality reservoirs in the eastern sink).

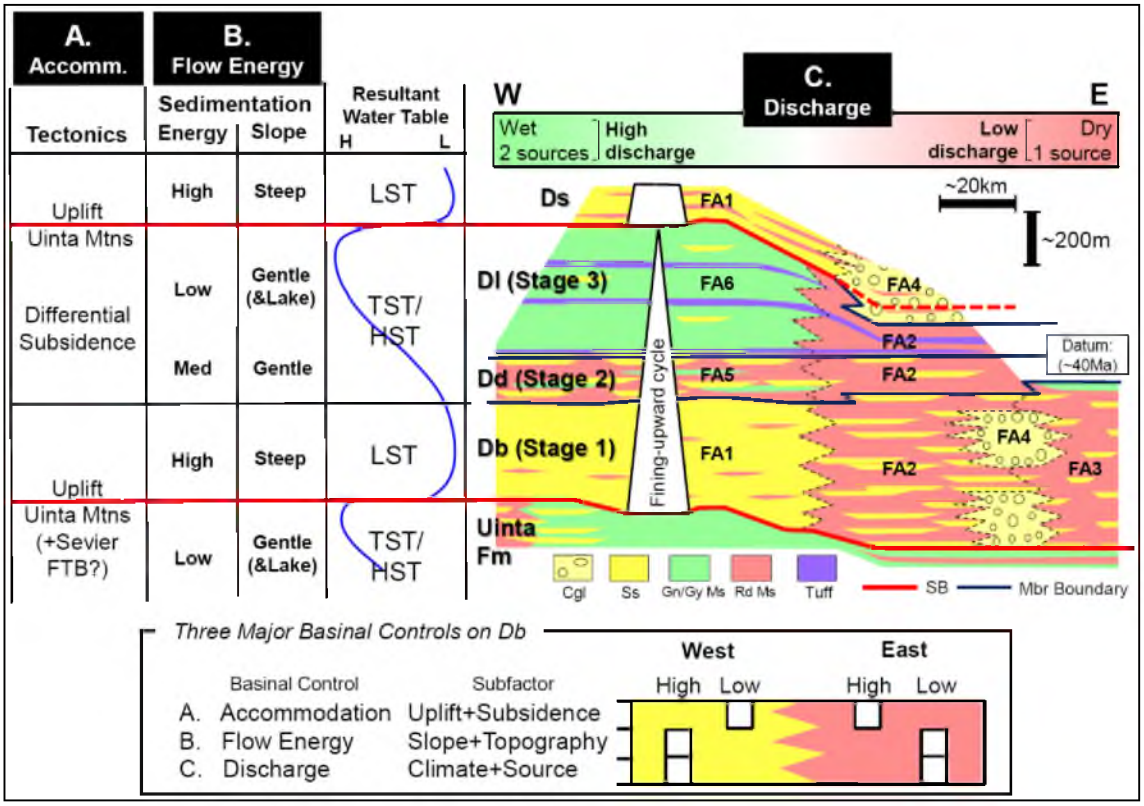

Figure 2.8. Sequence stratigraphic framework of the Duchesne River Formation and controlling factors. A tectonic event (uplift in the Uinta Mountains) had a primary influence on three major controlling factors of the basinal facies and sequence of the Duchesne River Formation: A) accommodation control, B) flow energy control, and C) discharge control. Specifically, the high NTG amalgamated braided river system in the western portion of Db resulted from high discharge (by wet climate and multiple source terrains), high flow energy (by steep slope with possibly confined river system along E-W basin axis), and relatively slow aggradation. On the other hand, the lower NTG braided, meandering, and isolated small river system in the eastern part of the basin resulted from lower discharge (by dry climate and single source terrain), low flow energy (by relatively gentle slope and unconfined river system), and relatively high aggradation.

2.6.1.2 Accommodation

Accommodation, which is related to a graded equilibrium profile in the fluvial environments, is largely controlled by tectonic uplift and subsidence. The accommodation space also controls stacking patterns of sediments. The basin-scale thickness change of Db indicates the relatively slow aggradation (repetitive cut-and-fill patterns of fluvial channels) in the western sink and high aggradation in the eastern sink (Fig. 2.8).

2.6.1.2 Flow Energy

Flow energy, which is related to a local topography and gradient/slope, controls a fluvial style. The amalgamated braided river system in the western part of the basin indicates high flow energy due to a steep slope with a confined river system along the E-W basin axis. This axial drainage system with long sediment transportation is important for development of texturally and compositionally mature (quart-rich) and high-quality (porous) sandstones in the sink. In contrast, relatively sinuous and isolated river system in the eastern part of the basin indicates low flow energy due to a relatively gentle slope with an unconfined river system, resulting in texturally and compositionally immature (abundant rock fragments) and low-quality sandstones in the sink (Fig. 2.8).

2.6.1.3 Discharge

Discharge, which is related to the local source climate and the number of source terrains, also controls a fluvial style. The high NTG fluvial system in the west indicates high discharge attributed to a wet climate and multiple source terrains, whereas the low NTG fluvial system in the east indicates low discharge due to a dry climate and a single source terrain (Fig. 2.9). It should be noted that a climatic contrast is observed even in the modern present-day Uinta Basin and surrounding ranges (Fig. 2.10): a wetter climate and higher precipitation in the western area and a drier climate and lower precipitation in the eastern area (Greer 1981; Jensen et al. 1990; Gillies and Ramsey 2009). Although the modern Green River flowing across the eastern Uinta Mountains gives a significant amount of discharge into the eastern dry Uinta Basin at present (Fig. 2.1), this large drainage system opened in the late Miocene or early Pliocene time (Hansen 1986) and did not exist in the Late Eocene.

2.6.2 Fluvial Sandstone Reservoir Exploration

Typical lacustrine basin-fill exhibits an upward-coarsening sequence from deep lacustrine, to deltaic and fluvial at the top. It is an ideal stratigraphic succession for a petroleum system because potential lacustrine source rocks are overlain by fluvial-deltaic sandstone

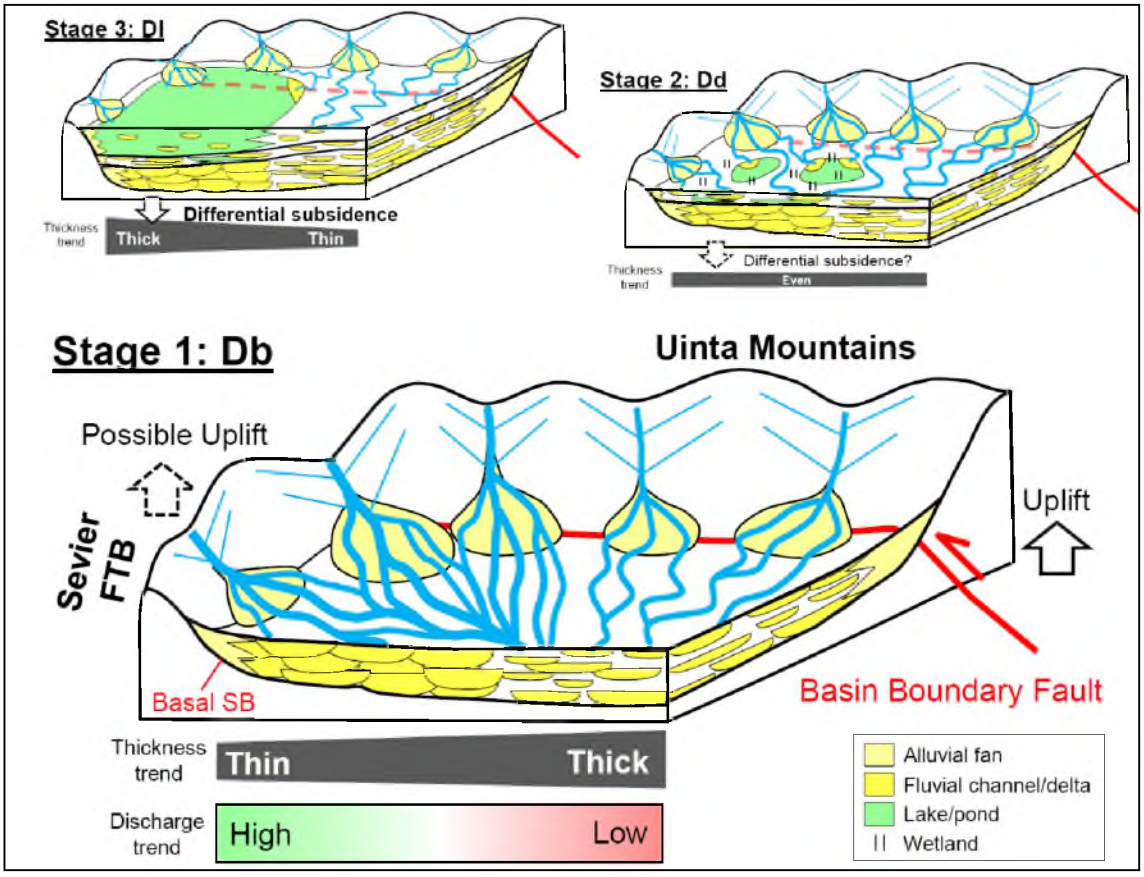

Figure 2.9. The tectonic-driven sequence stratigraphy with three-stages for the Duchesne River upward-fining sequence. Stage 1 (Db) marks high energy sedimentation on a steep slope after uplift(s) in the Uinta and possibly Sevier FTB. The high NTG braided river system in the west mainly reflects high discharge from two source terrains.

reservoirs, which could trap hydrocarbons from below. This type of petroleum system (i.e., lacustrine source rocks overlain by fluvial-deltaic reservoirs) is proven and common in global lacustrine basins, such as the Cretaceous rift basins in Sudan (Schull 1988), the Pre-salt rift basins of the West African Atlantic margin (Beglinger et al. 2012), and the Oligocene strata in the Indonesia Natuna Sea (Phillips et al. 1997).

In the Uinta Basin, the Duchesne River Formation also contains a significant amount of hydrocarbons (as tar sands) from the underlying lacustrine Green River shales. The significance of the Duchesne River Formation is that it is widely exposed and thus potential fluvial reservoir facies can be described and traced directly. The Duchesne River example exhibits the

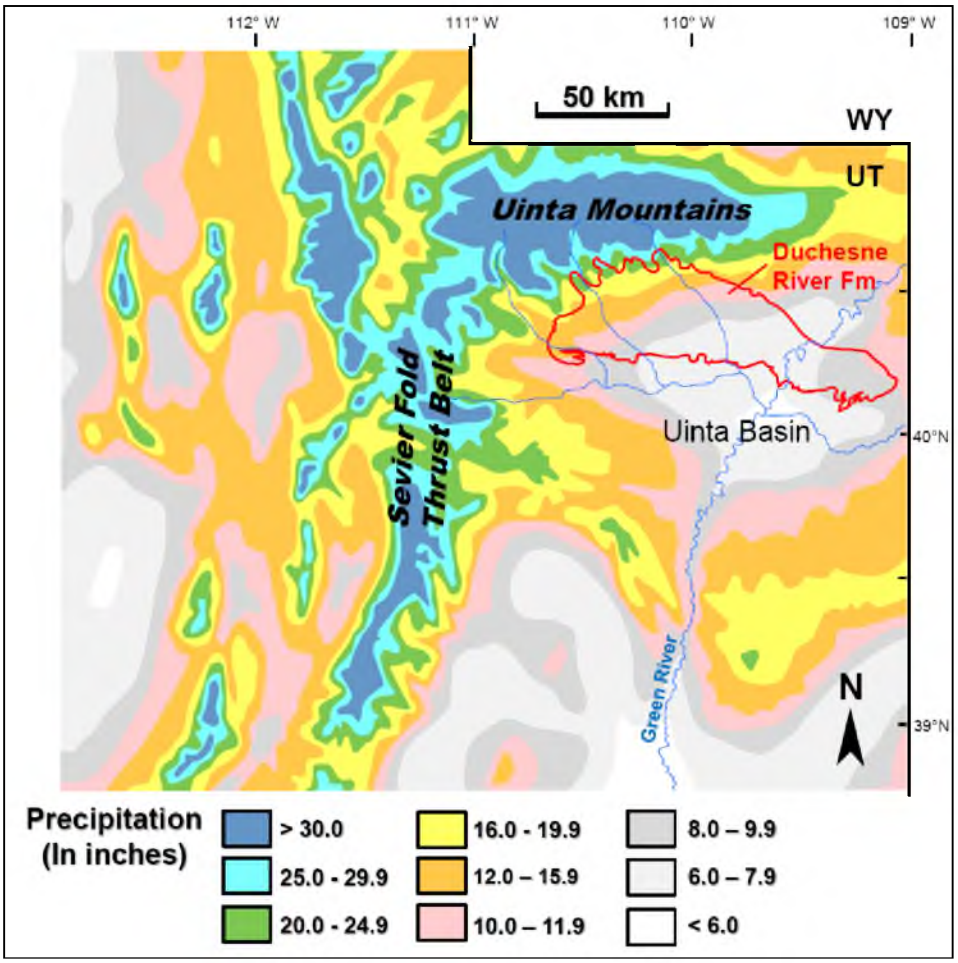

Figure 2.10. Modern precipitation in and around the Uinta Basin (modified after Greer et al. 1981). Note that a wetter climate and higher precipitation exist in the western part of the basin and adjacent mountain ranges (Uinta Mountains to the north and Sevier FTB to the west) and a drier climate and lower precipitation exist in the eastern part of the basin. This modern example implies local source tectonics have a great influence on discharge and fluvial systems in the basinal area.

importance of tectonics, location, and climate of sediment source terrains when trying to understand the distribution and amount of sandstone reservoirs in a sink. Specifically, the best sandstone reservoirs in terms of quantity and quality (porosity) are found in the central-western part of Db (around MS13 and MS24) where texturally and compositionally mature (quartz-rich), amalgamated braided channel sandstones developed due to: 1) high discharge from two wet source terrains; 2) high flow energy caused by a steep slope; 3) a lower aggradation rate (removal of fine-grained sediment by repetitive erosions); and 4) long sediment transportation

along the basin axis (i.e., an axial drainage system).

2.7 Conclusions

The combined approaches of outcrop-based stratigraphic correlations, paleocurrent analysis, and petrographic studies provided a detailed mechanism of a source-to-sink fluvial system of the widely exposed Tertiary Duchesne River basal member. This is a valuable analog example for the exploration of the fluvial reservoir system in the late-stage lacustrine basin fills as summarized below.

- Extensive outcrop data reveal a detailed basin-scale facies architecture, which shows significant differences in depositional facies within each Duchesne River member. In particular, the basal member shows a high net-to-gross braided river system in the western and a low net-to-gross braided, meandering, and isolated small river system in the eastern portion of the basin.
- Paleocurrents of the basal Brennan Basin Member (Db) shows dominant southeastward flows in the western part of the basin and south-southwestward or randomly directed flows in the eastern part of the basin. Correspondingly, there is a distinct difference in sandstone composition and texture/fabric between the east and west. Specifically, sandstones from the western part of the basin are richer in quartz (over 90% of total normalized grains) and more porous (point count porosities ranging from 14.7% to 17.6%) than those from the eastern portion. The texturally and compositionally mature sandstones in the western part of the basin indicate a long transport along the E-W basin axis derived from the multiple source terrains of the Uinta Mountains to the north and the Sevier FTB to the west.
- There are likely three major controls on the facies variations of the basal member: 1) accommodation, 2) flow energy, and 3) discharge. Especially, the high discharge river system, which was caused by a wetter climate and two source terrains in the western part of the basin, greatly contributed to development of a large-volume (more concentrated) and high-quality (porous) sandstone reservoir system in the western sink.

2.8 References

Allen, J.L., Johnson, C.L., Heumann, M.J., Gooley J., and Gallin, W., 2012, New technology and methodology for assessing sandstone composition: A preliminary case study using a quantitative electron microscope scanner (QEMScan): Geological Society of America Special Publication 487, p. 177-194.

Andersen, D.W., and Picard, M.D., 1972, Stratigraphy of the Duchesne River Formation (Eocene-Oligocene?), northern Uinta basin, northeastern Utah: Utah Geological and Mineral Survey Bulletin 97, 29 p.

Andersen, D.W., and Picard, M.D., I974, Evolution of synorogenic clastic deposits in the intermontane Uinta Basin of Utah, *in* Dickinson, W.R., editor, Tectonics and Sedimentation: SEPM Special Publication 22, p. 167-189.

Beglinger S.E., Doust, H., and Cloetingh, S., 2012, Relating petroleum system and play development to basin evolution; West African South Atlantic basins: Marine and Petroleum Geology, v. 30, p. 1-25.

Blackett, R.E., 1996, Tar-sand resources of the Uinta Basin, Utah (a catalog of deposits): Utah Geological Survey Open-File Report 335, 122 p.

Boden, T., and Tripp, B.T, 2012, Gilsonite veins of the Uinta Basin, Utah: Utah Geological Survey Special Study 141, 50 p.

Bruhn, R.L., Picard, M.D., and Beck, S.L., 1983, Mesozoic and early Tertiary structure and sedimentology of the central Wasatch Mountains, Uinta Mountains, and Uinta Basin: Utah Geological and Mineralogical Survey Special Studies 59, Salt Lake City, p. 63–105.

Bruhn, R.L., Picard, M.D., and Isby, J.S., 1986, Tectonics and sedimentation of Uinta arch, western Uinta Mountains and Uinta Basin, *in* Peterson. J.A., editor, Paleotectonics and sedimentation in Rocky Mountain region, United States: American Association of Petroleum Geologists Memoir 41, p. 333-352.

Bryant, B., 1992, Geologic and structure maps of the Salt Lake City 1°x 2° quadrangle, Utah and Wyoming: U.S. Geological Survey Miscellaneous Investigations Series Map I-1997.

Bryant, B., Naeser, C.W., Marvin, R.F., and Mehnert, H.H., 1989, Upper Cretaceous and Paleogene sedimentary rocks and isotopic ages of Paleogene tuffs, Uinta Basin, Utah: U.S. Geological Survey Bulletin 1787-J, 22 p.

Campbell, J.A., and Ritzma, H.R., 1979, Geology and petroleum resources of the major oil-impregnated sandstone deposits of Utah: Utah Geological and Mineral Survey Special Studies 50, 24 p.

Cashion, W.B., 1964, The distribution and quality of oil shale in the Green River Formation of the Uinta Basin, Utah-Colorado: U.S. Geological Survey Professional Paper 501-D, p. D86-D89.

Cashion, W.B., 1967, Geology and fuel resources of the Green River Formation, southeastern Uinta Basin, Utah and Colorado: U.S. Geological Survey Professional Paper 548, 48 p.

Covington, R.E., 1957, The bituminous sandstones of the Asphalt Ridge area, northeastern

Utah, *in* Seal, O.G., editor, Guidebook to the geology of the Uinta Basin: Intermountain Association of Petroleum, p. 172-175.

Covington, R.E., 1963, Bituminous sandstone and limestone deposits of Utah, *in* Crawford, A.L., editor, Oil and gas possibilities of Utah, re-evaluated: Utah Geological and Mineralogical Survey Bulletin 54, p. 225-247.

Covington, R.E., 1964, Bituminous sandstones in the Uinta Basin, *in* Sabatka, E.F., editor, Guidebook to the geology and mineral resources of the Uinta Basin-Utah's hydrocarbon storehouse: Intermountain Association of Petroleum Geologists, p. 227-242.

Dickinson, W.R., 1970, Interpreting detrital modes of graywacke and arkose: Journal of Sedimentary Petrology, v. 40, p. 695-707.

Dickinson, W.R., Beard, L.S., Brakenridge, G.R., Erjavec, J.L., Ferguson, R.C., Inman, K.F., Knepp, R.A., Lindberg, F.A., and Ryberg, P.T., 1983, Provenance of North American Phanerozoic sandstones in relation to tectonic setting: Geological Society of America Bulletin, v. 94, p. 222-235.

Dickinson, W.R., Klute, M.A., Hayes, M.J., Janecke, S.U., Lundin, E.R., McKittrick, M.A., and Olivares, M.D., 1988, Paleogeographic and paleotectonic setting of Laramide sedimentary basins in the central Rocky Mountain region: Geological Society of America Bulletin, v.100, p. 1023-1039.

Dickinson, W.R., Lawton, T.F., and Inman, K.F., 1986, Sandstone detrital modes, central Utah foreland region: Stratigraphic record of Cretaceous–Paleogene tectonic evolution: Journal of Sedimentary Petrology, v. 56, p. 276–293.

Fouch, T.D., 1975, Lithofacies and related hydrocarbon accumulations in Tertiary strata of the western and central Uinta Basin, Utah, *in* Bolyard, D.W., editor, Deep drilling frontiers of the central Rocky Mountains: Rocky Mountain Association of Geologists Symposium, Denver, Colorado, p. 163–173.

Folk, R.L., 1968, Petrology of sedimentary rocks: Hemphills's, Austin, 170 p.

Gazzi, P., 1966, Le arenarie del flysch sopracretaceo dell'Appennino modenese; correlazioni con il flysch di Monghidoro: Mineraologica e Petrografica Acta, v. 12, p. 69–97.

Gillies, R.R., and Ramsey, R.D., 2009, Climate of Utah, *in* Banner, R.E., Baldwin, B.D., and McGinty, E.L., editors, Rangeland Resources of Utah (revised): Utah State University, Cooperative Extension Service, p. 39-45.

Greer, D.C., Director, 1981, Atlas of Utah: Provo, Utah, Brigham Young University Press, 300 p.

Hansen, W.R., 1986, Neogene tectonics and geomorphology of the eastern Uinta Mountains in Utah, Colorado, and Wyoming: U.S. Geological Survey Professional Paper 1356, 78 p.

Hatcher, H.J., Meuzelaar, H.L.C., and Urban, D.T., 1992, A comparison of biomarkers in gilsonite, oil shale, tar sand, and petroleum from Threemile Canyon and adjacent areas in the Uinta Basin, Utah, *in* Fouch, T.D., Nuccio, V.F., and Chidsey, T.C., Jr., editors, Hydrocarbon and mineral resources of the Uinta Basin, Utah and Colorado: Utah Geological Association Guidebook 20, p. 271-288.

Hintze, L.F, Willis, G.C., Laes, D.Y.M., Sprinkel, D.A., and Brown, K.D., 2000, Digital geologic map of Utah 1:500000: Utah Geological Survey.

Ingersoll, R.V., Bullard, T.F., Ford, R.L., Grimm, J.P., Pickle, J.D., and Sares, S.W., 1984, The effects of grain size on detrital modes: A test of the Gazzi-Dickinson point-counting method: Journal of Sedimentary Petrology, v. 54, p. 103-116.

Jensen, D.T., Bingham, G.E., Ashcroft, G.L., Malek, E., McCurdy G.D., and McDougal, W.K., 1990, Precipitation pattern analysis Uinta Basin-Wasatch Front, Report to Division of Water Resources, State of Utah under Contract Number 90-3078: Office of the State Climatologist, Utah State University, Logan, Utah, 41 p.

Kayser, R.B., 1966, Bituminous sandstone deposits Asphalt Ridge: Utah Geological and Mineralogical Survey Special Studies 19, 62 p.

Kelly, T.S., Murphey, P.C., and Walsh, S.L., 2012, New records of small mammals from the middle Eocene Duchesne River Formation, Utah, and their implications for the Uintan-Duchesnean North American Land Mammal Age transition; Paludicola, v. 8, p. 208-251.

Lambiase, J.J., 1990, A model for tectonic control of lacustrine stratigraphic sequences in continental rift basins, *in* Katz, B.J., editor, Lacustrine Basin Exploration—Case Studies and Modern Analogs: American Association of Petroleum Geologists Memoir 50, p. 265–276.

McDowell, F.W., Wilson, J.A., and Clark, J., 1973, K-Ar dates for biotite from two paleontologically significant localities: Duchesne River Formation, Utah, and Chadron Formation, South Dakota: Isochron/West, v. 7, p. 11-12.

Phillips, S., Little, L., Michael, E., and Odell, V., 1997, Sequence stratigraphy of Tertiary petroleum systems in the West Natuna Basin: Indonesian Petroleum Association, Petroleum Systems of SE Asia and Australasia, Conference Proceedings, p. 381–390.

Picard, M.D., and High, L.R., 1972, Criteria for recognizing lacustrine rocks, *in* Rigby, J.K., and Hamblin, W.K., editors, Recognition of ancient sedimentary environments: SEPM Special Publication 16, p. 108-145.

Prothero, D.R. and Swisher, C.C., 1992, Magnetostratigraphy and geochronology of the terrestrial Eocene-Oligocene transition in North America, *in* Prothero, D.R., and Berggren, W.A., editors, Eocene-Oligocene climatic and biotic evolution: Princeton University Press, p. 46-74.

Ritzma, H.R., 1979, Oil-impregnated rock deposits of Utah: Utah Geological and Mineral Survey Map 47, 2 p.

Rowley, P.D., Hansen, W.R., Tweto, O., and Carrara, P.E., 1985, Geologic map of the Vernal 1ø x 2ø quadrangle, Colorado, Utah, and Wyoming: U.S. Geological Survey Miscellaneous Investigations Series I-1526.

Schull, T.J., 1988, Rift basins of interior Sudan: Petroleum exploration and discovery: American Association of Petroleum Geologists Bulletin, v. 72, p. 1128-1142.

Spieker, E.M, 1931, Bituminous sandstone near Vernal, Utah: U.S. Geological Survey Bulletin

822, p. 77-100.

Sprinkel, D.A., 2006, Interim geologic map of the Dutch John 30' x 60' quadrangle, Daggett and Uintah Counties Utah, Moffat County, Colorado, and Sweetwater County, Wyoming: Utah Geological Survey

Sprinkel, D.A., 2007, Interim geologic map of the Vernal 30' x 60' quadrangle, Uintah and Duchesne Counties, Utah, and Moffat and Rio Blanco Counties, Colorado: Utah Geological Survey.

Thomas, K.P., Barbour, R.V, Guffey, F.D., and Dorrence, S.M., 1977, Analysis of high-molecular-weight hydrocarbons in a Utah tar sand and produced oils: Special Volume - Canadian Institute of Mining and Metallurgy 17, p. 168-174.

Vanden Berg, M.D., 2008, Basin-wide evaluation of the uppermost Green River Formation's oil-shale resource, Uinta Basin, Utah and Colorado: Utah Geological Survey Special Study 128.

Visher, G.S., 1965, Use of vertical profile in environmental reconstruction: American Association of Petroleum Geologists Bulletin, v. 49, p. 41-61.

Wilson, J.A., 1978, Stratigraphic occurrence and correlation of early Tertiary vertebrate faunas, Trans-Pecos Texas; Part 1, Vieja area: Bulletin of the Texas Memorial Museum, v. 25, p. 1-42.

CHAPTER 3

TRACE FOSSILS AND FLUVIAL-LACUSTRINE ICHNOFACIES OF THE EOCENE UINTA AND DUCHESNE RIVER FORMATIONS, NORTHERN UINTA BASIN, UTAH

3.1 Abstract

Trace fossil assemblages in a fluvial-lacustrine sequence stratigraphy context hold significant potential for expanding our understanding of environmental controls and continental basin-fill history. The succession of the Eocene Uinta Formation and four members of the Duchesne River Formation is extremely well-exposed in the Uinta Basin of northeastern Utah, revealing a robust sequence stratigraphic framework to document broad-scale fluvial-lacustrine facies architectures and associated trace fossil assemblages. Dominant green/gray mudstones with interbedded tabular sandstones representing lacustrine environments contain trace fossils including ichnogenera *Arenicolites* and *Gordia* (=*Haplotichnus*). In contrast, dominant red mudstones with interbedded channelized sandstones representing upstream fluvial environments contain a variety of insect trace fossils including *Scoyenia, Ancorichnus*, and nest structures. Transitional, interfingering lithologies of wetland or shallow, short-lived lacustrine environments on the alluvial plain exhibit intermediate trace fossils including *Steinichnus*. Although there are many small-scale (bed-scale) physical structures and biogenic trace fossils of continental subenvironments, this study focuses on the large-scale (member scale) change in trace fossil assemblages, and this shows that the ichnofacies can corroborate continental sequence stratigraphic interpretations in a fluvial-lacustrine setting.

3.2 Introduction

The concept of ichnofacies, which was originally proposed by Seilacher (1967), has been refined or expanded by other workers over the last five decades (e.g., Frey and Pemberton 1984; Bromley and Asgaard 1993; Smith et al. 1993; Buatois and Mángano 1995; Genise et al. 2000; Ekdale et al. 2007; Genise et al. 2010). Initially, Seilacher (1967) proposed one continental ichnofacies that now has been expanded into six ichnofacies: *Scoyenia*, *Mermia*, *Corprinisphaera*, *Entradichnus, Termitichnus*, and *Celliforma* (Buatois and Mángano 2011) (Figs. 3.1 and 3.2). Additionally, the typical marine *Skolithos* ichnofacies is documented in coastal lacustrine environments (e.g., Buatois and Mángano 1995; Buatois and Mángano 2007). The collective works on marine ichnofacies concepts/models are useful for deciphering and reconstructing paleoenvironments through integrating sedimentological processes and paleontological or macrofossil data. However, there are far fewer studies of continental ichnofacies integrated with fluvial-lacustrine sedimentology and sequence stratigraphy context (Buatois and Mángano 2004, 2009).

The purpose of this study is to document the continental ichnology of a well-exposed fluvial-lacustrine depositional system of the uppermost Uinta and Duchesne River Formation of the northern Uinta Basin. Observed trace fossils, which are identified to the ichnogenus level, are placed in a sequence stratigraphic context, and vertical change in trace fossil assemblages or ichnofacies is discussed.

3.3 Geological Context

3.3.1 Geological Setting

The Uinta Basin is a prolific oil-producing basin located in northeastern Utah. It is a part of the Laramide lake basin system straddling Wyoming, Colorado, and Utah (Fig. 3.3), which emerged during the latest Cretaceous to early Paleogene (Dickinson et al. 1988). The Uinta Basin is surrounded by several hinterlands such as the Uinta Mountains to the north, Sevier Fold Thrust Belt (FTB) to the west, Douglas Creek arch to the east, and Uncompahgre uplift and San Rafael Swell to the south. The basin shows an asymmetric basin shape northerly bounded

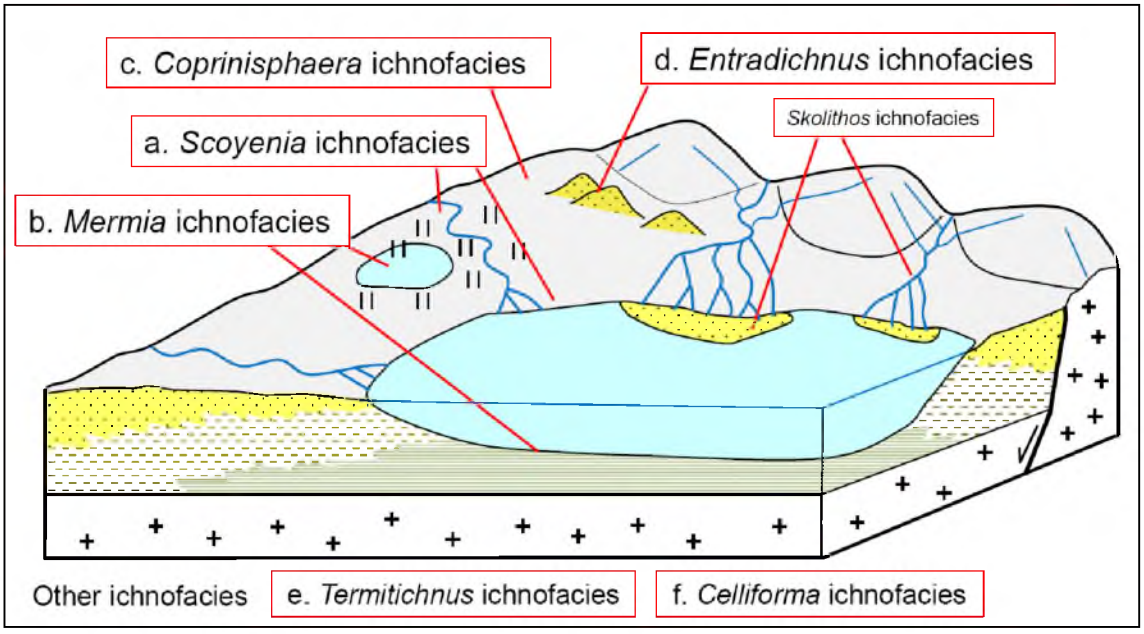

Figure 3.1. Six continental ichnofacies (a to f) and marginal lacustrine *Skolithos* ichnofacies in a continental depositional setting (modified from Buatois and Mángano 2007).

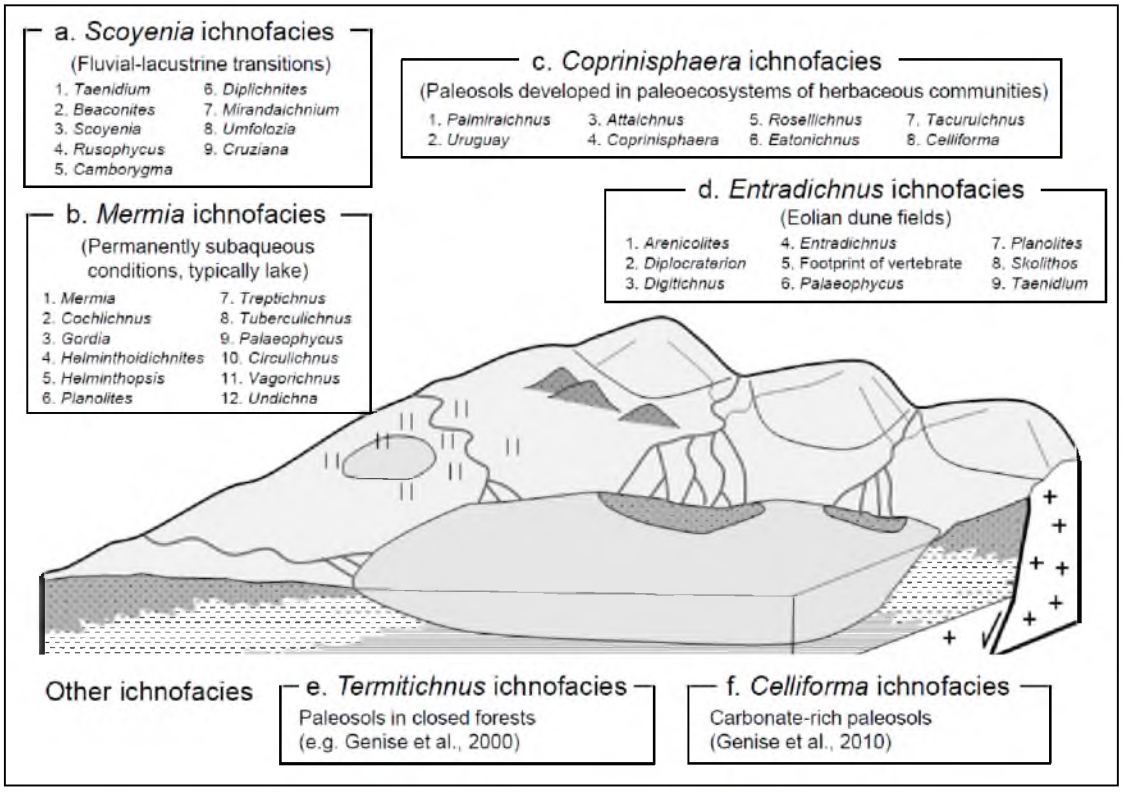

Figure 3.2. Trace fossil (ichnongenus) compositions of continental ichnofacies models. a) *Scoyenia* ichnofacies (data from Buatois and Mángano 2007), b) *Mermia* ichnofacies (data from Buatois and Mángano 2007), c) *Coprinisphaera* ichnofacies (data from Buatois and Mángano 2007) and d) *Entradichnus* ichnofacies (data from Ekdale et al. 2007).

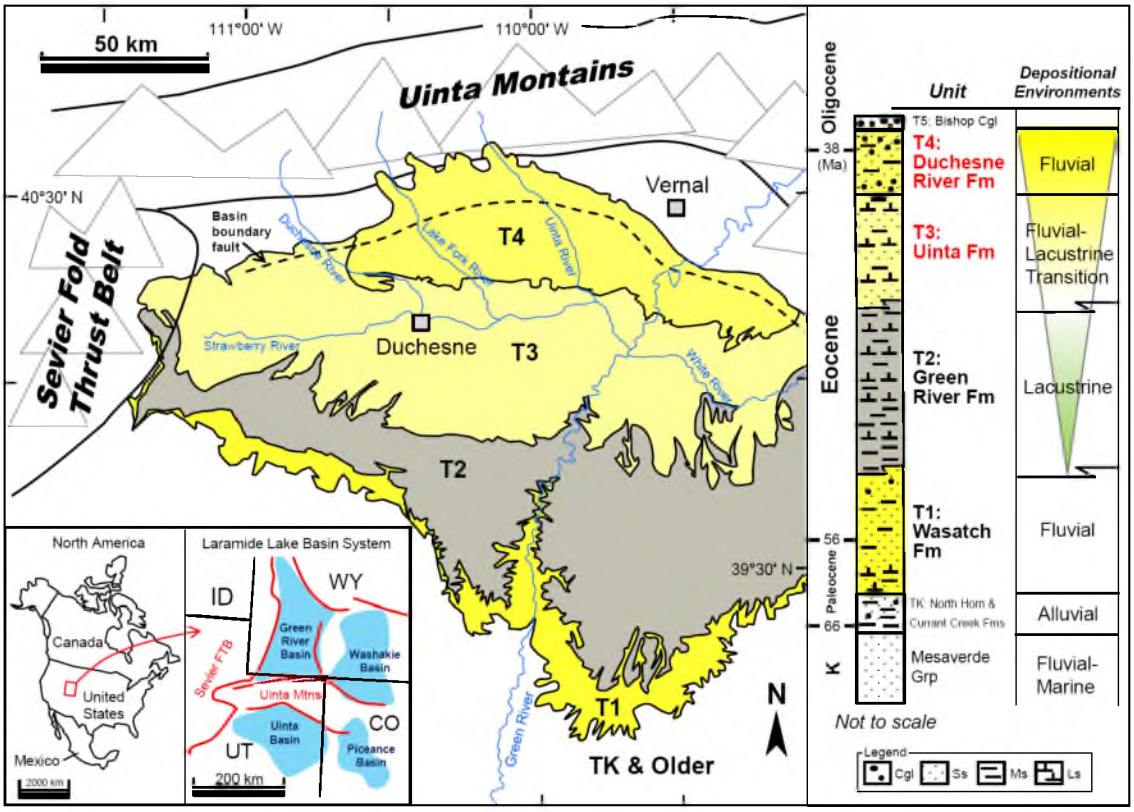

Figure 3.3. Index map and schematic geologic column showing the Paleogene sequence of the Uinta Basin. The basin is surrounded by high mountain ranges of the Uinta Mountains and Sevier Fold Thrust Belt (FTB). T2 to T4 exhibits a typical upward-coarsening/shallowing lacustrine basin-fill succession. The map of Laramide Lake Basin System is from Dickinson et al. (1988). The geological map is modified from Andersen and Picard (1974), Bryant et al. (1989), Bryant (1992), Hintze et al. (2000), and Sprinkel (2006, 2007).

by a high-angle reverse fault at the foothills of the Uinta Mountains (e.g., Fouch 1975; Bruhn et al. 1983, 1986).

Paleocene-Eocene strata of the Uinta Basin consist of the Wasatch (fluvial), Green River (lacustrine), Uinta (fluvial-lacustrine transition), and Duchesne River (fluvial) Formations (Fig. 3.3). This study focuses on late-stage basin-fills of the uppermost Uinta and Duchesne River Formations, which are generally comprised of coarser grained deposits than the underlying, renowned petroleum source rock of the Green River Shale. The Duchesne River Formation is subdivided into four lithologically distinct units, Brennan Basin (Db), Dry Gulch Creek (Dd), Lapoint (Dl), and Starr Flat (Ds) members in ascending order (Andersen and Picard

1972). A regional study detailed in the Chapter 1 of this thesis depicts a robust sequence stratigraphic framework and detailed basin-scale facies architectures of the Duchesne River Formation (Figs. 3.4 and 3.5).

3.3.2 Previous Studies

A relatively small number of studies have reported on the Uinta and Duchesne River Formation despite their excellent exposures, whereas the Green River Formation including that in Wyoming has received much attention documenting sequence stratigraphy and ichnology (e.g., Bohac et al. 2000; Keighley et al. 2003; Bohac et al. 2007). Andersen and Picard (1972) presented a comprehensive regional stratigraphy and proposed the four member subdivisions of the Duchesne River Formation used here. D'Alessandro et al. (1987) is the only known ichnological study of the Duchesne River Formation. It should be noted that the study area of D'Alessandro et al. (1987) is situated in the western part of the Uinta Basin where the "Undivided Duchesne River Formation" was proposed by Bryant et al. (1989), and it includes proximal fluvial deposits time-equivalent to distal lacustrine deposits of the Uinta and Green River Formations (Bryant et al. 1989) (detailed nomenclatural history in Appendix A). The formation studied by D'Alessandro et al. (1987) is probably time-equivalent to the Uinta or Green River Formation, and thus not covered by this study. There is no comprehensive ichnology study on the Uinta Formation, although some continental trace fossils from this formation were reported in Hasiotis (2002).

3.4 Methods

Basin-wide field work was conducted throughout the E-W and N-S exposure of the uppermost Uinta and Duchesne River Formations. The acquired measured geological sections at 35 locations (a total of 2,970 m in length, described at resolution of 10-20 cm) were regionally correlated (Figs. 3.4 and 3.5). In this chapter, trace fossils and their assemblages were described in relation to depositional environments on the basis of their presence-absence. Although trace fossils are abundant at some locations, identifications of ichnogenera are

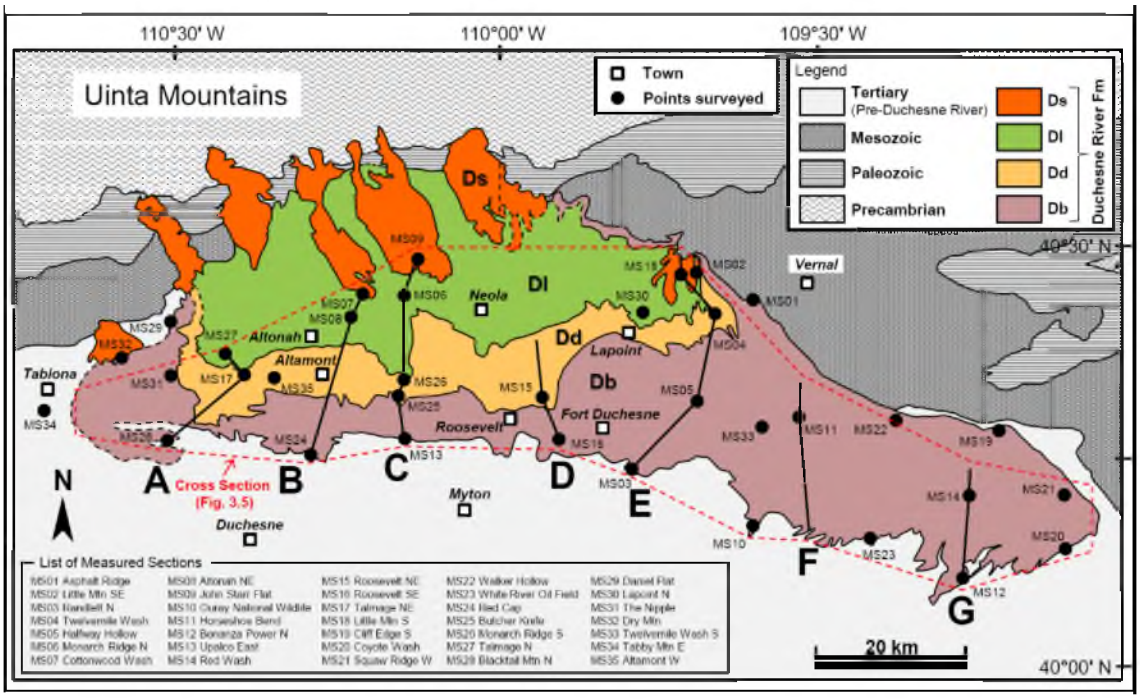

Figure 3.4. Geological map of the Duchesne River Formation and surrounding area. Regional dip is to the north and the Duchesne River members (Db: Brennan Basin Member, Dd: Dry Gulch Creek Member, Dl: Lapoint Member and Ds: Starr Flat Member) get progressively younger toward the Uinta Mountains. The locations of 35 measured sections (MS), composite sections A to G (black lines), and the location of the cross section in Fig. 3.5 (dotted red polygon) are shown on the map. The map is modified after Andersen and Picard (1974), Rowley et al. (1985), Bryant et al. (1989), and Sprinkel (2006 and 2007).

sometimes challenging due to poor preservation conditions including modern weathering.

3.5 Observed Trace Fossils and Paleoenvironmental Interpretations

The succession of the uppermost Uinta and Duchesne River Formations exhibits distinct fluvial-lacustrine facies changes in response to primarily tectonic uplift and subsidence of the Uinta Mountains and the adjacent basinal area (Figure 3.5). Correspondingly, there are significant changes in observed trace fossils and their assemblages. In this section, lithofacies, biofacies (e.g., body fossil occurrence), and observed trace fossils of each unit are first described. Subsequently, depositional environments are interpreted, and also the trace fossil assemblages observed in this study are compared with the known/reported continental ichnofacies models and their components. The uppermost unit of the Duchesne River

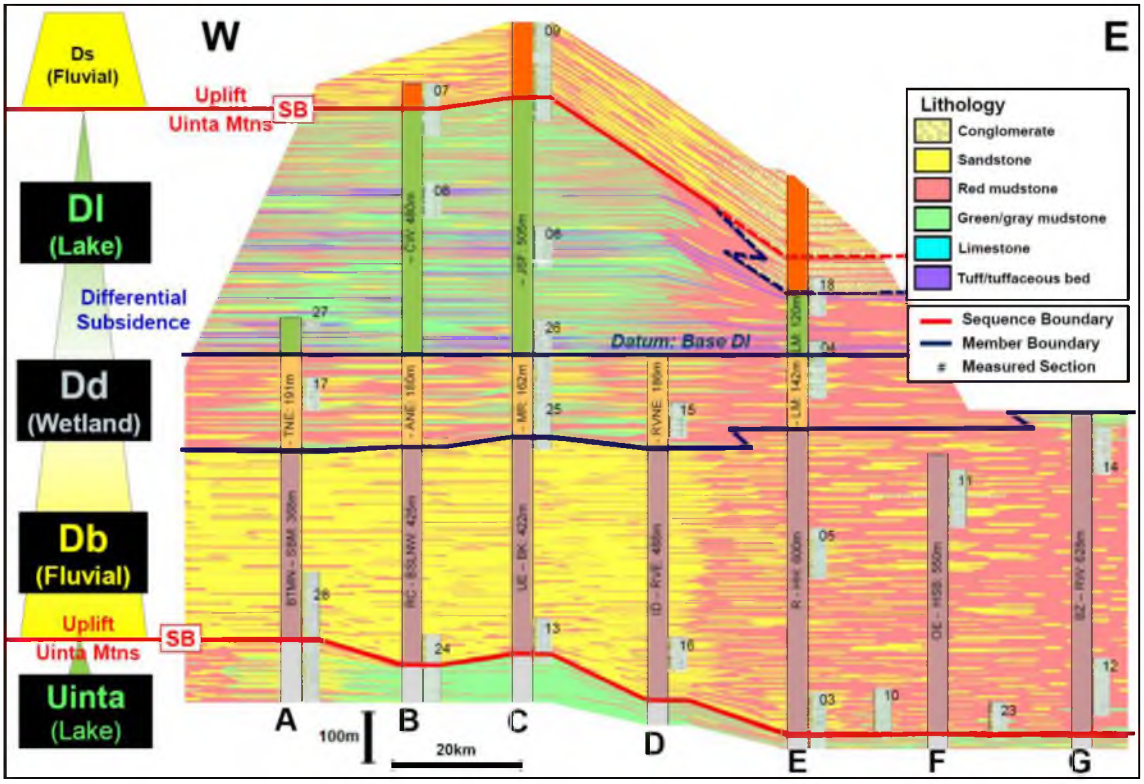

Figure 3.5. E-W regional correlations of composite sections A to G showing the stratigraphic framework and detailed basin-scale facies architectures of the uppermost Uinta and Duchesne River Formations. The stratigraphic datum is set at the base of Dl, which can be regarded as a nearly isochronous boundary (~40 Ma). The succession of the uppermost Uinta and the Duchesne River Formation is characterized by upward-fining continental cycles.

Formation (Ds) is excluded from this ichnological study due to the insufficient amount of trace fossil data.

3.5.1 Uppermost Uinta Formation

3.5.1.1 Description

The lithofacies of the uppermost Uinta Formation is characterized by alternating beds of sandstones, mudstones, and limestones (Fig. 3.6), typically comprised of upward-coarsening progradational prarasequences. The formation is green and gray mudstone-dominated at the basin center (e.g., MS13, MS24), and gradually becomes sandy to the west (e.g., MS28) (Fig. 3.5). Between composite sections A and D, the formation occasionally contains conspicuous

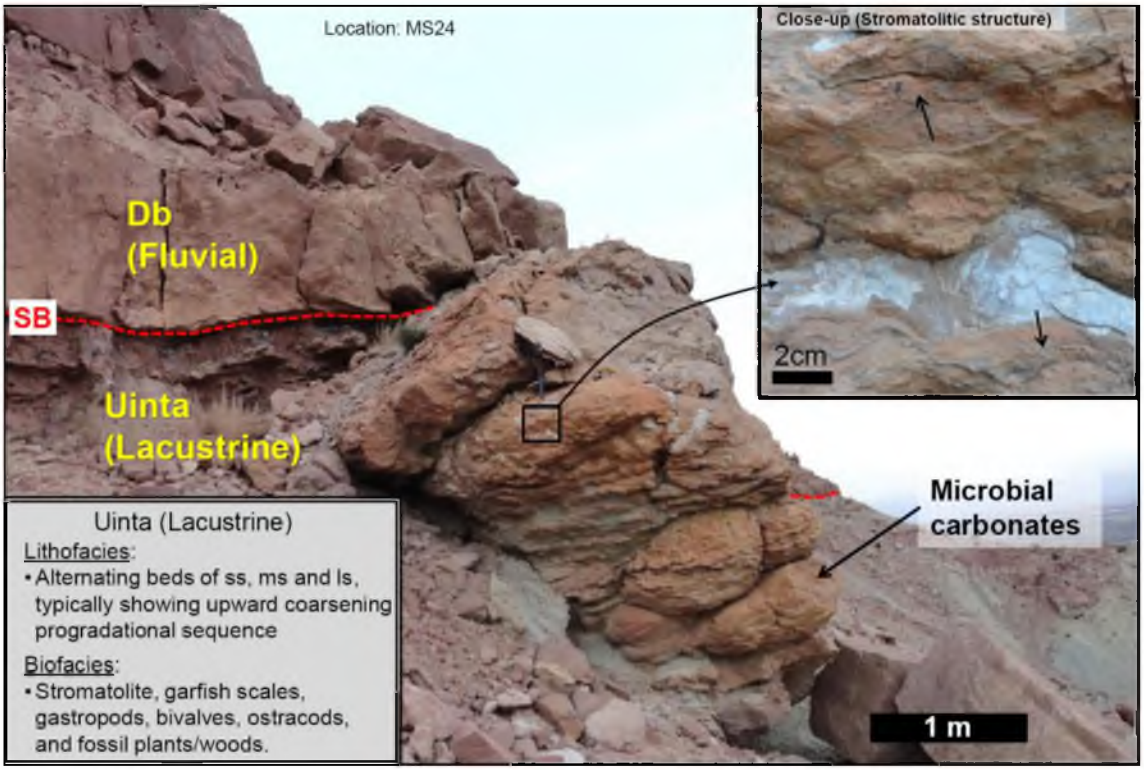

Figure 3.6. The uppermost Uinta Formation at MS24, showing stacked microbial carbonate mounds with stromatolitic structures. Lithofacies and biofacies of the uppermost Uinta Formation are also summarized.

stromatolitic limestone mounds (Fig. 3.6) and thin-layered fossiliferous limestones including garfish scales, gastropods, bivalves, and ostracods.

Trace fossils are generally less abundant than in the overlying unit (Db). Most of the traces are observed in epirelief on the top surfaces of tabular sandstones. They include *Arenicolites* isp. (U-shaped burrow with no wall) and *Taenidium* isp. (horizontal burrow with meniscate backfill) and *Gordia* (=*Haplotichnus*) isp. (horizontal, small, simple burrow, sometimes self-overcrossing) are observed within the same sandstone bed with symmetrical wave ripples at MS24 (Figs. 3.7 and 3.8). Buatois et al. (1998) suggested that *Gordia* Emmons 1844 is synonymous with *Haplotichnus* (Miller 1889), and I agree with that interpretation and therefore refer all such traces to *Gordia* in this thesis. Additionally, *Planolites* isp. (horizontal, simple, straight to gently curved burrow), Unidentified Trace Fossil A (horizontal to oblique, a series of ball-shaped burrows with distinct thick walls) (Fig. 3.8), and Unidentified B (slightly U-

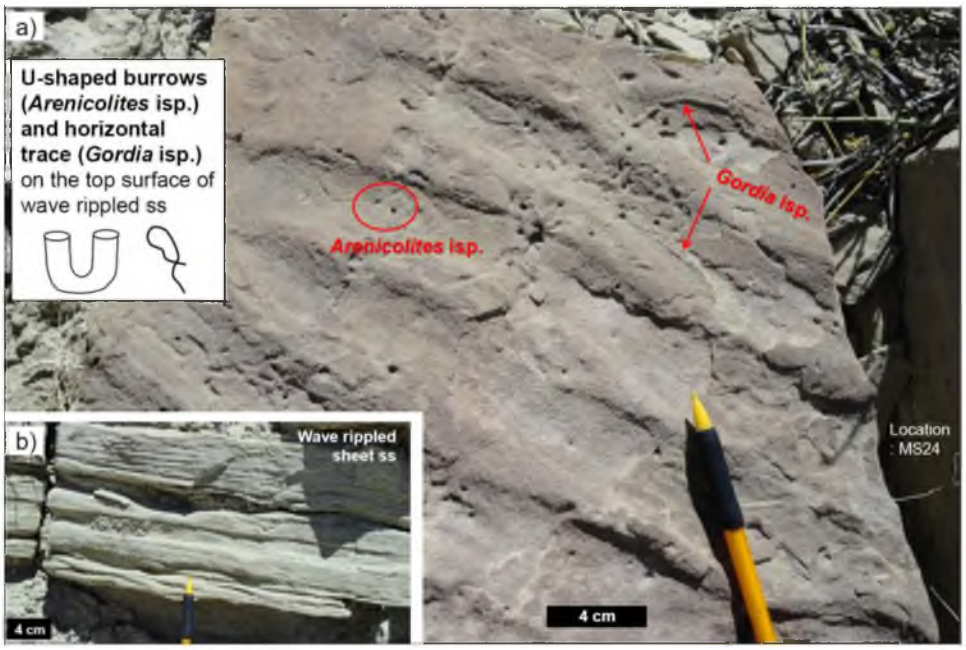

Figure 3.7. Trace fossils observed in the uppermost Uinta Formation at MS24. a) *Arenicolites* isp. (U-shape burrow with no wall) and *Gordia* isp. (horizontal, small, simple burrow, sometimes self-overcrossing) appear on the top surface of asymmetric wave-rippled sandstone. b) Sectional view of the asymmetric wave-rippled sandstone.

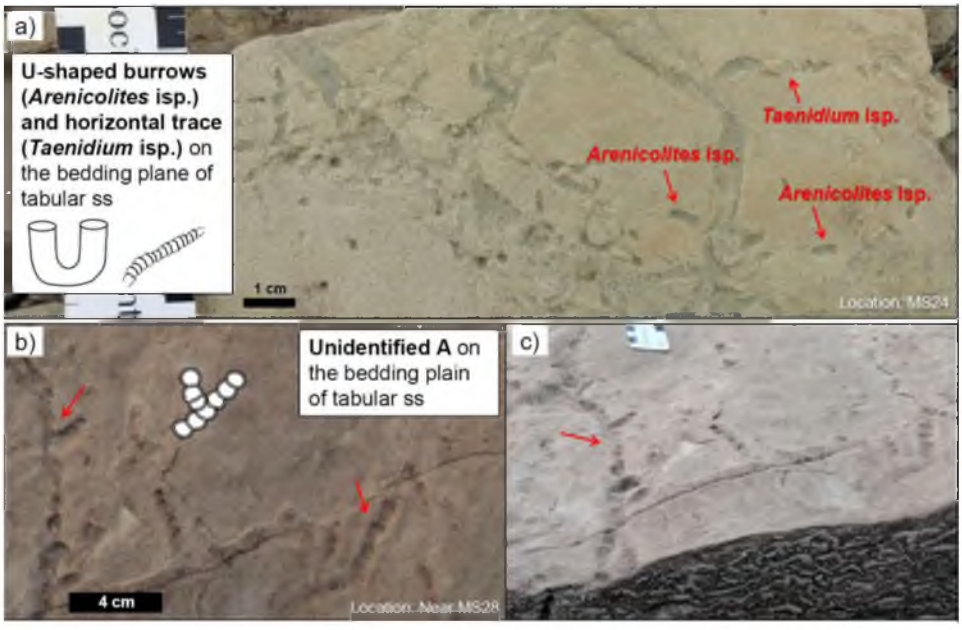

Figure 3.8. Trace fossils observed in the uppermost Uinta Formation at MS24 and MS28. a) *Arenicolites* isp. (U-shape burrow with no wall) and *Taenidium* isp. *(horizontal burrow with meniscate backfill)* on the bedding plane of tabular sandstone. b) & c) Unidentified Trace Fossil A (horizontal to oblique, a series of ball-shaped burrows with distinct thick walls) on the bedding plane of tabular sandstone.

shaped, clustered, horizontal tubes) are shown in this unit.

3.5.1.2 Interpretation

The lithofacies of dominant green and gray mudstones with limestones and wave-rippled sandstones and conspicuous stromatolitic limestone mounds clearly indicate an extensive lacustrine environment in the basin center. Gradual increase in sandstones to the western part of the basin indicates a transition into a marginal deltaic and fluvial system to the west. A lake environment of the Uinta Formation has been also documented by several previous workers (Bruhn et al. 1986; Bryant et al. 1989; Davis et al. 2009).

The Uinta trace fossil assemblage (Fig. 3.9) shows dominantly horizontal grazing traces (pascichnia). The trace fossil composition in this unit indicates a mixture of *Mermia* (e.g., *Gordia* isp.), *Scoyenia* (e.g., *Taenidium* isp.), and *Skolithos* (e.g., *Arenicolites* isp.) ichnofacies (Fig. 3.9). All these ichnofacies can occur in lake environments: *Mermia*: low energy permanent subaqueous conditions, *Scoyenia*: low to moderate energy fluvial-lacustrine transitions, and *Skolithos*: moderate to high energy shorelines and delta (Buatois and Mángano 2007), and are consistent with the above paleoenvironmental interpretation based on lithofacies and biofacies.

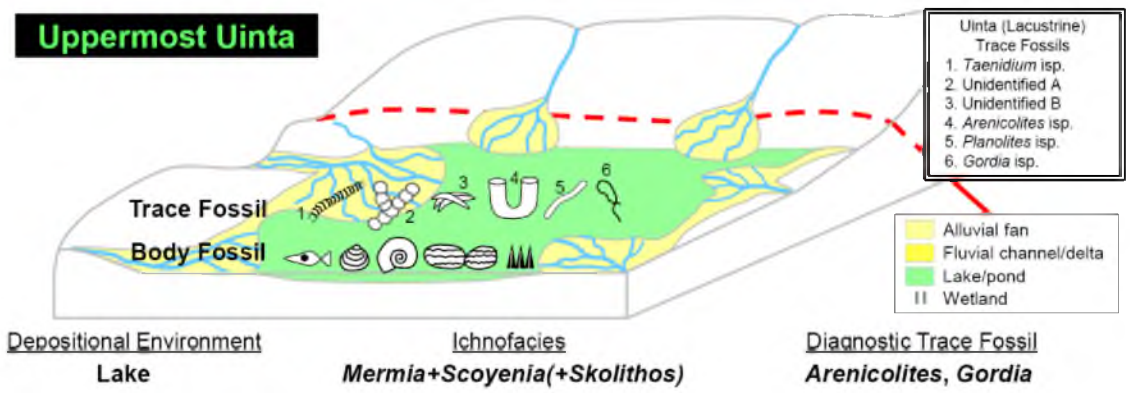

Figure 3.9. Paleoenvironmental reconstruction and trace fossil assemblage of the uppermost Uinta. A lake environment developed during the deposition of the uppermost Uinta Formation. Trace fossil composition in this unit indicates a mixture of *Mermia*, *Scoyenia,* and *Skolithos* ichnofacies. *Arenicolites* isp. and *Gordia* isp. are interpreted to be diagnostic trace fossils to represent the uppermost Uinta environment.

3.5.2 Brennan Basin Member (Db)

3.5.2.1 Description

The lithofacies of the basal member (Db) of the Duchesne River Formation is dominated by trough-cross stratified, channelized sandstones, thin-layered sandstones and siltstones, and red mudstones (commonly mottled), typically showing upward-fining parasequences (Fig. 3.10). Db exhibits a significant contrast of lithofacies: a high net-sand-to-gross-thickness ratio (NTG) facies in the western and a lower NTG facies in the eastern part of the basin (Fig. 3.5). Body fossils are scarce in this unit, although some mammal teeth (e.g., rodent) and bones (e.g., rhinocerotoid) were previously reported (e.g., Rasmussen et al. 1999, Kelly et al. 2012). A large (but unidentified) mammal's bone was found in channelized sandstone at MS33 during the field work of this study (Fig. 3.10).

Trace fossils are very abundant, especially in the eastern part of the basin. Most of the traces are observed both in hyporelief and epirelief, and sometimes in fullrelief. Meniscate trace fossils such as *Scoyenia* isp. (meniscate backfill with ornamented wall), *Ancorichnus* isp. (meniscate backfill with smoothly lined wall), *Beaconites* isp. (distinct, texturally heterogeneous meniscate backfill), and *Naktodemasis* isp. (thin and tightly spaced meniscate backfill) commonly and intensively occur in this unit (Figs. 3.11, 3.12, and 3.13). Also insect nest structures such as *Termitichnus* isp. (large trunk burrow with spherical-shaped holes), *Celliforma* isp. (trunk burrow with oval-shaped cells/chambers), and *Parawanichnus* isp. (large interconnected burrow system with galleries and chambers), and unidentified ant nest or plant root structures (network or branching burrows with 2-3 millimeter diameters) are common in sandstones or siltstones (Figs. 3.12 and 3.13). Additionally, *Skolithos* isp., *Planolites* isp., and *Palaeophycus* isp. are ubiquitous.

3.5.2.2 Interpretation

Lithofacies (channelized sandstones with red mudstones) and biofacies (mammal teeth and bones) indicate an extensive alluvial plain environment developed throughout the deposition of this unit. It indicates the progradation of the fluvial deposits of Db and the

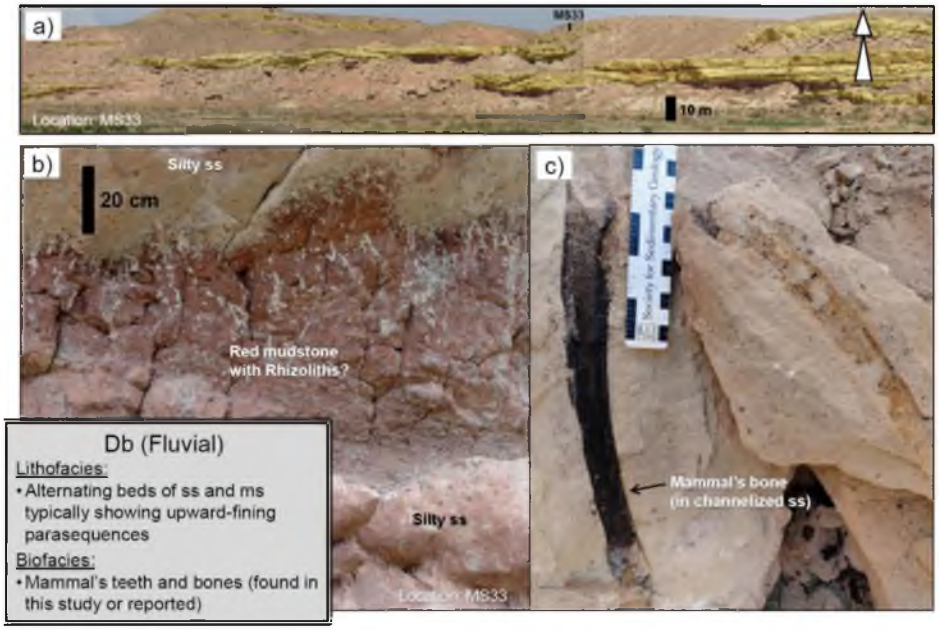

Figure 3.10. The basal member of the Duchesne River Formation (Db) at MS33 showing typical lithofacies and biofacies. a) Alternating beds of sandstones and mudstones typically showing upward-fining parasequeces of basal channelized sandstones (highlighted by yellow) and capped red mudstones. b) Close-up photo of MS33 showing mottled red mudstone (including Rhizoliths?) and silty sandstones. c) Mammal's bone found in channelized sandstone.

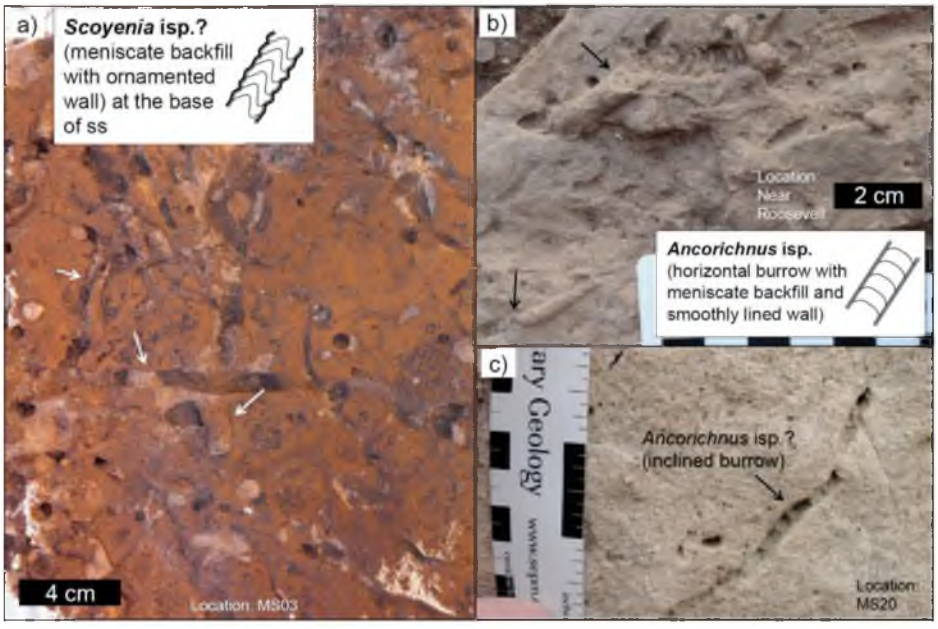

Figure 3.11. Trace fossils observed in Db (1). a) *Scoyenia* isp. (meniscate backfill with ornamented wall) at the base of sandstone (hyporelief). b) *Ancorichnus* isp. (meniscate backfill with smoothly lined wall) at the base of sandstone. c) *Ancorichnus* isp.(?) (inclined burrow with meniscate backfill and smoothly lined wall) within sandstone (sectional view).

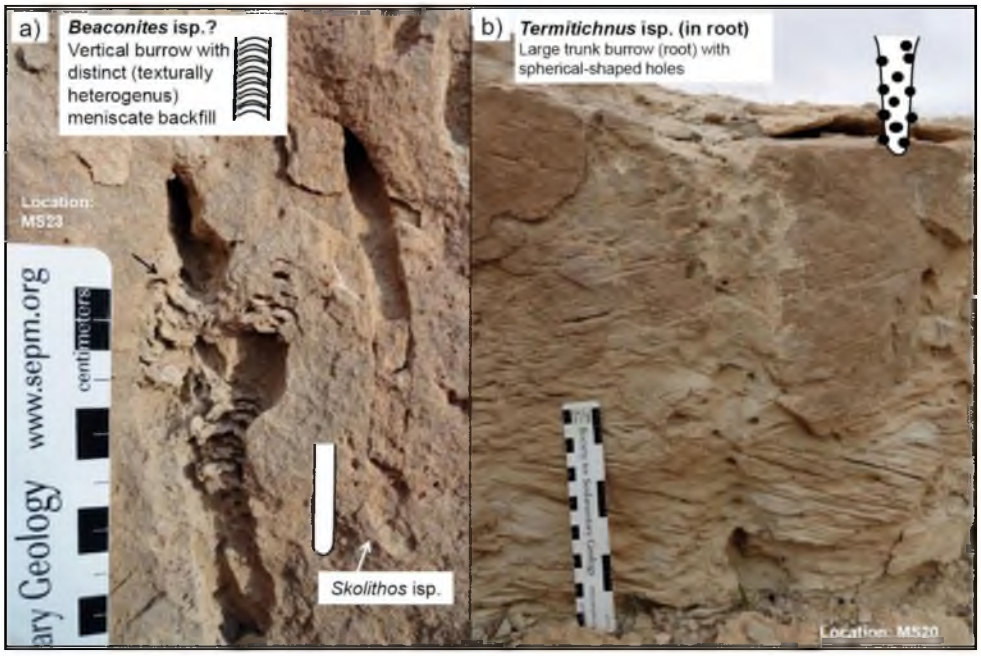

Figure 3.12. Trace fossils observed in Db (2). a) *Beaconites* isp.(?) (distinct, texturally heterogenus meniscate backfill) and *Skolithos* isp. (simple, vertical cylindrical burrow) in a sectional view of sandstone. b) *Termitichnus* isp. in root (large trunk burrow with spherical-shaped holes) in a sectional view of trough cross-stratified sandstone.

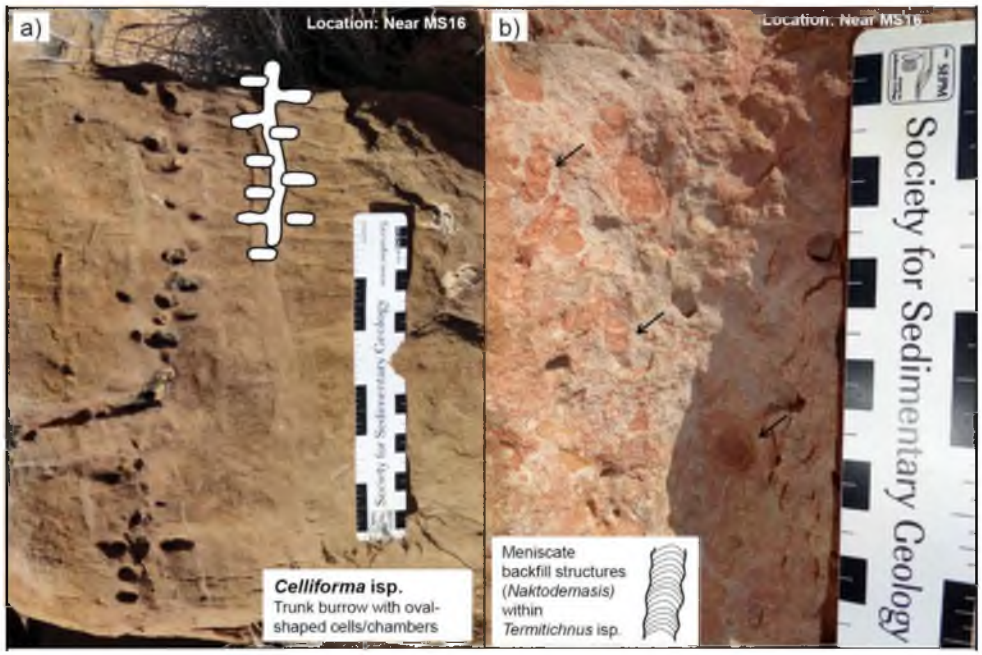

Figure 3.13. Trace fossils observed in Db (3). a) *Celliforma* isp. (trunk burrow with oval-shaped cells/chambers) in a sectional view of trough cross-stratified sandstone. b) Meniscate backfill structures (*Naktodemasis* isp.) within *Termitichnus* isp.

cessation of lake deposition of the Uinta Formation. Db exhibits a significant contrast of fluvial styles between the west (an amalgamated braided fluvial system) and east (a relatively sinuous fluvial system) (Fig. 3.5). This contrast is greatly influenced by the difference in climate and the number of source terrains (i.e., discharge control) (see the details in Chapter 1).

The trace fossil composition in this unit indicates a mixture of *Scoyenia* (e.g., several types of meniscate backfill traces) and *Coprinisphaera* (e.g., insect nesting structures) ichnofacies (Fig. 3.14). Most of the intensively burrowed structures occur in contact with red mudstones indicating well-drained paleosols or within silty sandstones indicating pedogenically-altered overbank deposits. Therefore, we can merely interpret this assemblage as dominantly *Coprinisphaera* ichnofacies (i.e., paleosol trace fossil suites), because meniscate burrows can also be a part of this ichnofacies (e.g., Buatois and Mangano 2007). The Db trace fossil assemblage shows a distinct difference from the underlying Uinta Formation (lake) assemblage.

3.5.3 Dry Gulch Creek Member (Dd)

3.5.3.1 Description

The second member (Dd) of the Duchesne River Formation has a transitional lithofacies between the underlying sandstone-dominated Db and overlying mudstone-dominated Dl. Dd typically shows alternating beds of channelized and tabular sandstones and green and red mudstones (commonly mottled) including intensive gypsum veins and fragmented fossil plant/coaly layers. Dd exhibits contrasting mudstone colors: mixed green and red mudstones in the west and dominant red mudstones in the eastern part of the basin (Fig. 3.5). Body fossils are scarce except for fossil plants found in the western part of this unit (Figure 3.15).

Trace fossils (in the western part of the basin) are abundant and recognized both in hyporelief and epirelief, and even in fullrelief. Meniscate trace fossils such as *Scoyenia* isp., *Ancorichnus* isp., *Beaconites* isp., and *Naktodemasis* isp. commonly occur in this unit. *Steinichnus* isp. (large-diameter horizontal burrows with crossing scratch patterns) was observed at the base of a cross-stratified sandstone at MS15 (Fig. 3.16). Additionally, *Skolithos* isp., *Planolites* isp., *Palaeophycus* isp., Unidentified Trace Fossil A (Fig. 3.17) (see the

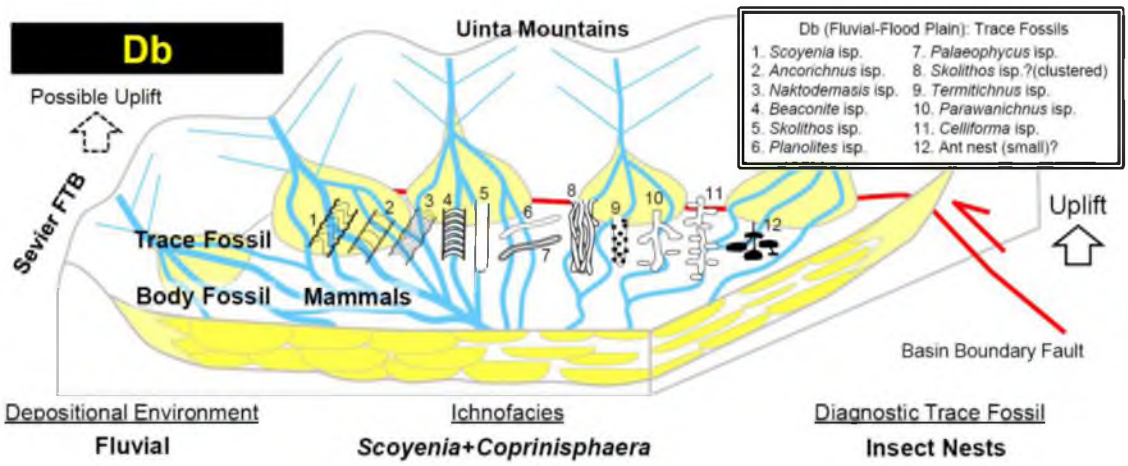

Figure 3.14. Paleoenvironmental reconstruction and trace fossil assemblage of Db. Lake Uinta disappeared and fluvial systems developed on a widespread alluvial plain during the deposition of Db. Trace fossil composition in this unit indicates a mixture of *Scoyenia* and *Coprinisphaera* ichnofacies. Insect nests (e.g., *Termitichnus* isp., *Parawanichnus* isp., *Celliforma* isp.) are interpreted to be diagnostic trace fossils to represent the Db environment.

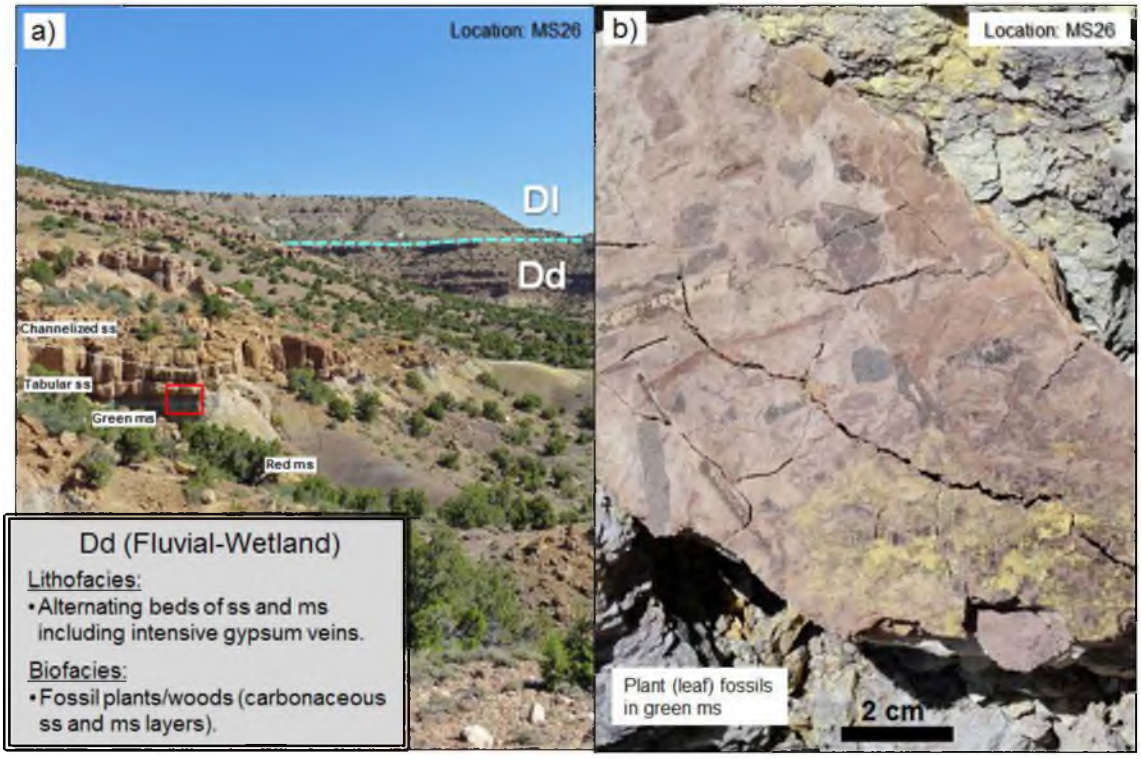

Figure 3.15. The second member of the Duchesne River Formation (Dd) at MS26 showing typical lithofacies and biofacies. a) Alternating beds of channelized and tabular sandstones and green and red mudstones of Dd. b) Fossil plants/woods in green mudstone of Dd.

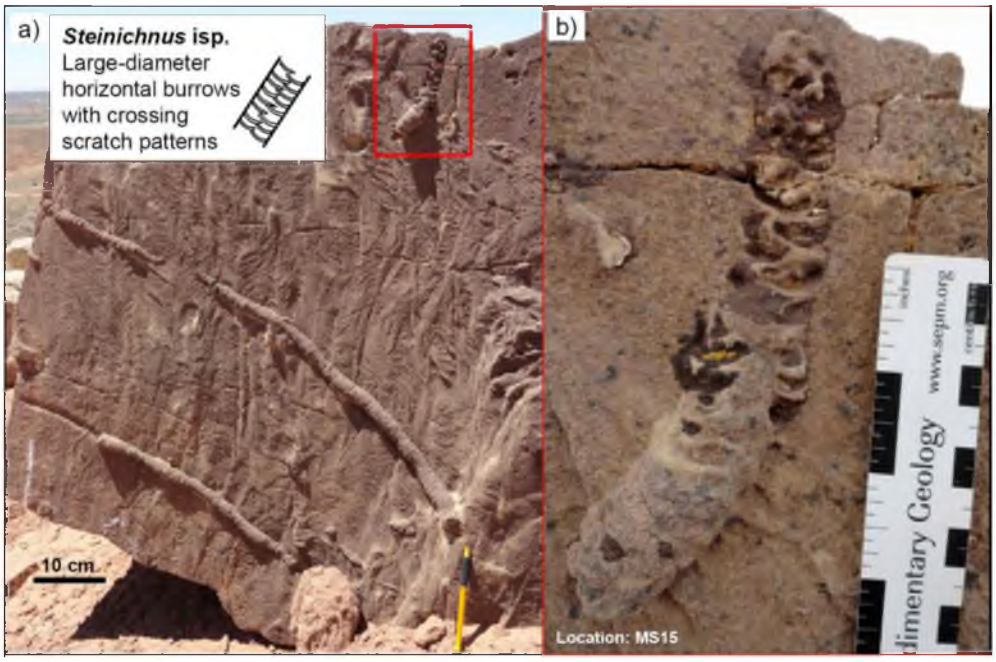

Figure 3.16. Trace fossils observed in the western part of Dd (1). a) *Steinichnus* isp. (large-diameter horizontal burrow with crossing scratch patterns) observed at the base of cross-stratified sandstone at MS15. b) Close-up photo of *Steinichnus* isp.

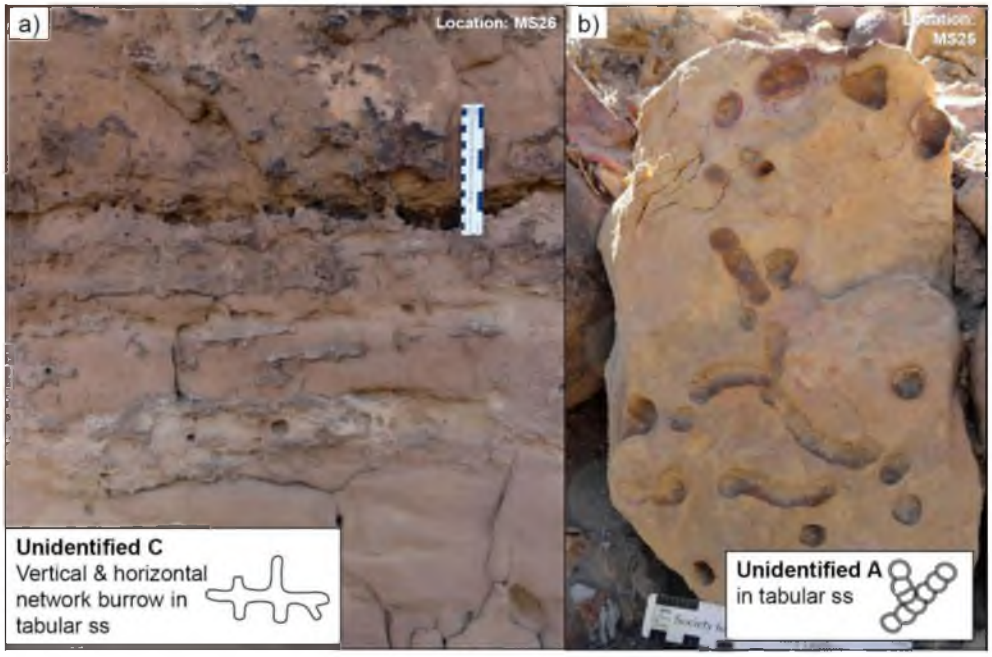

Figure 3.17. Trace fossils observed in the western part of Dd (2). a) Unidentified Trace Fossil C (vertical and horizontal branching network burrow with no wall) in a sectional view of tabularly-bedded (deltaic) sandstone. b) Unidentified Trace Fossil A (horizontal to oblique, a series of ball-shaped burrow with distinct thick wall).

description in the section of the uppermost Uinta Formation), Unidentified Trace Fossil C (Fig. 3.17) (vertical and horizontal branching network burrow with no wall), and unidentified nest or root structures (network/branching burrows with 2-3 millimeter diameters, small ant nest?) are recognized in the western part of this unit.

3.5.3.2 Interpretation

Lithofacies (mixed green and red mudstones with interbedded channelized and tabular sandstones) and biofacies (layered fossil plants/woods) indicate frequent interventions of shallow and short-lived lacustrine or wetland environments on an extensive alluvial plain in the western part of the basin (i.e., to the west of MS15 NE Roosevelt). Trace fossil composition in this unit indicates a transitional ichnofacies (i.e., a mixture of *Scoyenia*, *Coprinisphaera,* and *Skolithos* ichnofacies) between those in the underlying Db and overlying Dl (Fig. 3.18). Although most of the ichnogenera in this unit are also recognized in Db, occurrences of Unidentified Trace Fossils A (observed in the lacustrine Uinta Formation as described above) and *Steinichnus* isp. indicate some interventions of short-lived lake or wetland environments in Dd. It is noted that ichnogenus *Steinichnus* possibly made by insects such as beetles or mole crickets (Bromley and Asgaard 1979, Bohacs et al. 2007) is reported to be distributed in a higher water table environment than the insect nesting traces (Bohacs et al. 2007).

3.5.4 Lapoint Member (Dl)

3.5.4.1 Description

The third member (Dl) of the Duchesne River Formation is characterized by fine-grained deposits (i.e., mudstones and tuff/tuffaceous fine-grained rocks). It exhibits dominant green and gray mudstones interbedded with tabular sandstones (occasionally wave-rippled), tuffs and limestones in the western part of the basin (Fig. 3.19), and dominant red mudstones in the eastern part of the basin (Fig. 3.5). Body fossils are generally scarce, although shell-rich (gastropods and bivalves) limestones and coaly/carbonaceous mudstone layers are observed in some locations (e.g. MS06) in the western part of the basin (Fig. 3.19).

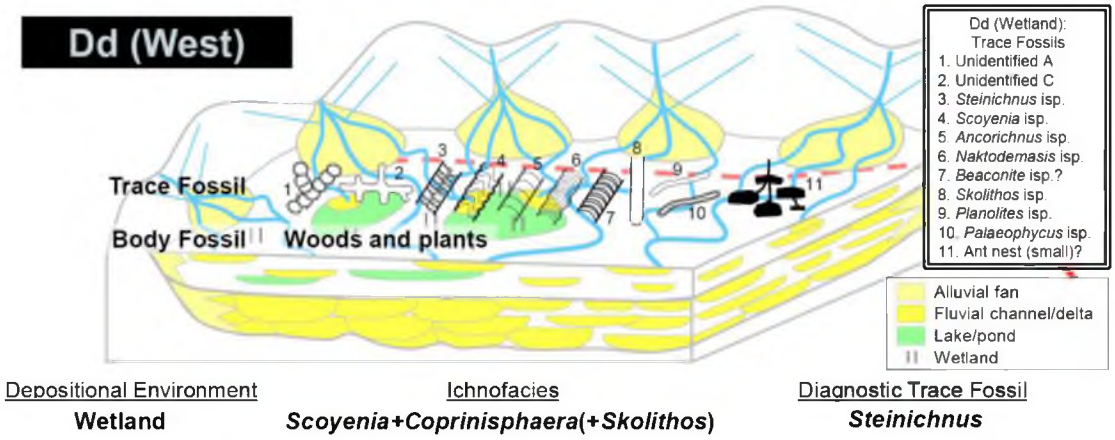

Figure 3.18. Paleoenvironmental reconstruction and trace fossil assemblage of Dd. Short-lived lake or wetland environments developed in the western part of the basin during the deposition of Dd. Trace fossil composition in this unit indicates a transitional ichnofacies (i.e., a mixture of *Scoyenia*, *Coprinisphaer*a, and *Skolithos* ichnofacies) between those in Db and Dl. *Steinichnus* isp. might be a diagnostic trace fossil for this unit as it is reported to be distributed in a higher water table environment than insect nesting traces (Bohacs et al. 2007).

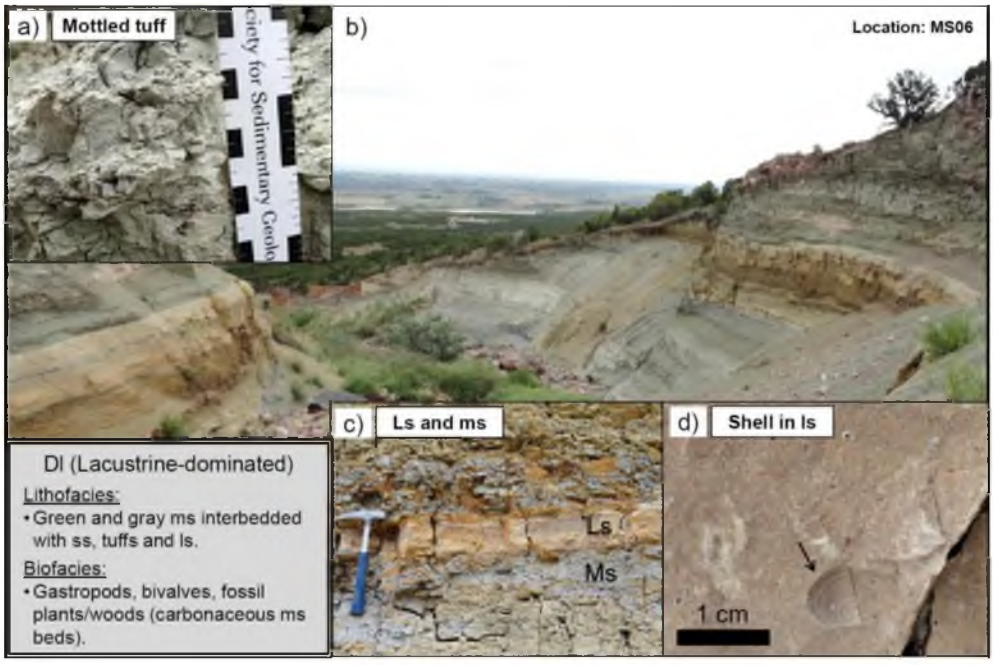

Figure 3.19. The third member of the Duchesne River Formation (Dl) at MS06 showing typical lithofacies and biofacies. a) Close-up of mottled (biotite-rich) tuff observed at MS06. b) Overlook of green mudstone-dominated Dl. c) Green mudstone with thin fossiliferous limestone (ls) including gastropods and bivalves. d) Close-up of shell (bivalves) in limestone.

Trace fossils in the western part of this unit are sparse and tend to occur in epirelief on the top surface of tabular sandstones. Trace fossils observed in this unit are *Arenicolites* isp., *Gordia* isp., *Taenidium* isp., and *Planolites* isp. (Fig. 3.20), which are similar in assemblage to those of the uppermost Uinta Formation.

3.5.4.2 Interpretation

Lithofacies (dominant green/gray mudstones with wave-rippled tabular sandstones) and biofacies (gastropods and bivalves within fossiliferous limestones) indicate a widespread lacustrine environment in the western half of the basin. This extensive lake environment developed due to differential subsidence of the basin (detailed discussion in Chapter 1). The trace fossil composition in this unit indicates a mixture of the *Mermia*, *Scoyenia*, and *Skolithos* ichnofacies (Fig. 3.21), which is very similar to ichnofacies of the uppermost Uinta Formation. This evidence demonstrates the recurrence of lake organisms' communities and a distinct difference from the fluvial-flood plain trace fossil assemblage observed in the underlying Db.

Figure 3.20. Trace fossils observed in the western part of Dl. a) *Arenicolites* isp. (U-shape burrow) on the top surface of tuffaceous silty sandstone, b) *Taenidium* isp. (horizontal burrow with meniscate backfill) on the top surface of silty sandstone.

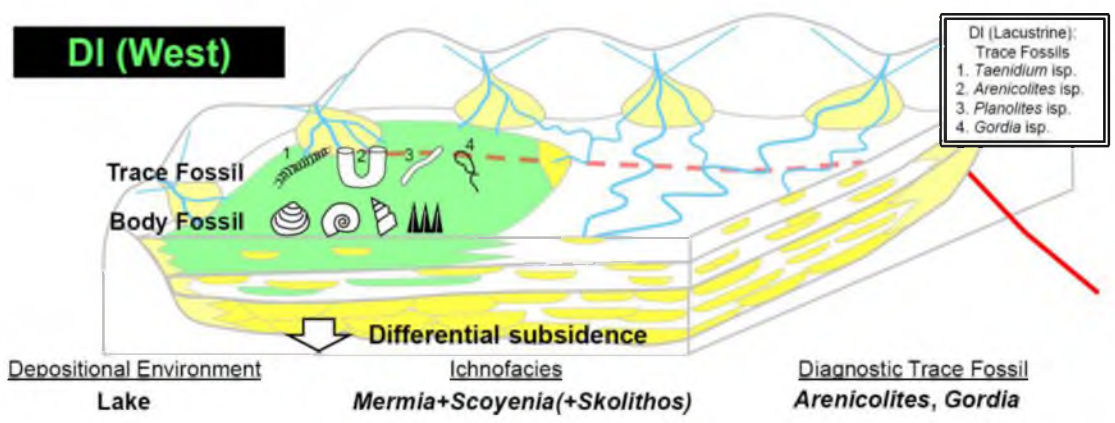

Figure 3.21. Paleoenvironmental reconstruction and trace fossil assemblage of Dl. An extensive lake environment developed during the deposition of Dl. Trace fossil composition in this unit indicates a mixture of *Mermia*, *Scoyenia*, and *Skolithos* ichnofacies, demonstrating the recurrence of lake organisms' communities.

3.6 Synthesis and Discussion

The sequence of the Duchesne River Formation was primarily controlled by tectonics (sequence stratigraphic framework construction detailed in Chapter 1). The uplift(s) in the Uinta Mountains and possibly the Sevier FTB caused distinct sequence boundaries at the base of Db and Ds, and led to the development of an upward-fining fluvial sequence from Db (LST: lowstand systems tract) to Dd and Dl (TST/HST: transgressive/highstand systems tract) (Fig. 3.22). The trace fossil compositions examined in this chapter show distinct changes according to these systems tracts or relative water table level changes (Fig. 3.22): *Mermia*, *Scoyenia*, and *Skolithos* ichnofacies of the uppermost Uinta Formation (TST/HST), dominant *Coprinisphaera* ichnofacies of Db (LST), *Scoyenia*, *Coprinisphaera*, and *Skolithos* ichnofacies of Dd (TST/HST), and *Mermia*, *Scoyenia*, and *Skolithos* ichnofacies of Dl (TST/HST). These changes correspond to the large-scale (i.e., member-scale) changes in depositional environment, and thus this study cannot offer either rigorous bed-by-bed analyses or interpretations on specific small-scale continental environments, such as channel, bar, and levee. In the future, such detailed bed-scale analysis may lead to decoding a high-resolution sequence and to the extraction of more specific trace fossil assemblage (ichnofacies). An ichnofabric approach might be useful for this high-resolution analysis, because there are possibly multiple communities recorded within a

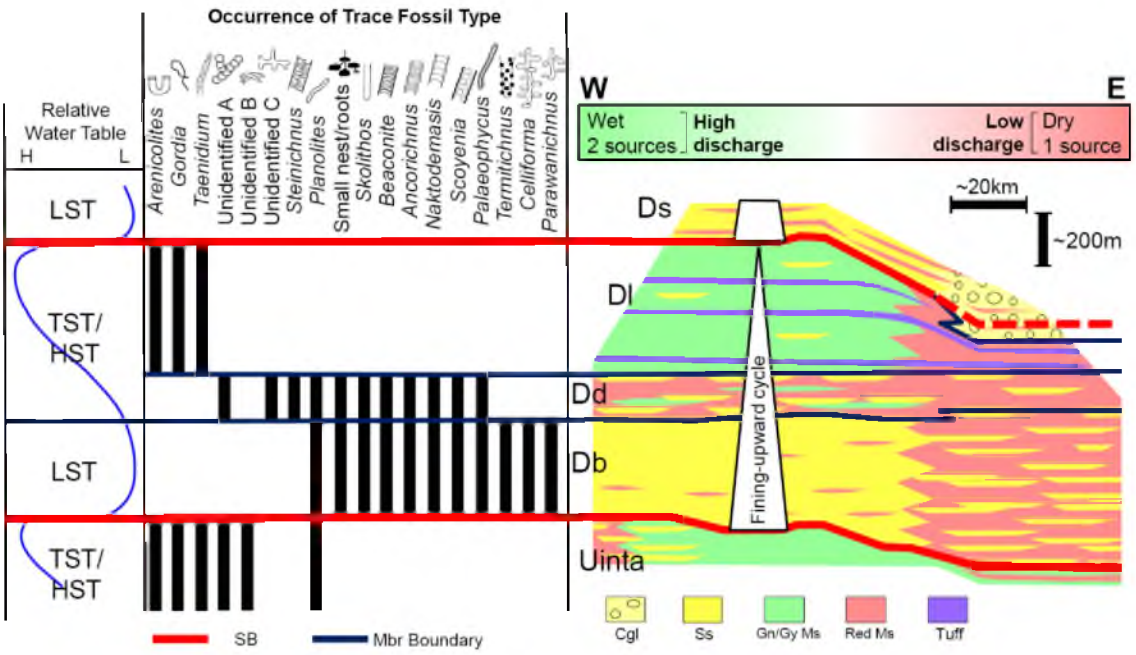

Figure 3.22. Synthesis of sequence stratigraphic framework and trace fossil occurrences of the uppermost Uinta and Duchesne River Formations. The uplift(s) in the Uinta Mountains and possibly in the Sevier FTB caused distinct sequence boundaries at the base of Db and Ds, and led to the development of an upward-fining sequence from Db (LST) to Dl (TST/HST). It is noted that trace fossils show distinct changes in their assemblages according to the relative water table level.

sandstone bed. For example, traces in fluvial channels could be overwritten by the later paleosol communities after these channels are abandoned.

3.7 Conclusion

A regional outcrop-based study revealed the sequence stratigraphic framework and detailed basin-scale facies architectures of the uppermost Uinta and Duchesne River Formations. This chapter documented remarkable changes in continental trace fossil assemblages according to fluctuations in the relative water table level (i.e., member-scale sedimentary facies changes). Specifically, the uppermost Uinta Formation and third member of the Duchesne River Formation (Dl) indicate extensive lacustrine environments and the corresponding trace fossil assemblage including *Arenicolites* and *Gordia*. By contrast, the basal member of the Duchesne River Formation (Db) exhibits a widespread fluvial environment and

the corresponding trace fossil assemblage characterized by a variety of insect trace fossils (e.g., *Scoyenia*, *Ancorichnus*, nest structures). The second member of the Duchesne River Formation (Dd) shows a transitional (i.e., wetland) environment where the intermediate trace fossil assemblage including *Steinichnus* are present. The large-scale (member scale) change in trace fossil assemblages shows how the ichnofacies can corroborate continental sequence stratigraphic interpretations and can serve as a valuable indicator of paleoenvironmental change in a fluvial-lacustrine setting. The uppermost Uinta and Duchesne River Formations offer an invaluable example to record dramatic changes in living communities (trace making organisms) in response to the tectonic control in the dynamic intermontane basin.

3.8 References

Andersen, D.W., and Picard, M.D., 1972, Stratigraphy of the Duchesne River Formation (Eocene-Oligocene?), northern Uinta basin, northeastern Utah: Utah Geological and Mineral Survey Bulletin, v. 97, 29 p.

Andersen, D.W., and Picard, M.D., I974, Evolution of synorogenic clastic deposits in the intermontane Uinta Basin of Utah, *in* Dickinson, W.R., ed., Tectonics and Sedimentation: SEPM Special Publication, v. 22, p. 167-189.

Bohacs, K.M., Carroll, A.R., Neal, J.E., and Mankiewicz, P.J., 2000, Lake-basin type, source potential, and hydrocarbon character: an integrated-sequence-stratigraphic–geochemical framework, *in* Gierlowski-Kordesch E.H., and Kelts, K.R., eds., Lake basins through space and time: American Association of Petroleum Geologists Studies in Geology 46, p. 3–34.

Bohacs, K.M., Hasiotis, S.T., and Demko, T.M., 2007, Continental ichnofossils of the Green River and Wasatch Formations, Eocene, Wyoming: a preliminary survey, proposed relation to lake-basin type, and application to integrated paleo-environmental interpretation, The Mountain Geologist, v. 44, p. 79-108.

Bromley, R.G., and Asgaard, U., 1979, Triassic freshwater ichnocoenoses from Carlsberg Fjord, East Greenland: Palaeogeography, Palaeoclimatology, Palaeoecoloy, v. 28, p. 39-80.

Bromley, R.G., and Asgaard, U., 1993, Two bioerosion ichnofacies produced by early and late burial associated with sea−level change, Geologische Rundschau v. 82, p. 276–280.

Bruhn, R.L., Picard, M.D., and Beck, S.L., 1983, Mesozoic and early Tertiary structure and sedimentology of the central Wasatch Mountains, Uinta Mountains, and Uinta Basin: Utah Geological and Mineralogical Survey Special Studies 59, Salt Lake City, p. 63–105.

Bruhn, R.L., Picard, M.D., and Isby, J.S., 1986, Tectonics and sedimentation of Uinta arch, western Uinta Mountains and Uinta Basin, *in* Peterson. J.A., ed., Paleotectonics and sedimentation in Rocky Mountain region, United States: American Association of Petroleum Geologists Memoir 41, p. 333-352.

Bryant, B., Naeser, C.W., Marvin, R.F., and Mehnert, H.H., 1989, Upper Cretaceous and

Paleogene sedimentary rocks and isotopic ages of Paleogene tuffs, Uinta Basin, Utah: U.S. Geological Survey Bulletin 1787-J, 22 p.

Bryant, B., 1992, Geologic and structure maps of the Salt Lake City 1 degree x 2 degrees quadrangle, Utah and Wyoming: U.S. Geological Survey Miscellaneous Investigations Series Map I-1997.

Buatois, L.A., and Mángano, M.G., 1995. The paleoenvironmental and paleoecologic significance of the lacustrine *Mermia* ichnofacies: an archetypical subaqueous nonmarine trace fossil assemblage, Ichnos, v. 4, p. 151-161.

Buatois, L.A., and Mángano, M.G., 2004, Animal-substrate interactions in freshwater ecosystems: applications of ichnology in facies and sequence stratigraphic analysis of fluvio-lacustrine successions, *in* McIlroy, D., ed., The application of ichnology to paleoenvironmental and stratigraphic analysis: Geological Society of London, Special Publication v. 228, p. 311-333.

Buatois, L.A., and Mángano, M.G., 2007, Invertebrate ichnology of continental freshwater environments: i*n* Miller, W. III, ed., Trace Fossils: Concepts, Problems, Prospects: Elsevier, Amsterdam, p. 285-323.

Buatois, L.A., and Mángano, M.G., 2009, Applications of ichnology in lacustrine sequence stratigraphy: Potential and limitations: Palaeogeography, Palaeoclimatology, Palaeoecology, v. 272, p. 127-142.

Buatois, L.A., and Mángano, M.G., 2011, Ichnology: Organism-Substrate Interactions in Space and Time, Cambridge University Press, 358 p.

Buatois, L.A, and Mángano, M.G., Maples, C.G., and Lanier, W.P., 1998, Ichnology of an Upper Carboniferous fluvio-estuarine paleovalley: the Tonganoxie Sandstone, Buildex Quarry, Eastern Kansas, USA, Journal of Paelontology, v. 72, p. 152-180.

D'Alessandro, A., Ekdale, A.A., Picard, M.D., 1987, Trace fossils in fluvial deposits of the Duchesne River Formation (Eocene), Uinta Basin, Utah, Palaeogeography, Palaeoclimatology, Palaeoecology, v. 61, p. 285-301.

Davis, S.J., Mulch, A., Carroll, A.R., Horton T.W., and Chamberlain, C.P., 2009, Paleogene landscape evolution of the central North American Cordillera: Developing topography and hydrology in the Laramide Foreland: Geological Society of America Bulletin, v. 121, p. 100-116.

Dickinson, W.R., Klute, M.A., Hayes, M.J., Janecke, S.U., Lundin, E.R., McKittrick, M.A., and Olivares, M.D., 1988, Paleogeographic and paleotectonic setting of Laramide sedimentary basins in the central Rocky Mountain region: Geological Society of America Bulletin, v.100, p. 1023-1039.

Ekdale, A.A., Bromley, R.G., and Loope, D.B., 2007, Ichnofacies of an ancient erg: a climatically influenced trace fossil association in the Jurassic Navajo Sandstone, southern Utah, U.S.A.: *in* Miller, W., III, ed., Trace Fossils: Concepts, Problems, Prospects: Elsevier, Amsterdam, p. 562-574.

Emmons, E., 1844, The Taconic System: Based on Observations in New York, Massachusetts, Maine, Vermont and Rhode Island: Caroll and Cook, Albany, 68 p.

Fouch, T.D., 1975, Lithofacies and related hydrocarbon accumulations in Tertiary strata of the western and central Uinta Basin, Utah, *in* Bolyard, D.W., ed., Deep drilling frontiers of the central Rocky Mountains: Rocky Mountain Association of Geologists Symposium, Denver, Colorado, p. 163–173.

Genise, J.F., Mangano, M.G., Buatois, L.A., Laza, J.H., and Verde, M., 2000, Insect trace fossil associations in palaeosols: the *Coprinisphaera* ichnofacies, Palaios, v. 15, p. 49–64.

Genise, J.F., Melchor, R.N., Bellosi, E.S., Verde, M., 2010, Invertebrate and vertebrate trace fossils in carbonates: *in* Alonso-Zarza, A.M., Tanner, L., eds., Carbonates in Continental Settings, Developments in Sedimentology, v. 61, Elsevier Publishing Group, Amsterdam, p. 319–369.

Hasiotis, S.T., 2002, Continental Trace Fossils, SEPM Short Course Notes no. 51, Tulsa, OK, 134 p.

Hintze, L.F, Willis, G.C., Laes, D.Y.M., Sprinkel, D.A., and Brown, K.D., 2000, Digital geologic map of Utah 1:500000: Utah Geological Survey.

Keighley, D., Flint, S., Howell, J., and Moscariello, A., 2003, Sequence stratigraphy in lacustrine basins: a model for part of the Green River Formation (Eocene), southwest Uinta Basin, Utah: Journal of Sedimentary Research, v. 73, p. 987-1006.

Kelly, T.S., Murphey, P.C., and Walsh, S.L., 2012, New records of small mammals from the middle Eocene Duchesne River Formation, Utah, and their implications for the Uintan-Duchesnean North American Land Mammal Age transition; Paludicola, v. 8, p. 208-251.

Miller, S.A., 1889, North American geology and paleontology for the use of amateurs, students and scientists: Western Methodist Book Concern, Cincinnati, Ohio, 664 p.

Rasmussen, D.T., Hamblin, A.H., and Tabrum, A.R., 1999, The mammals of the Eocene Duchesne River Formation, *in* Gillette, D.D., ed., Miscellaneous Publication, Utah Geological Survey 99-1, p. 421-427.

Rowley, P.D., Hansen, W.R., Tweto, O., and Carrara, P.E., 1985, Geologic map of the Vernal 1ø x 2ø quadrangle, Colorado, Utah, and Wyoming: U.S. Geological Survey Miscellaneous Investigations Series I-1526.

Seilacher, A., 1967, Bathymetry of trace fossils, Marine Geology, v. 5, p.413-428.

Smith, R.M.H., Mason, T.R., and Ward, J.D., 1993, Flash-flood sediments and ichnofacies of the Late Pleistocene Homeb Silts, Kuiseb River, Namibia, Sedimentary Geology, v. 85, p. 579-599.

Sprinkel, D.A., 2006, Interim geologic map of the Dutch John 30' x 60' quadrangle, Daggett and Uintah Counties Utah, Moffat County, Colorado, and Sweetwater County, Wyoming: Utah Geological Survey.

Sprinkel, D.A., 2007, Interim geologic map of the Vernal 30' x 60' quadrangle, Uintah and Duchesne Counties, Utah, and Moffat and Rio Blanco Counties, Colorado: Utah Geological Survey.

CHAPTER 4

FLUVIAL AND LACUSTRINE SANDSTONE RESERVOIR MODELS AND CHARACTERIZATION: EOCENE UINTA AND DUCHESNE RIVER FORMATIONS, NORTHERN UINTA BASIN, UTAH

4.1 Abstract

Over the last two decades, stochastic reservoir modeling techniques have progressed to the point where they are now commonplace in workflows for asset teams performing reserve estimates and recovery predictions. There are multiple approaches to building reservoir models that can generate thousands of different realizations, constrained to a limited number of control wells. The outcrop reference provides an invaluable ground truth to guide reservoir modeling for the most realistic outcomes.

Lacustrine deposits of the Uinta Formation and overlying fluvial deposits of Duchesne River Formations represent the late-stage filling of the intermontane Uinta Basin. These formations are well-exposed at Blacktail Mountain in the western part of the basin, revealing a vertical cliff-face section of 206 m with 1856 m of lateral exposure. A photo panorama, four vertical measured sections, and surface gamma ray data were used to interpret the detailed facies architecture (defined five facies in the lacustrine deposits and three facies in the fluvial deposits) of Blacktail cliff-face. These field data were also compared to subsurface well logs covering the same stratigraphic levels in a 30 km west-east section. The combined data sets provided statistics of fluvial channel geometry and distribution.

Facies interpretations of the Blacktail cliff-face were translated into a pixel-based reference (geomodel) with ~120,000 cells (dimensions dx = 10 m, dy = 10 m, dz = 1 m), in which facies were manually assigned to each cell. This outcrop reference of the fluvial unit

(Duchesne River Formation), which exhibits the most complicated reservoir (channel) architectures, was compared to reservoir models generated by three techniques: 1) indicator kriging, 2) sequential indicator simulation, and 3) object-based modeling. All models were constrained by: a) two measured sections as hard data, b) global facies proportions of 50% fluvial channel and 50% flood plain, and c) channel geometries (variogram or width:depth statistics). A static sandbody connectivity analysis was used to evaluate which modeling technique most closely reproduced the reservoir characteristics of the outcrop reference. This analysis showed that object-based models fit the outcrop reference best in terms of wellbore connectivity. Overall, this study provides an important analog example that leverages statistical inputs in geological modeling, and demonstrates which stochastic modeling techniques best represent observed depositional patterns derived from outcrop data.

4.2 Introduction

Stochastic reservoir modeling is a relatively recent discipline as its earlier practices date back to the mid-1980s. The study of the statistics of reservoir bodies and their application to generating quantitative reservoir models, however, began much earlier (see reviews by Bryant and Flint 1993; Keogh et al. 2007; Howell et al. 2014). Several modeling techniques or approaches have now been developed and are standard tools in the oil industry. Since an infinite number of geomodels (facies distributions) can be generated using different modeling techniques, approaches, and parameters, geoscientists often struggle to choose the most realistic one. Thus, reference outcrops are greatly beneficial to reservoir modeling as a ground truth example. Outcrop-based modeling studies, in which outcrops are directly integrated into geocellular models, are commonplace today (e.g., Dutton et al. 2002; Ciftci et al. 2004; White et al. 2004; Falivene et al. 2006; Labourdette and Jones 2007; Pranter et al. 2007; Sech et al. 2009; Pranter and Sommer 2011). However, high-quality outcrops that enable us to capture reservoir body characteristics (e.g., shape and continuity) at the usual scale of well spacing (a few hundred to a few thousand meters) are not quite so common (Howell et al. 2014). This research focuses on a well-exposed cliff-face over 200 m in height and 1800 m wide, which is

suitable for understanding detailed sand body geometry, architecture, and connectivity at the scale of normal well spacing.

The purpose of this chapter is to: 1) describe the stratigraphic framework with fluvial-laucstrine facies architecture and sandbody (reservoir) geometries on the well-exposed cliff-face of the Blacktail Mountain, 2) test several stochastic modeling techniques on the fluvial unit (Duchesne River Formation), and 3) evaluate which technique best represents the actual sandbody (fluvial channel) characteristics of the outcrop reference.

4.3 Geological Context

4.3.1 Geological Setting

The Uinta Basin is a prolific oil-producing province situated in northeastern Utah. It is a part of the Laramide intermontane lake basin system that straddles Wyoming, Colorado, and Utah (Fig. 4.1). This system emerged during the latest Cretaceous to early Paleogene (Dickinson et al. 1988). The Uinta Basin is surrounded by several highlands such as the Uinta Mountains to the north, Sevier Fold Thrust Belt (FTB) to the west, Douglas Creek Arch to the east, and Uncompahgre Uplift and San Rafael Swell to the south. The basin has an asymmetrical shape, bounded in the north by a high-angle reverse fault at the foothills of the Uinta Mountains (e.g., Fouch 1975; Bruhn et al. 1983, 1986).

Paleocene-Eocene strata of the Uinta Basin are composed of the Wasatch (fluvial), Green River (lacustrine), Uinta (fluvial-lacustrine transition), and Duchesne River (fluvial) Formations (Fig. 4.1). This stratigraphic succession corresponds in a general way to the staged lacustrine basin-fill model (Lambiase 1990): stage 1 – Early basin (Wasatch Formation); stage 2 – Basin deepening (Green River Formation); stage 3 – Basin filling (Uinta Formation); and stage 4 – Late basin filling (Duchesne River Formation) (Keighley et al. 2003).

This chapter focuses on the uppermost Uinta Formation and the basal member of the Duchesne River Formation (Brennan Basin Member: Db), which are exposed at Blacktail Mountain in the western Uinta Basin. Here, the Uinta Formation is composed of upward-coarsening sequences of green mudstones and tabular sandstones that represent a

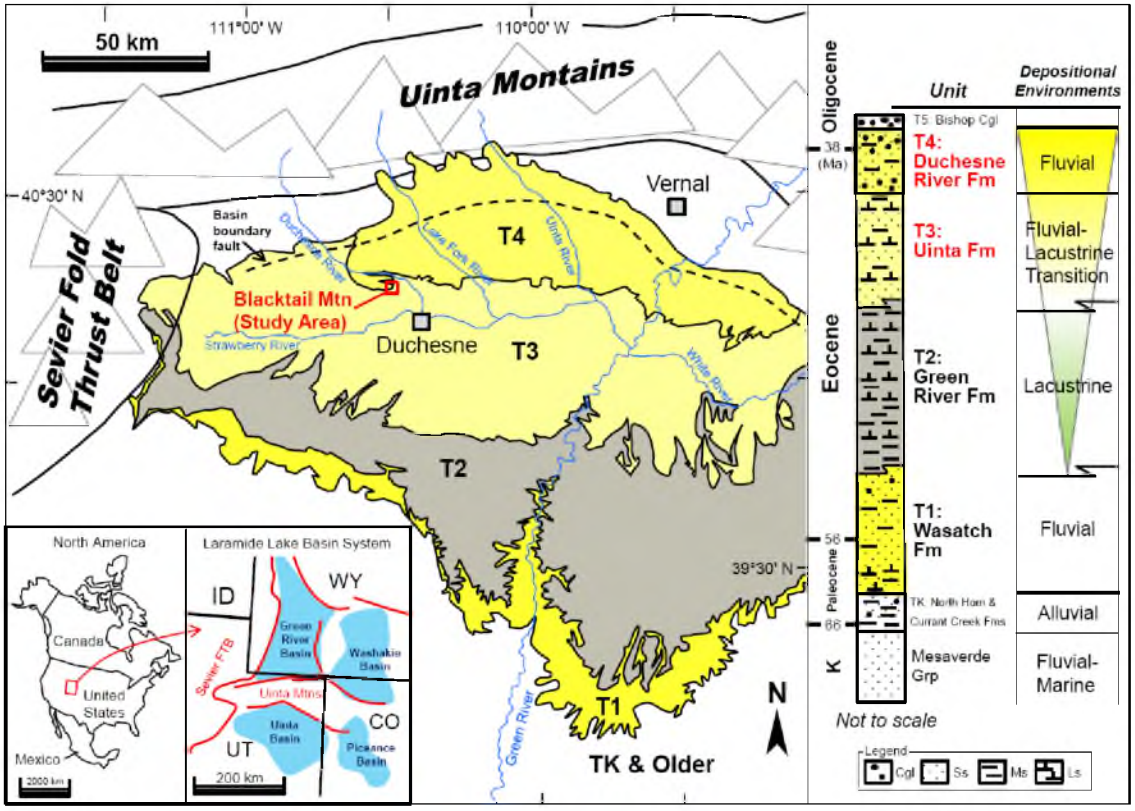

Figure 4.1. Index map and schematic geologic column showing the Paleogene sequence of the Uinta Basin. The regional dip is to the north and formations get progressively younger toward the Uinta Mountains. The basin is surrounded by the high mountain ranges of the Uinta Mountains and Sevier Fold Thrust Belt (FTB). Units T2 to T4 exhibit a typical upward-coarsening/shallowing lacustrine basin-fill sequence. The map of Laramide Lake Basin System is from Dickinson et al. (1988). The geological map is modified from Andersen and Picard (1974), Bryant et al. (1989), Bryant (1992), Hintze et al. (2000), and Sprinkel (2006, 2007).

lacustrine deltaic system, and the overlying Db is characterized by upward-fining sequences of channelized sandstones and red mudstones that represent a braided fluvial system.

4.3.2 Previous Studies

Only a limited number of papers have reported the stratigraphy and sedimentology of the Uinta and Duchesne River Formations, probably because of their lesser economic significance compared with the underlying renowned Green River Formation. Andersen and Picard (1972) published a comprehensive stratigraphic study of the Duchesne River Formation, and defined the four currently accepted members of this formation. This builds upon a recent

regional sequence stratigraphic study of the Duchesne River Formation (Chapter 1 of this paper). However, there is no comprehensive stratigraphic or sedimentological study available on the Uinta Formation, although some general stratigraphic and sedimentological descriptions and paleogeographic interpretations are given in older studies (e.g., Stagner 1941; Bruhn et al. 1983, 1986; Bryant 1989).

Moore et al. (2012) and Archer et al. (2012) studied the lacustrine deltaic sandstones of the Green River Formation of the Uinta Basin, which involved outcrop-based reservoir characterization and modeling. However, reservoir studies of the overlying Uinta and Duchesne River Formations that can provide new perspectives on a fluvial system are presented here for the first time.

4.4 Data Collection and Methods

A GigaPan photo and four measured sections (MS-1, MS-2, MS-3, and MS-4, totaling 673 m in length) were acquired from a cliff-face 206 m high by 1856 m wide, on the eastern flank of Blacktail Mountain (Figs 4.2a and 4.2b). Although the photo was acquired from a location perpendicular to the cliff-face, there are still substantial distortions along the vertical axis, which make it difficult to extract geological data (e.g., channel size) consistent enough for quantitative analysis. Therefore, a scale correction factor "s" (0.85 to 1.22 depending on the height of the cliff-face) was calculated based on the difference between measured section lengths and photo-based lengths, in order to obtain a more realistic vertical thickness (Fig. 4.2a).

A hundred ninety-three (193) paleocurrent measurements were collected to improve our understanding of the regional depositional system and to make geometric corrections to the sedimentary bodies (channels) (Fig. 4.2c). In addition, 118 m of surface gamma ray data (average data point interval: 0.3 m) were acquired along MS-1, to allow us to recognize log patterns and the cyclicity of exposed formations, which support sequence stratigraphic interpretations on this cliff-face. These data are also used for a regional correlation with subsurface well data. Six oil wells drilled in the 1992 to 2011 were chosen for their proximity to

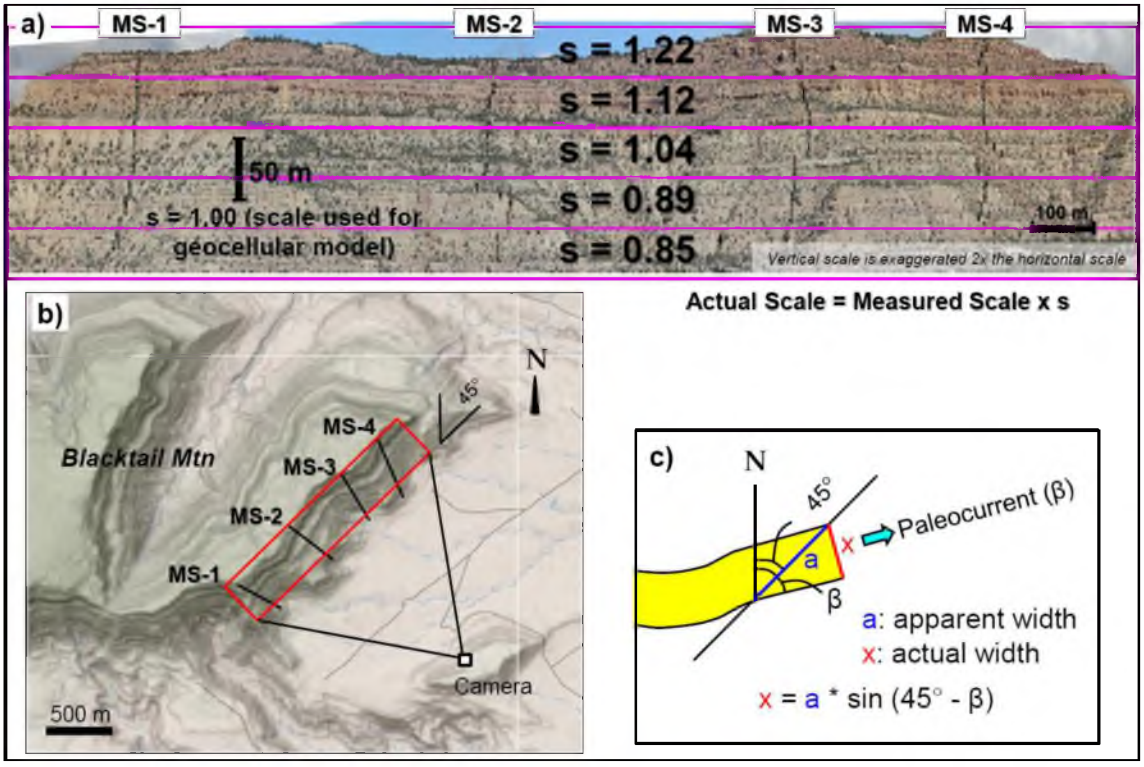

Figure 4.2. Blacktail outcrop photo. a) A GigaPan photo showing the locations of four measured sections and scale correction factors "s". b) Locations of cliff-face with measured sections, also showing where the GigaPan photo was taken from (square labeled "camera"). Topographic base map is from Utah Oil and Gas Map 2.0.0 (Utah Department of Natural Resources). c) An example of geometric correction to obtain the actual width of a fluvial channel using cliff-face strike (45°), apparent width (a), and paleocurrent orientation (β).

the Blacktail locality (within 30 km), provided by the Utah oil and gas well database (Utah Department of Natural Resources).

The following workflow was applied to build the outcrop-based geomodels: 1) sedimentary facies definition and recognition on measured sections; 2) construction of a sequence stratigraphic framework with detailed outcrop interpretations; and 3) grid/cell geometry set-up and translation of photo interpretations into a pixel-based geomodel. These tasks are sequentially described in the next section, and then several reservoir modeling techniques are evaluated and also the model strengths and weaknesses are discussed in the later sections.

4.5 Facies Classification and Outcrop Interpretation

4.5.1 Sedimentary Facies Classification and Gamma Ray Log

Five facies (F1 to F5) in lacustrine deposits (Uinta Formation) and three facies (F6 to F8) in fluvial deposits (Duchesne River Formation) were defined in measured sections (detailed lithological descriptions and interpreted depositional environments for each facies are given in Table 4.1). Lacustrine deposits are comprised of: F1 (distributary channel): fine- to very coarse-grained, trough cross-stratified sandstones with channelized shapes; F2 (delta plain): dominant massive or mottled mudstones and siltstones with interbedded sandstones; F3 (stream mouth bar): tabular sandstones with minor thin-layered siltstones and mudstones; F4 (distal delta front – prodelta): dominant laminated mudstones with interbedded sandstones, siltstones, and limestones; and F5 (debris/mass flow): large, angular mudstone, limestone, and sandstone blocks floating in mudstone matrix. Fluvial deposits are comprised of: F6 (fluvial channel): fine- to very coarse-grained, trough cross-stratified sandstones with channelized shapes; F7 (flood plain): dominant mottled mudstones with interbedded thin-layered sandstones and siltstones; and F8 (overbank sandstone >1 m thick): very fine- to medium-grained, massive or trough cross-stratified (occasionally indistinct) sandstones.

Typically, these facies are organized in regular, cyclic patterns in the lacustrine and fluvial units. The lacustrine deposits form upward-coarsening/shallowing parasequences (see idealized parasequences and gamma ray log patterns in Fig. 4.3a). Here, facies F4A (distal delta front) and F4B (prodelta) are generally distinguishable. However, they are not always possible to distinguish in this outcrop, because both are muddy slope-forming facies and tend to be covered. The fluvial deposits form upward-fining parasequences (see idealized parasequences and gamma ray log patterns in Fig. 4.3b). Here, facies F8 (overbank sandstone >1 m thick) could strictly be part of facies F7 (flood plain). However, because sandstones more than 1 m thick are recognizable and traceable in the GigaPan photo, and it is meaningful to distinguish those sandstones from the viewpoint of reservoir characterization, facies F8 (overbank sandstone >1 m thick) was separated from facies F7 (flood plain) in this study.

Table 4.1. Interpreted Facies Classifications and Descriptions

	Name (Depositional Environment)	Descriptive Name	Lith	Grain Size	Color	Sorting	Shape	Sedimentary Structures	Other Remarks	NTG
Five Facies in Lacustrine Uin	F1. Distributary Channel / TDC	Ss	Ss	Fine to very coarse	Orange, yellowish gray, light gray	Poor to well	Channelized	Trough cross-bedding	Erosional base, rip-up clasts, rarely thin mudstone drapes	0.97
	F2. Delta Plain (Overbank)	Dominant ms and slts with interbeded ss	Ss	Very fine- to very coarse	Orange, yellowish gray, light gray, reddish gray	Very poor to well	Tabular or channelized	Intistinct trough cross-bedding, massive, or wave rippled,	Occasionally bioturbated	0.19
			Slts/Ms	Clay to silt	(Slts) Green to yellow, (Ms) Green to red	N/A	N/A	(Ms) Massive or mottled	(Slts) Occasionally carbonaceous materials	
	F3. Stream Mouth bar	Ss with minor slts/ms	Ss	Fine- to medium	Yellowish gray/white, orange	Moderate to well	Tabular	Commonly parallel and planar cross-bedding, occasionally trough cross-bedding, current and wave ripple	Interbedded with thin-layered or laminated green and yellow slts or ms.	0.87
	F4. Distal Delta Front (F4A) – Prodelta (F4B)	F4A - Alternating beds of ss, ms, slts and ls F4B - Ms with minor ls and ss/slts	Ss/Slts	Silt-sized to fine	Yellowish white	Moderate to well	Tabular, thin-layered	Massive or parallel laminated	N/A	0.05
			Ms	Clay	Green and dark gray	N/A	N/A	Thinly-laminated	N/A	
			Ls	Clay-size	Tan, dark gray	N/A	Mounded or thin-layered	Massive, occasionally stromatolitic structures	N/A	
	F5. Debris/Mass Flow	Large, angular ms, ls and ss blocks floating in red ms matrix, characterized by slumping structures (e.g., abnormal structural dip).								0.48
Three Facies in Fluvial Unit	F6. Fluvial Channel	Ss	Ss	Fine to very coarse, granule in part	Yellowish gray, reddish gray, orange, light gray	Poor to well	Channelized	Trough cross-bedding	Erosional base, rip-up clasts, rarely thin and lenticular red ms interbedded	0.98
	F7. Flood Plain	Dominant ms with interbedded ss and slts	Ms	Clay to silt	Red to maroon,	N/A	N/A	Mottled	Commonly bioturbated	0.27
			Ss/Slts	Silt-sized to medium-grained	Yellowish gray, reddish gray, orange	Poor to well sorted	Thin-layered	Massive or indistinct trough cross-bedding	Occasionally bioturbated, accumulation of clays	
	F8. Overbank Sandstone (>1 m)	Ss	Ss	Very fine to medium, silty in part	Yellowish gray, reddish gray, orange	Poor to well sorted	Tabular to channelized	Massive or indistinct trough cross-bedding	Occasionally bioturbated, accumulation of clays	0.8

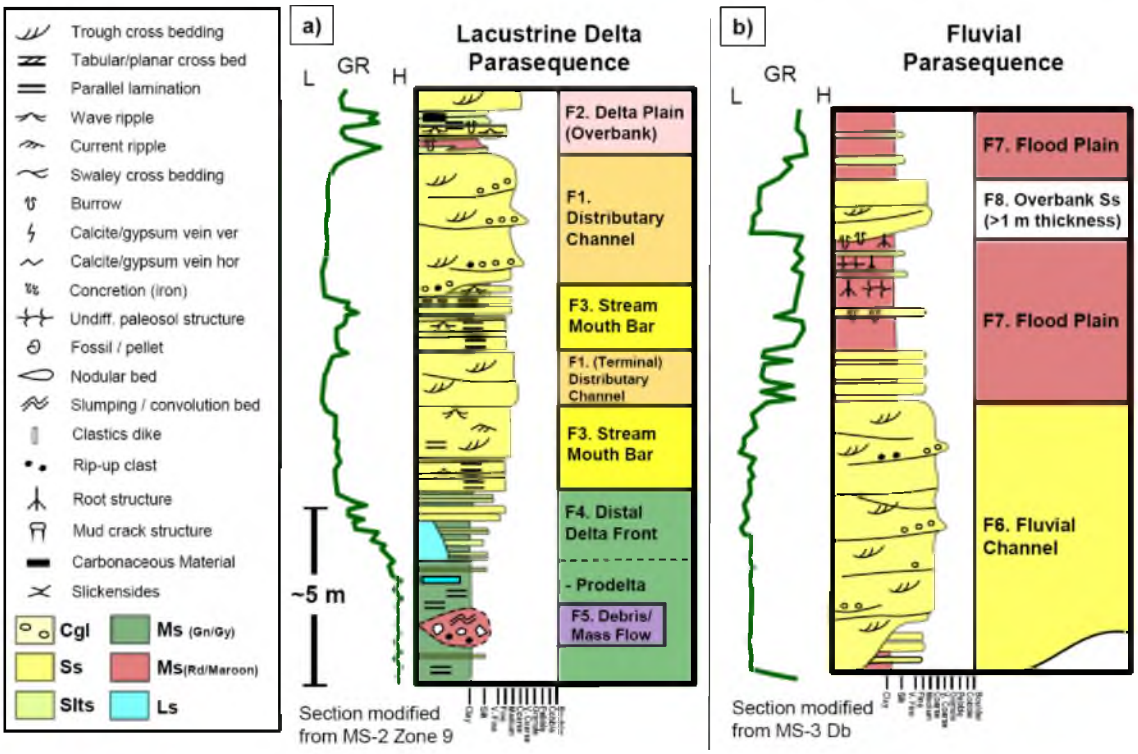

Figure 4.3. Idealized parasequences. a) lacustrine deltaic parasequence and gamma ray (GR) log pattern. The upward-shallowing sequence consists of five lacustrine facies (F1 to F5). b) fluvial parasequence and gamma ray (GR) log pattern. The upward-fining sequence consists of three fluvial facies (F6 to F8). See Table 4.1 for detailed descriptions of each facies.

The acquired measured section gamma ray data along MS-1 exhibit log patterns typical of a lacustrine deltaic prograding system (e.g., Bohacs 2012) and fluvial sequence (e.g., Bridge and Tye 2000). These data were correlated reasonably well to the subsurface well logs covering the same stratigraphic levels in a 30 km west-east section (Fig. 4.4).

4.5.2 Outcrop Interpretation (Sequence Stratigraphic Framework and Zonation)

To produce a sequence stratigraphic framework for the Blacktail outcrop, initially the sequence boundary (i.e., formation boundary between the Uinta and Duchesne River formations) was placed at the unconformable base of the first occurrence of fluvial channels (Fig. 4.5). Then nine major flooding surfaces (FS1 to FS9) distinguish nine major parasequences (unit name: U1 to U9) in the lacustrine Uinta Formation that range ~10-20 m thick. In addition, five minor flooding surfaces (FS1.5, FS2.5, FS6.5, F7.5, FS9.5) were

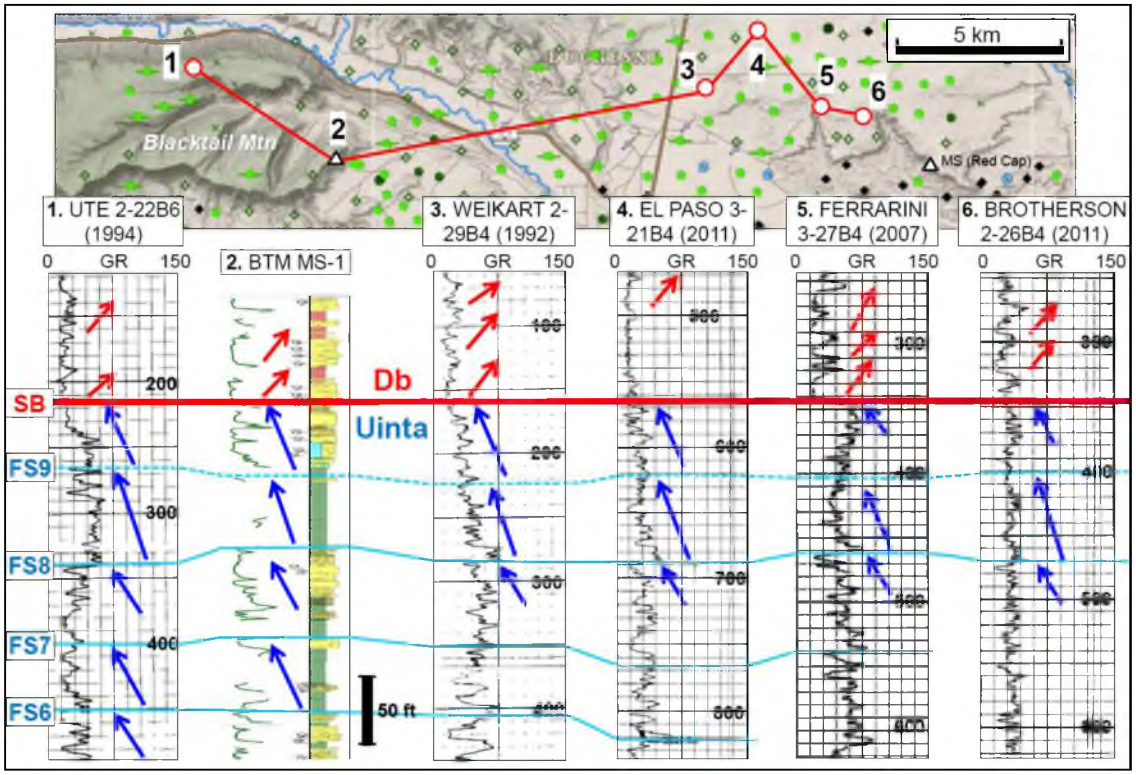

Figure 4.4. Surface (MS-1) to subsurface (six wells) gamma ray correlations in a 30 km west-east section. The uppermost Uinta Formation exhibits typical upward-coarsening parasequences (i.e., prograding lacustrine deltaic system), whereas the basal member of the Duchesne River Formation (Db) shows typical upward-fining parasequences (i.e., aggradational fluvial system).

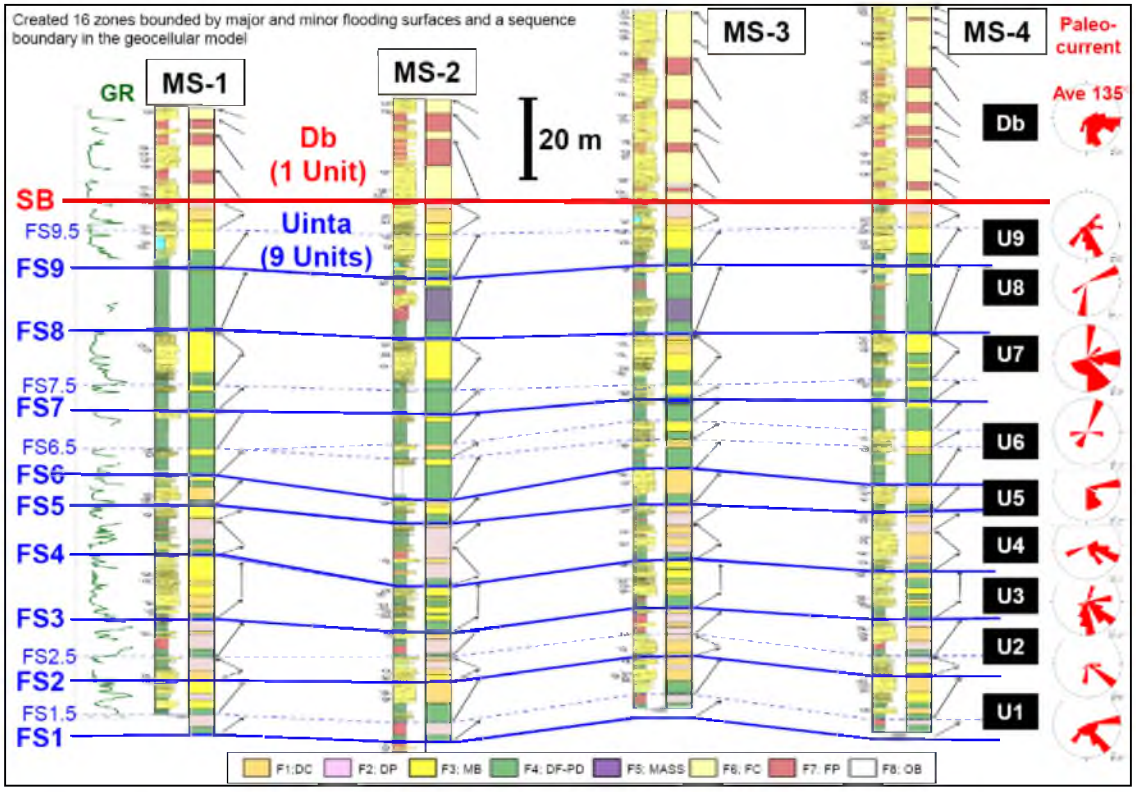

Figure 4.5. Sequence stratigraphic framework of the Blacktail outcrop. The Uinta Formation consists of nine units bounded by major flooding surfaces (FS) and Db has one unit, bounded by a basal sequence boundary (SB). Facies (DC = Distributary Channel, DP = Delta Plain, MB = Mouth Bar, DF-PD = Distal Delta Front to Prodelta, MASS = Mass/Debris flow, FC = Fluvial Channel, FP = Flood Plain, OB = Overbank Ss >1 m) were defined along each measured section.

interpreted to constrain smaller, thinner (<10 m thick) parasequences (subunits), resulting in 15 zones (units + subunits) bounded by major and minor flooding surfaces (Fig. 4.5). In contrast, because no regionally traceable surface is recognized within the fluvial deposits of Db except the basal sequence boundary, Db was treated as only one unit/zone (Fig. 4.5).

Then the facies interpretations were overlain on the high-resolution GigaPan photo (Fig. 4.6). It should be noted that only a sandbody or bundled sandbodies (with thin, minor mudstones) > 1 m thick could be recognized in this photo. In other words, sandbodies < 1 m thick could not be evaluated in this study.

Quantitative sandbody geometry data, such as channel width:thickness ratio, are useful for the spatial prediction of geological objects (e.g., Fielding and Crane 1987; Hirst 1991;

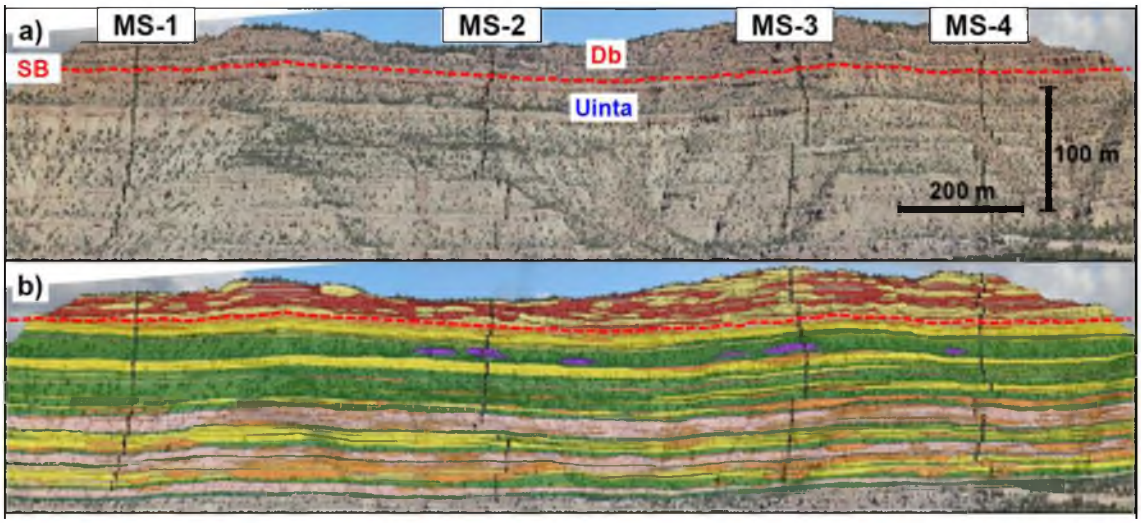

Figure 4.6. Blacktail outcrop interpretation. a) Original outcrop and b) interpreted GigaPan photo of the Blacktail cliff-face. Vertical scale is twice the horizontal scale. See the color code in Figure 4.5 for key to interpreted facies.

Reynolds 1999; Gibling 2006). Because channel geometrical statistics were essential for reservoir modeling, fluvial channel geometry data were extracted from this photo interpretation of the fluvial unit (Db). The widths of fluvial channels that intersect measured sections were corrected using measured paleocurrent data. The widths of channels that do not intersect measured sections were corrected using the average orientation (135°) of 59 paleocurrent measurements (based on trough cross-bedding in channelized sandstones) from Db, so these data must be treated with caution (Fig. 4.7). Aspect ratios (thickness divided by width) vary from 0.015 to 0.12 and histograms of channel thickness and channel width exhibit highly skewed, lognormal-like distributions (Fig. 4.7).

4.5.3 Translation into Outcrop Reference

Outcrop interpretations (bounding surfaces and facies) were precisely translated into a pixel-based geomodel (i.e., outcrop reference), which has 160 (I) x 4 (J) x 189 (layer) = 120,960 cells (18,871 cells in Db) (Fig. 4.8). In this outcrop reference, facies (F1 to F8) were assigned manually into each cell. A horizontal cell size of 10 m x 10 m and an average cell height of 1 m were used to represent outcrop-based interpretations.

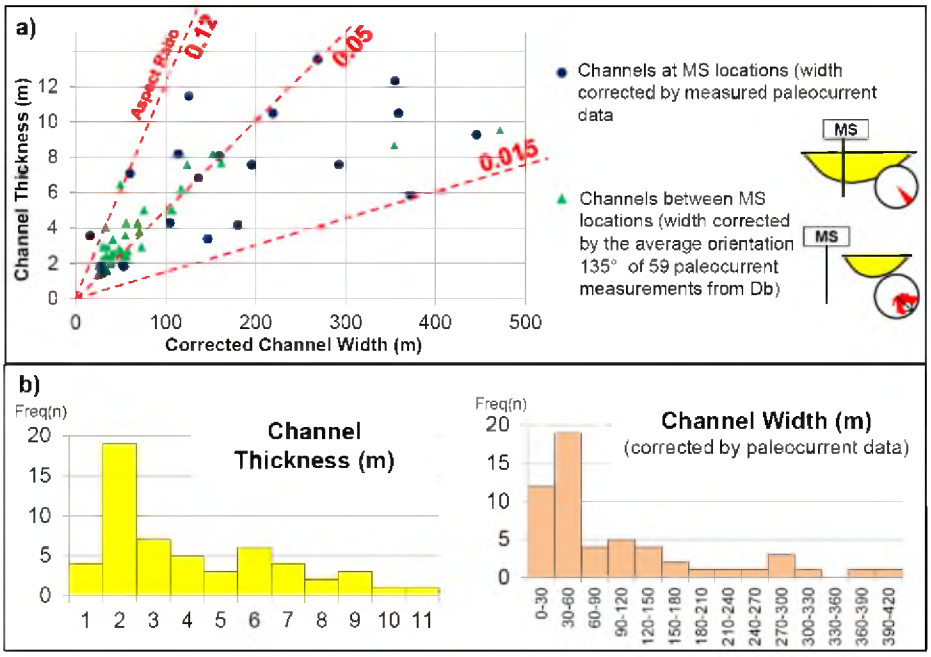

Figure 4.7. Quantitative sandbody geometry data extracted from the fluvial unit (Db). a) Cross-plot of channel width (X-axis) and thickness (Y-axis). The resulting aspect ratios (thickness divided by width) vary from 0.015 to 0.12. Green triangles show supplemental data with channel widths corrected by the average paleocurrent direction, 135° (because there was no direct paleocurrent measurement). b) Histograms of channel thickness and corrected width, showing highly skewed, lognormal-like distributions.

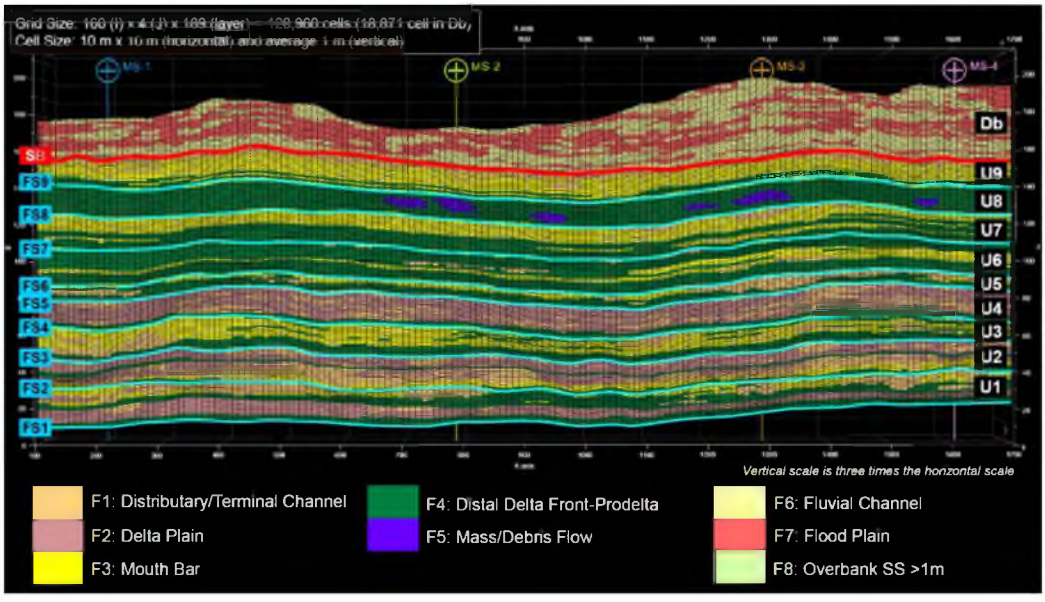

Figure 4.8. A pixel-based geomodel based on the outcrop interpretation (i.e., outcrop reference) in which facies were assigned manually into each cell. Vertical scale is three times the horizontal scale.

4.6 Evaluation of Reservoir Modeling Techniques

In many subsurface studies with a limited number of vertical wells, there is a common challenge to justify a reservoir modeling technique, define input parameters, and evaluate resulting models/realizations. Here, several common modeling techniques and input parameters are tested focusing on the fluvial unit (Db) which exhibits the most complicated reservoir (fluvial channel) architectures. The resulting models/realizations are evaluated by using the outcrop reference that should be the best answer through modeling technique/parameter tests. This section presents geomodels of the fluvial unit (Db) generated by three techniques: 1) indicator kriging; 2) sequential indicator simulation; and 3) object-based modeling (Table 4.2), in which two measured sections (MS-1 and MS-4) were used as constraints (hard data). Subsequently, these models are compared and evaluated, using static connectivity analysis to determine which modeling technique most closely reproduced the static sandbody connectivity characteristics of the outcrop reference.

4.6.1 Geomodel Generations by Three Different Techniques

4.6.1.1 Indicator Kriging (IK)

A simple deterministic interpolation method, indicator kriging, was first tested by using a variogram model with a long horizontal range, greater than well spacing (variogram setting: isotropic; horizontal range: 2000 m). As expected, the resulting geomodel revealed unrealistically continuous facies architectures (Fig. 4.9a).

4.6.1.2 Sequential Indicator Simulation (SIS)

SIS is a variogram-based stochastic modeling approach typically applied to facies modeling. Variogram models used for this simulation were derived from the analysis of the outcrop reference (geomodel) of Db. The vertical variogram model was well fitted by an exponential model with a 5 m range and 0.0001 nugget. However, the horizontal variogram model was best fitted by exponential models with a range of 70–100 m and 0.0001 nugget. This study therefore tested two scenarios, with horizontal variogram ranges of 100 m and 70 m,

Table 4.2. Geomodels Examined

Geomodel Name (ID)	Method	Scenario	No. of Realizations
IK	Indicator Kriging	Deterministic; one scenario only	n/a
SIS1 R1 to R10 SIS2 R1 to R10	Sequential Indicator Simulation (SIS)	Scenario 1: Horizontal Range: 100 m Scenario 2: Horizontal Range: 70 m	10 realizations for each scenario
OB R1 to R10	Object-based (Stochastic) Modeling	One scenario only, using skewed distribution based on measured channel thickness and width	10 realizations

respectively. A global facies fraction of 50% for F6 (fluvial channel) and 50% for F7 (flood plain) and F8 (overbank), which was calculated from the outcrop reference, was used as another constraint for SIS, for comparability with the outcrop reference. Because this method is stochastic, 10 realizations were obtained for each scenario to understand the variability among realizations. The resulting geomodels/realizations better represent discontinuous fluvial channel features (some examples of realizations are shown in Fig. 4.9b to 4.9e). Realizations from the scenario with a longer horizontal variogram range seem to have slightly more continuous channel facies than those from the second scenario.

4.6.1.3 Object-based Stochastic Modeling (OB)

Object-based stochastic modeling (also known as Boolean modeling) is commonly used for facies modeling. In this method, geological objects such as channels and mounds are stochastically distributed based on their geometric parameters and orientations. Because the width:thickness statistics and flow directions of fluvial channels were obtained from the outcrop reference of Db (Fig. 4.7), similar statistics were used for OB modeling. The applied statistics were: a) channel width (m) – skewed triangle distribution (min: 15, med: 45, max: 150); b) channel thickness (m) – skewed triangle distribution (min: 1, med: 2, max: 6); and c) channel

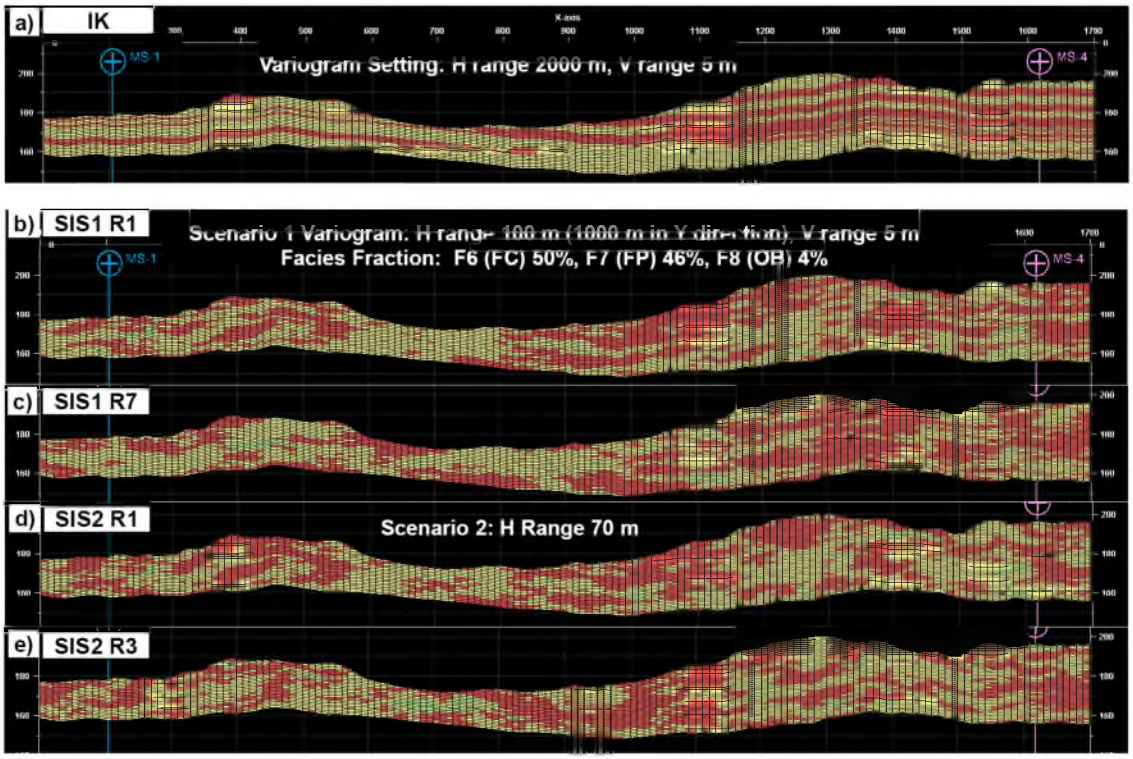

Figure 4.9. Examples of geomodels generated by a) indicator kriging (IK), b) and c) sequential indicator simulation (SIS) scenario 1, and d) and e) SIS scenario 2. Two measured sections (MS-1 and MS-4) were used as constraints (hard data).

orientation – normal to cliff-face ±50° (Fig. 4.10). In addition, a global facies fraction of F6 (fluvial channel): 50% and F7 (flood plain) and F8 (overbank): 50% was used as another constraint in order to ensure comparability with the outcrop reference. Because this method is stochastic, 10 realizations were obtained to quantify the variability among realizations. The resulting geomodels/realizations show a reasonable approximation of discontinuous fluvial channel features (Fig. 4.11).

4.6.2 Geomodel Comparisons and Evaluations (Static Connectivity Analysis)

There are several ways to select the geomodel that best fits the outcrop reference, such as examinations of: 1) similarity in reservoir cell location; 2) reservoir connectivity; 3) reservoir volumetrics; and 4) dynamic behavior/flow simulations. This study examined a static (wellbore) connectivity analysis (Larue and Hovadik 2006; Pranter and Sommer 2011), because it is a

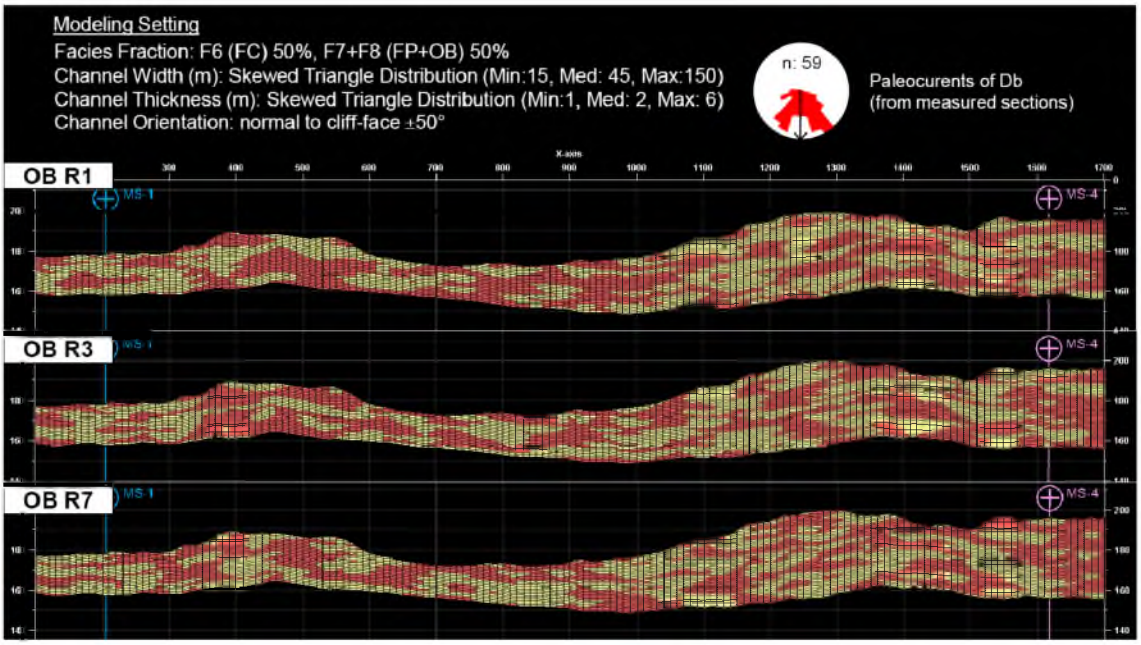

Figure 4.10. Examples of geomodels generated by object-based (OB) stochastic modeling. Two measured sections (MS-1 and MS-4) were used as constraints (hard data).

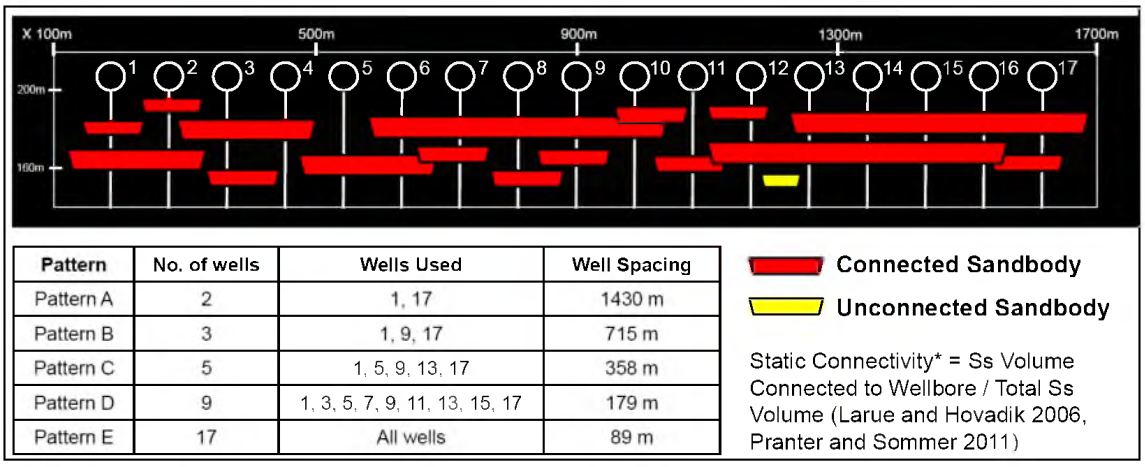

Pattern	No. of wells	Wells Used	Well Spacing
Pattern A	2	1, 17	1430 m
Pattern B	3	1, 9, 17	715 m
Pattern C	5	1, 5, 9, 13, 17	358 m
Pattern D	9	1, 3, 5, 7, 9, 11, 13, 15, 17	179 m
Pattern E	17	All wells	89 m

Connected Sandbody

Unconnected Sandbody

Static Connectivity* = Ss Volume Connected to Wellbore / Total Ss Volume (Larue and Hovadik 2006, Pranter and Sommer 2011)

Figure 4.11. Five patterns of well deployment and locations of 17 wells, with schematic connected and unconnected fluvial channels. Note that static (wellbore) connectivity is evaluated in stages at the scale of general well spacing (a few hundred to a few thousand meters). *In this study, cell number-based proportion (proportion of the number of "fluvial channel" cells connected to wellbore) was used rather than strict cell volume, although there is very little difference between the two methods.

simple concept closely associated with dynamic flow behaviors. Static connectivity has been defined by a simple equation: "sandstone volume connected to wellbore divided by total sandstone volume" (Pranter and Sommer 2011). In this study, cell number-based proportion (i.e., proportion of the number of F6: fluvial channel facies cells connected to the wellbore) was used rather than strict cell volume, although there is very little difference between the two methods because variation in cell size is small. Five patterns of well deployment (Pattern A to Pattern E), with a maximum of 17 wells (Fig. 4.11), were set to evaluate the trends in two-dimensional static connectivity along the wells for all geomodels/realizations.

The resulting plots of well patterns (A to E) versus connectivity (%) are shown in Figure 4.12. The plot of the outcrop reference (black line) has an s-shaped curve, as connectivity rapidly increases when well spacing decreases from 715 m (Pattern B) to 358 m (Pattern C). The IK geomodel (light green line) has an extremely high connectivity (> 95%) throughout. The SIS scenario 1 geomodels/realizations (Fig. 4.12a) tend to have higher connectivity than the outcrop reference, although some of the realizations fit the reference well. The SIS scenario 2 geomodel/realizations (Fig. 4.12b) fit the outcrop reference better than the SIS scenario 1 realizations. However, overall, there is great variability among the SIS geomodels/realizations. The OB geomodels/realizations (Fig. 4.12c) tend to fit the outcrop reference (black line) best, with s-shaped curves correctly reproduced in most realizations. However, there was one notable outlier: OB R1 (see Fig. 4.10), with extremely high connectivity (Fig. 4.12c). Average curves of geomodels generated by each stochastic method (SIS scenario 1, SIS scenario 2, and OB) also indicate that the OB geomodels/realizations fit the outcrop reference best (Fig. 4.13).

Collectively, the OB geomodels tend to fit the outcrop reference best in terms of two-dimensional static wellbore connectivity, if parameters for channel geometry are appropriately provided. However, an important lesson that this analysis highlights is that we should examine and compare multiple models/realizations carefully before selecting a representative model, because there may be substantial errors or outliers in stochastic models.

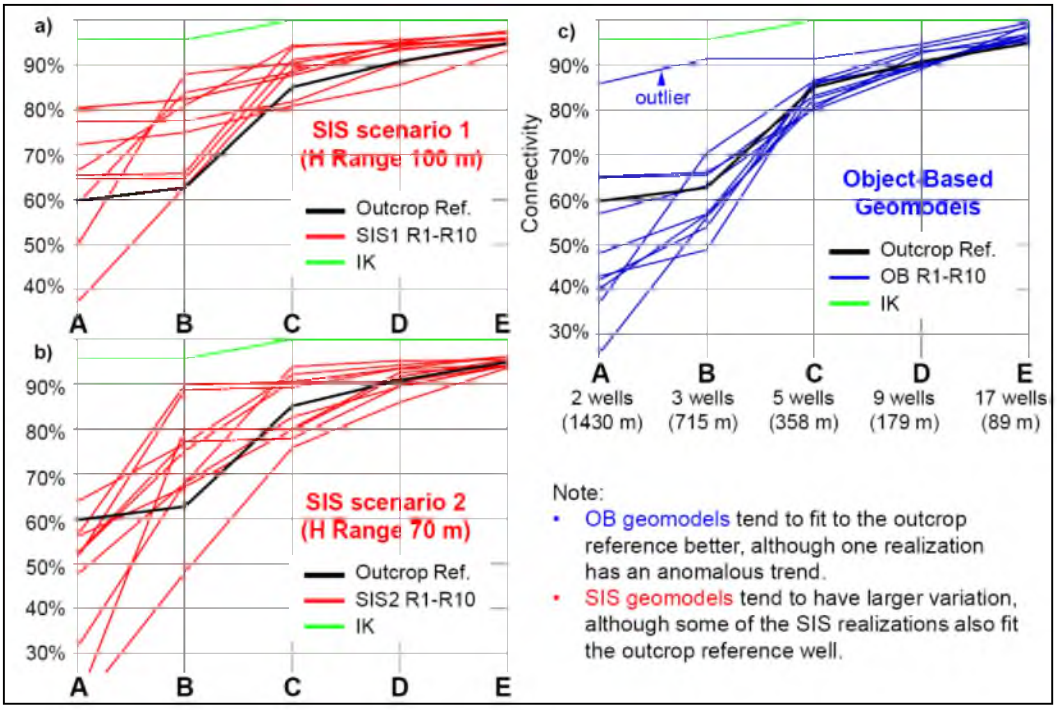

Figure 4.12. Static connectivity analysis (plots of well patterns A to E versus connectivity). Panels show comparisons of the outcrop reference and the IK model with 10 geomodels/realizations of (a) SIS scenario 1, (b) SIS scenario 2, and (c) the OB modeling.

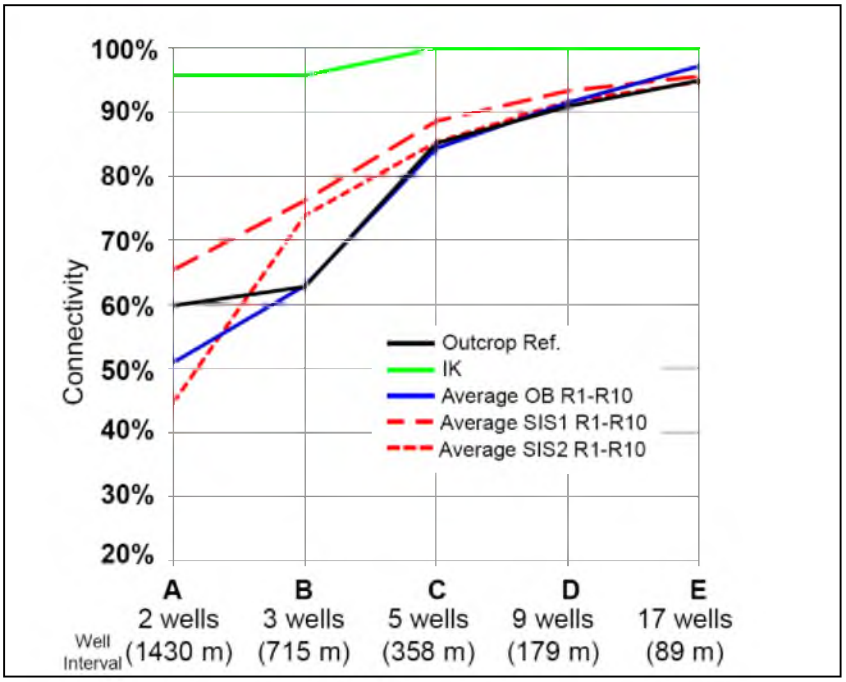

Figure 4.13. Comparisons of the static connectivity curve of the outcrop reference with average curves of geomodels/realizations by SIS scenario 1, SIS scenario 2, and OB modeling. Note that the average curve of OB geomodels fits the outcrop reference best.

4.6.3 Strengths and Weaknesses of Examined Modeling Techniques

This section summarizes strengths and weaknesses of modeling techniques examined in this study. Indicator kriging (IK) is a simple deterministic interpolation method and generally makes a smooth and laterally continuous geomodel. Thus, this method would work for laterally continuous facies (e.g., offshore mudstones) between control points/wells, whereas it is not suitable for modeling discontinuous geological patterns such as channels or mounds.

Sequential indicator simulation (SIS) is a variogram-based stochastic modeling technique, and is generally suitable to generate heterogeneous facies distributions. The advantage of this method is to leverage variogram models that can be obtained through data analysis of control well data, even if specific statistics of geological patterns (e.g., channel size) are unknown. However, this method is not suitable to depict specific geological shapes such as channel and mound.

In object-based stochastic modeling (Boolean modeling), geological objects such as channels and mounds are stochastically distributed based on their geometric parameters and orientations. Although this method is suitable to depict different sizes and shapes of specific geological objects (e.g., channel), it is not always easy to obtain accurate input geometric parameters from a limited number of control wells. If we use wrong input parameters, there may be fatal errors in the resulting geomodels.

4.7 Discussion

In this study, geological models were evaluated by examining two-dimensional (i.e., sectional) sandbody connectivity. However, some researchers have demonstrated that three-dimensional sandbody connectivity is much higher than two-dimensional (e.g., King 1990; Larue and Hovadik 2006; Hovadik and Larue 2007). In addition, sandstones on flood plains (overbank deposits), which were not considered as reservoir bodies in this outcrop reference, are still likely to act as conduits because of their porosity and lateral continuity. These assumptions need to be tested in order to construct more sophisticated three-dimensional geological models that realistically reflect dynamic flow behavior in subsurface layers.

Another aspect to explore is using the net-sandstone-to-gross-thickness ratio (NTG) as a variable in the models. It is commonly known that cross-plots of NTG (%) and connectivity (%) show an s-curve with a cascade zone, i.e., connectivity drastically increases at a certain NTG ratio (e.g., Allen 1978; Larue and Hovadik 2006; Pranter and Sommer 2011). Only the case of a 50% NTG (i.e., fluvial channel: 50% and flood plain: 50%) was tested in this study, based on the actual outcrop reference interpretation. Because a variety of fluvial systems exists worldwide, an investigation of the sensitivity of NTG to static connectivity will be an important topic for global applications.

Multiple-point statistics (MPS) is a modeling technique that makes use of training images, i.e., a database of geological patterns (Caers 2001; Strebelle 2002; Caers and Zhang 2004). This technique is becoming increasingly popular, and it is used in some outcrop-based studies (e.g., Falivene et al. 2006). In the future, it may be worth investigating the application of this method to the Blacktail Mountain outcrop in order to compare with other techniques examined in this chapter.

Lacustrine deltaic sandstones of the Uinta Formation generally have more laterally continuous shapes than those of the fluvial unit (Db) on the Blacktail Mountain cliff-face. Although this study did not investigate a reservoir modeling technique to model this lacustrine unit, this may be worth doing if there is a substantial difference in the properties (e.g., porosity and permeability) of the mouth bar and the distributary channel sandstones. Stochastic reservoir modeling techniques would be useful to model such heterogeneous reservoir distributions.

4.8 Conclusions

This study provided a robust sequence stratigraphic framework and detailed facies architecture (defined five facies in lacustrine deposits and three facies in fluvial deposits) on the Blacktail Mountain outcrop, using a GigaPan photo (covering a cliff-face 206 m high x 1856 m wide), four measured sections, and surface gamma ray data. This outcrop interpretation, which reveals facies and reservoir body characteristics (e.g., shape and size/continuity) at the usual

scale of well spacing (over a thousand meters), is a valuable analog example for reservoir modeling in similar fluvial-lacustrine settings in subsurfaces.

Several reservoir modeling techniques (indicator kriging, sequential indicator simulation, and object-based modeling) were tested on the fluvial unit (Db), constrained by: a) two measured sections as hard data, b) global facies proportions of 50% fluvial channel and 50% flood plain, and c) channel geometries (variogram or width:depth statistics). The resulting geomodels were compared with the outcrop reference and quantitatively evaluated by the static sandbody connectivity analysis. This analysis showed that object-based geomodels fit the outcrop reference best in terms of wellbore connectivity, although one realization showed a large deviation from the reference. This reservoir modeling study revealed the utility of input parameters such as statistics of channel geometries for computer-based geological modeling projects, and successfully demonstrated which stochastic modeling techniques best represent the observed depositional patterns derived from outcrop data.

4.9 References

Allen, J.R.L., 1978, Studies in fluviatile sedimentation: An exploratory quantitative model for the architecture of avulsion-controlled alluvial sites: Sedimentary Geology, v. 21, p. 129–147.

Andersen, D.W., and Picard, M.D., I974, Evolution of synorogenic clastic deposits in the intermontane Uinta Basin of Utah, *in* Dickinson, W.R., ed., Tectonics and Sedimentation: SEPM Special Publication, v. 22, p. 167-189.

Archer, R., Robbana, E., Ritts, B.D., Moore, J., Johnson, C., and Taylor, A., 2012, Reservoir simulation models of an Eocene Lacustrine Delta, Green River Formation, Southwest Uinta Basin, Utah, *in* Baganz, O.W., Bartov, Y., Bohacs, K., and Nummedal, D., eds., Lacustrine sandstone reservoirs and hydrocarbon systems: American Association of Petroleum Geologists Memoir, v. 95, p.209-221.

Bohacs, K.M., 2012, Relation of hydrocarbon reservoir potential to Lake-Basin type: An integrated approach to unraveling complex genetic relations among Fluvial, Lake-Plain, Lake Margin, and Lake Center Strata, *in* Baganz, O.W., Bartov, Y., Bohacs, K., and Nummedal, D., eds., Lacustrine sandstone reservoirs and hydrocarbon systems: American Association of Petroleum Geologists Memoir, v. 95, p. 13-56.

Bruhn, R.L., Picard, M.D., and Beck, S.L., 1983, Mesozoic and early Tertiary structure and sedimentology of the central Wasatch Mountains, Uinta Mountains, and Uinta Basin: Utah Geological and Mineralogical Survey Special Studies 59, Salt Lake City, p. 63–105.

Bruhn, R.L., Picard, M.D., and Isby, J.S., 1986, Tectonics and sedimentation of Uinta arch, western Uinta Mountains and Uinta Basin, *in* Peterson. J.A., ed., Paleotectonics and sedimentation in Rocky Mountain region, United States: American Association of Petroleum Geologists Memoir, v. 41, p. 333-352.

Bridge, J.S., and Tye, R.S., 2000, Interpreting the dimensions of ancient fluvial channel bars, channels, and channel belts from wireline-logs and cores: American Association of Petroleum Geologists Bulletin, v. 84, p. 1205-1228.

Bryant, B., Naeser, C.W., Marvin, R.F., and Mehnert, H.H., 1989, Upper Cretaceous and Paleogene sedimentary rocks and isotopic ages of Paleogene tuffs, Uinta Basin, Utah: U.S. Geological Survey Bulletin 1787-J, 22 p.

Bryant, B., 1992, Geologic and structure maps of the Salt Lake City 1 degree x 2 degrees quadrangle, Utah and Wyoming: U.S. Geological Survey Miscellaneous Investigations Series Map I-1997.

Bryant, I.D., and Flint, S.S., 1993, Quantitative clastic reservoir geological modelling: problems and perspectives, *in* Flint, S.S., and Bryant, I.D., eds., The geological modelling of hydrocarbon reservoirs and outcrop analogues: International Association of Sedimentologists Special Publication, v. 15, p. 3-20.

Caers, J., and Zhang, T., 2004, Multiple-point geostatistics: A quantitative vehicle for integrating geologic analogs into multiple reservoir models, in Integration of outcrop and modern analogs in reservoir modeling: American Association of Petroleum Geologists Memoir, v. 80, p. 383-394.

Ciftci, B.N., Aviantara, A.A., Hurley, N.F., and Kerr, D.R., 2004, Outcrop-based three-dimensional modeling of the Tensleep Sandstone at Alkali Creek, Bighorn Basin, Wyoming, *in* Grammer, G.M., Harris, P.M., and Eberli, G.P., eds., Integration of outcrop and modern analogs in reservoir modeling: American Association of Petroleum Geologists Memoir, v. 80, p. 235 – 259.

Dickinson, W.R., Klute, M.A., Hayes, M.J., Janecke, S.U., Lundin, E.R., McKittrick, M.A., and Olivares, M.D., 1988, Paleogeographic and paleotectonic setting of Laramide sedimentary basins in the central Rocky Mountain region: Geological Society of America Bulletin, v.100, p. 1023-1039.

Dutton, S.P., White, C.D., Willis, B.J., and Novakovic, D., 2002, Calcite cement distribution and its effect on fluid flow in a deltaic sandstone, Frontier Formation, Wyoming: American Association of Petroleum Geologists Bulletin, v. 86, p. 2007-2021.

Falivene, O., Arbues, P., Gardiner, A., Pickup, G., Munoz, J.A., and Cabrera, L., 2006, Best practice stochastic facies modeling from a channel-fill turbidite sandstone analog (the Quarry outcrop, Eocene Ainsa basin, northeast Spain): American Association of Petroleum Geologists Bulletin, v. 90, p. 1003-1029.

Fielding, C.R., and Crane, R., 1987, An application of statistical modelling to the prediction of hydrocarbon recovery factors in fluvial reservoir sequences, *in* Ethridge, F.C., Flores, R.M., and Harvey, M.D., eds., Recent developments in fluvial sedimentology: SEPM Special Publication, v. 39, p. 321-327.

Fouch, T.D., 1975, Lithofacies and related hydrocarbon accumulations in Tertiary strata of the western and central Uinta Basin, Utah, *in* Bolyard, D.W., ed., Deep drilling frontiers of the central Rocky Mountains: Rocky Mountain Association of Geologists Symposium, Denver, Colorado, p. 163–173.

Gibling, M.R., 2006, Width and thickness of fluvial channel bodies and valley fills in the geological record: a literature compilation and classification, Journal of Sedimentary Research, v. 76, p. 731–770.

Hintze, L.F, Willis, G.C., Laes, D.Y.M., Sprinkel, D.A., and Brown, K.D., 2000, Digital geologic

map of Utah 1:500000: Utah Geological Survey.

Hirst, J.P.P., 1991, Variations in alluvial architecture across the Oligo–Miocene Huesca fluvial system, Ebro basin, Spain, *in* Miall, A.D., and Tyler, N., eds., The three-dimensional facies architecture of terrigenous clastic sediments and its implications for hydrocarbon discovery and recovery: SEPM Concepts in Sedimentology and Paleontology, v. 3, p. 111-121.

Hovadik, J.M., and Larue, D.K., 2007, Static characterizations of reservoirs: refining the concepts of connectivity and continuity: Petroleum Geoscience, v. 13, p. 195–211.

Howell, J.A., Martinius, A.W., and Good, T.R., 2014, The application of outcrop analogues in geological modelling: a review, present status and future outlook: *in* Martinius, A.W., Howell, J.A., and Good, T.R., eds., Sediment-body geometry and heterogeneity: analogue studies for modelling the subsurface: Geological Society, London, Special Publications, v. 387, p. 1-25.

Keighley, D., Flint, S., Howell, J., and Moscariello, A., 2003, Sequence stratigraphy in lacustrine basins: a model for part of the Green River Formation (Eocene), southwest Uinta Basin, Utah: Journal of Sedimentary Research, v. 73, p. 987-1006.

Keogh, K.J., Martinius, A.W., and Osland, A., 2007, The development of fluvial stochastic modelling in the Norwegian oil industry: a historical review, subsurface implementation: Sedimentary Geology v. 202, p. 249–268.

King, P.R., 1990, The connectivity and conductivity of overlapping sand bodies, *in* Buller, A.T., Berg, E., Hjelmeland, O., Kleppe, J., Torsæter, O., and Aasen, J.O., eds., North Sea oil and gas reservoirs—II: London, Graham and Trotman, p. 353–362.

Labourdette, R., and Jones, R.R., 2007, Characterization of fluvial architectural elements using a three-dimensional outcrop data set: Escanilla braided system, South-Central Pyrenees, Spain: Geosphere, v. 3, p. 422-434.

Lambiase, J.J., 1990, A model for tectonic control of lacustrine stratigraphic sequences in continental rift basins, in Katz, B.J., ed., Lacustrine Basin Exploration—Case Studies and Modern Analogs: American Association of Petroleum Geologists Memoir 50, p. 265–276.

Larue, D.K., and Hovadik, J., 2006, Connectivity of channelized reservoirs: a modelling approach: Petroleum Geoscience, v. 12, p. 291-308.

Moore, J., Taylor, A., Johnson, C., Ritts, B.D., and Archer, R., 2012, Facies analysis, reservoir characterization, and LIDAR modeling of an Eocene Lacustrine Delta, Green River formation, Southwest Uinta basin, Utah, *in* Baganz, O.W., Bartov, Y., Bohacs, K., and Nummedal, D., eds., Lacustrine sandstone reservoirs and hydrocarbon systems: American Association of Petroleum Geologists Memoir, v. 95, p. 183-208.

Pranter, M.J., Ellison, A.I., Cole, R.D., and Patterson, P.E., 2007, Analysis and modeling of intermediate-scale reservoir heterogeneity based on a fluvial point-bar outcrop analog, Williams Fork Formation,Piceance Basin, Colorado: American Association of Petroleum Geologists Bulletin, v. 91, p. 1025-1051.

Pranter, M.J., and Sommer, N.K., 2011, Static connectivity of fluvial sandstones in a lower coastal-plain setting: An example from the Upper Cretaceous lower Williams Fork Formation, Piceance Basin, Colorado: American Association of Petroleum Geologists Bulletin, v. 95, p. 899-923.

Reynolds, A.D., 1999, Dimensions of paralic sandstone bodies: American Association of Petroleum Geologists Bulletin, v. 83, p. 211–229.

Sech, R.P., Jackson, M.D., and Hampson, G.J., 2009, Three-dimensional modeling of a shoreface-shelf parasequence reservoir analog: Part 1. Surface-based modeling to capture high-resolution facies architecture: American Association of Petroleum Geologists Bulletin, v. 93, p. 1155-1181.

Sprinkel, D.A., 2006, Interim geologic map of the Dutch John 30' x 60' quadrangle, Daggett and Uintah Counties Utah, Moffat County, Colorado, and Sweetwater County, Wyoming: Utah Geological Survey.

Sprinkel, D.A., 2007, Interim geologic map of the Vernal 30' x 60' quadrangle, Uintah and Duchesne Counties, Utah, and Moffat and Rio Blanco Counties, Colorado: Utah Geological Survey.

Stagner, W. L., 1941, The paleogeography of the eastern part of the Uinta Basin during Uinta B (Eocene) time: Annals of Carnegie Museum, v. 28, p. 273-308.

White, C.D., Willis, B.J., Dutton, S.P., Bhattacharya, J.P., and Narayanan, K., 2004, Sedimentology, statistics, and flow behavior for a tide-influenced deltaic sandstone, Frontier Formation, Wyoming, United States, *in* Grammer, G.M., Harris, P.M., and Eberli, G.P., eds., Integration of outcrop and modern analogs in reservoir modeling: American Association of Petroleum Geologists Memoir, v. 80, p. 129-152.

APPENDIX A

PREVIOUS STUDIES AND GEOLOGICAL AGE

A detailed history of early studies on the Duchesne River Formation is described in chronological order in Andersen and Picard (1972). Here, we largely follow the Andersen and Picard (1972) work, and briefly review the previous studies with a focus on the nomenclatural history and age definition. Peterson and Kay (1931) first separated this formation into the "Upper Uinta" from the underlying Tertiary formation. The name "Duchesne" was introduced by Scott (1932) and Peterson (1932) in order to avoid confusion. Eventually, Kay (1934) proposed the new name "Duchesne River" because the term "Duchesne" had already been used elsewhere in North American nomenclature. He also divided this Duchesne River formation into three units: Randlett, Halfway, and Lapoint horizons in ascending order. However, these subdivisions were not regionally traceable very far from their type localities. Thus, Warner (1963) later divided the formation into two members, a lower minor bentonite member and an upper major bentonite member on the basis of the bentonite content. Also, Warner (1963) recognized two facies in either half of the formation: a sandy facies in the western half, and a muddy facies in the eastern half. The related regional maps showing the distributions of members and facies are available in Warner (1965, 1966). Because Warner's members were not proposed formally in accordance with the American Commission on Stratigraphic Nomenclature, Andersen and Picard (1972) proposed different subdivisions that consist of four lithostratigraphic units: Brennan Basin (Db), Dry Gulch Creek (Dd), Lapoint (Dl), and Starr Flat (Ds) members in ascending order. They correlated these new subdivisions with the previously defined units by Kay (1934) and Warner (1963). Although Andersen and Picard (1972) concluded that these new members are all traceable and presented some regional

correlations of measured sections, they did not show the distributions of the new members on a geologic map. Only a crude outline of the Duchesne River Formation distribution is mapped in their later works (Andersen and Picard 1974; Picard and Andersen 1975). Rowley et al. (1985) and Bryant et al. (1989) were the first to map these four members defined by Andersen and Picard (1972) over the entire basin. However, Bryant et al. (1989) could not trace the base of the Duchesne River Formation in the western part of the basin (to the west of Duchesne) because the upper part of the Uinta Formation becomes very sandy in this area, making it difficult to differentiate from the overlying Duchesne River Formation. Bryant et al. (1989) thus defined and mapped this area as "Undivided Duchesne River Formation", which includes the formations time-equivalent to the Uinta or Green River Formations. This mapping was subsequently incorporated into a regional 1° x 2° geological map of the Salt Lake City quadrangle (Bryant 1992) that was later digitized and modified (Bryant 2010). The geological maps of eastern half of the Duchesne River Formation distribution (Dutch John 30' x 60' quadrangle and Vernal 30' x 60' quadrangle) have recently been updated by Sprinkel (2006, 2007).

Macro body fossils, including both vertebrates and invertebrates, are scarce in the Duchesne River Formation. The epoch and age of this formation had been debated in some early works, i.e., whether it should be included in the Eocene or Oligocene. Based on fauna from this formation, Wood et al. (1941) established the Duchesnean North American Land Mammal Age (NALMA) as the youngest subdivision of the Eocene Epoch. However, this Duchesnean NALMA continued to be a controversial topic among some researchers (e.g., Wilson, 1978; Emry, 1981). Lucas (1992) reviewed the history of the discussion and redefined the "type" fauna of the Duchesnean Land Mammal Age. It has been generally accepted as Eocene LMA on the basis of mammalian fossils from other parts of North America (Rasmussen et al. 1999). Andersen and Picard (1972) noticed the uppermost unit (Ds) was still undated and could be much younger; possibly Oligocene in age. Subsequently, Rasmussen et al. (1999) and the more recently published Kelly et al. (2012) describe some new records of mammalian fossils from the Duchesne River Formation, although there is still no diagnostic mammal for age

definition recovered from the uppermost member of Ds.

The absolute ages reported in early works are a K-Ar age of 40 Ma from an ashy siltstone bed at the base of Dl (Andersen and Picard, 1974), a biotite K-Ar age of 40.3 Ma from a tuff at the base of the Dl east of Lapoint from which Duchesnean fauna was originally defined (McDowell et al. 1973), and biotite K-Ar ages of 38 and 35.7 Ma from tuff at the top of the Dd (Mauger 1977). Bryant et al. (1989) report fission track ages of zircons and biotite K-Ar ages from all over the basin. However, the results are quite discordant and controversial because there are significant gaps and discrepancies in ages determined using the two different methods (zircon ages for the Duchesne River Formation range from 30 to 38 Ma, while K-Ar ages are 7 to 11 Ma older). Prothero and Swisher (1992) reported six biotite $^{40}Ar/^{39}Ar$ dates from the Lapoint Ash with an average of 39.74±0.07 Ma. Kelly el al. (2012) recalibrated this finding by using the new Fish Canyon Tuff standard of 28.20 Ma, and determined an age of 40.26±0.08 Ma.

A.1 References Cited

Andersen, D.W., and Picard, M.D., 1972, Stratigraphy of the Duchesne River Formation (Eocene-Oligocene?), northern Uinta basin, northeastern Utah: Utah Geological and Mineral Survey Bulletin 97, 29 p.

Andersen, D.W., and Picard, M.D., I974, Evolution of synorogenic clastic deposits in the intermontane Uinta Basin of Utah, *in* Dickinson, W.R., editor, Tectonics and Sedimentation: SEPM Special Publication 22, p. 167-189.

Bryant, B., 1992, Geologic and structure maps of the Salt Lake City 1° x 2° quadrangle, Utah and Wyoming: U.S. Geological Survey Miscellaneous Investigations Series Map I-1997.

Bryant, B., 2010, Geologic map of the east half of the Salt Lake City 1° x 2° (Duchesne and Kings Peak 30 x 60 quadrangles), Duchesne, Summit, and Wasatch Counties, Utah, and Uinta County, Wyoming (digitized and modified from U.S. Geological Survey Miscellaneous Investigations Series Map I-1997): Utah Geological Survey.

Bryant, B., Naeser, C.W., Marvin, R.F., and Mehnert, H.H., 1989, Upper Cretaceous and Paleogene sedimentary rocks and isotopic ages of Paleogene tuffs, Uinta Basin, Utah: U.S. Geological Survey Bulletin 1787-J, 22 p.

Emry, R.J., 1981, Additions to the mammalian fauna of the type Duchesnean, with comments on the status of the Duchesnean "Age": Journal of Paleontology, v. 55, p. 563-570.

Kay, J.L., 1934, Tertiary formations of the Uinta Basin, Utah: Annals of Carnegie Museum, v. 23, p. 357-372.

Kelly, T.S., Murphey, P.C., and Walsh, S.L., 2012, New records of small mammals from the

middle Eocene Duchesne River Formation, Utah, and their implications for the Uintan-Duchesnean North American Land Mammal Age transition; Paludicola, v. 8, p. 208-251.

Lucas, S.G., 1992, Redefinition of the Duchesnean Land Mammal "Age," late Eocene of western North America, *in* Prothero, D.R., and Berggren, W.A., editors, Eocene-Oligocene climatic and biotic evolution, Princeton University Press, p. 88-105.

Mauger, R.L., 1977, K-Ar ages of biotites from tuffs in Eocene rocks of the Green River, Washakie, and Uinta basins, Utah, Wyoming, and Colorado: University of Wyoming Contributions to Geology, v. 15, p. 17-41.

McDowell, F.W., Wilson, J.A., and Clark, J., 1973, K-Ar dates for biotite from two paleontologically significant localities: Duchesne River Formation, Utah, and Chadron Formation, South Dakota: Isochron/West, v. 7, p. 11-12.

Peterson, O.A., 1932, New species from the Oligocene of the Uinta: Annals of Carnegie Museum, v. 21, p. 61-78.

Peterson, O.A., and Kay, J.L., 1931, The Upper Uinta Formation of northeastern Utah: Annals of Carnegie Museum, v. 20, p. 293-306.

Picard, M.D., and Andersen, D.W., 1975, Paleocurrent analysis and orientation of sandstone bodies in the Duchesne River Formation (Eocene-Oligocene?), northern Uinta Basin, northeastern Utah: Utah Geology, v. 2, p. 1-15.

Prothero, D.R. and Swisher, C.C., 1992, Magnetostratigraphy and geochronology of the terrestrial Eocene-Oligocene transition in North America, *in* Prothero, D.R., and Berggren, W.A., editors, Eocene-Oligocene climatic and biotic evolution: Princeton University Press, p. 46-74.

Rasmussen, D.T., Hamblin, A.H., and Tabrum, A.R., 1999, The mammals of the Eocene Duchesne River Formation, *in* Gillette, D.D., editor, Miscellaneous Publication, Utah Geological Survey 99-1, p. 421-427.

Rowley, P.D., Hansen, W.R., Tweto, O., and Carrara, P.E., 1985, Geologic map of the Vernal 1ø x 2ø quadrangle, Colorado, Utah, and Wyoming: U.S. Geological Survey Miscellaneous Investigations Series I-1526.

Scott, W.B., 1932, An introduction to geology, 3rd ed.: New York, Macmillan, 441 p.

Sprinkel, D.A., 2006, Interim geologic map of the Dutch John 30' x 60' quadrangle, Daggett and Uintah Counties Utah, Moffat County, Colorado, and Sweetwater County, Wyoming: Utah Geological Survey

Sprinkel, D.A., 2007, Interim geologic map of the Vernal 30' x 60' quadrangle, Uintah and Duchesne Counties, Utah, and Moffat and Rio Blanco Counties, Colorado: Utah Geological Survey.

Warner, M.M., 1963, Sedimentation of the Duchesne River Formation, Uinta Basin, Utah: Ph. D. Dissertation, Department of Geology, State University of Iowa, 339 p.

Warner, M.M., 1965, Cementation as a clue to structure, drainage patterns, permeability, and other factors: Journal of Sedimentary Petrology, v. 35, p. 797-804.

Warner, M.M., 1966, Sedimentational analysis of the Duchesne River Formation, Uinta Basin, Utah: Geological Society of America Bulletin v. 77, p. 945-957.

Wilson, J.A., 1978, Stratigraphic occurrence and correlation of early Tertiary vertebrate faunas,

Trans-Pecos Texas; Part 1, Vieja area: Bulletin of the Texas Memorial Museum, v. 25, p. 1-42.

Wood, H.E., Chaney, R.W., Clark, J., Colbert, E.H., Jepsen, G.L., Reeside, J.B., and Stock, C., 1941, Nomenclature and correlation of the North American continental Tertiary: Geological Society of America Bulletin, v. 52, p. 1-48.

APPENDIX B

MEASURED SECTIONS

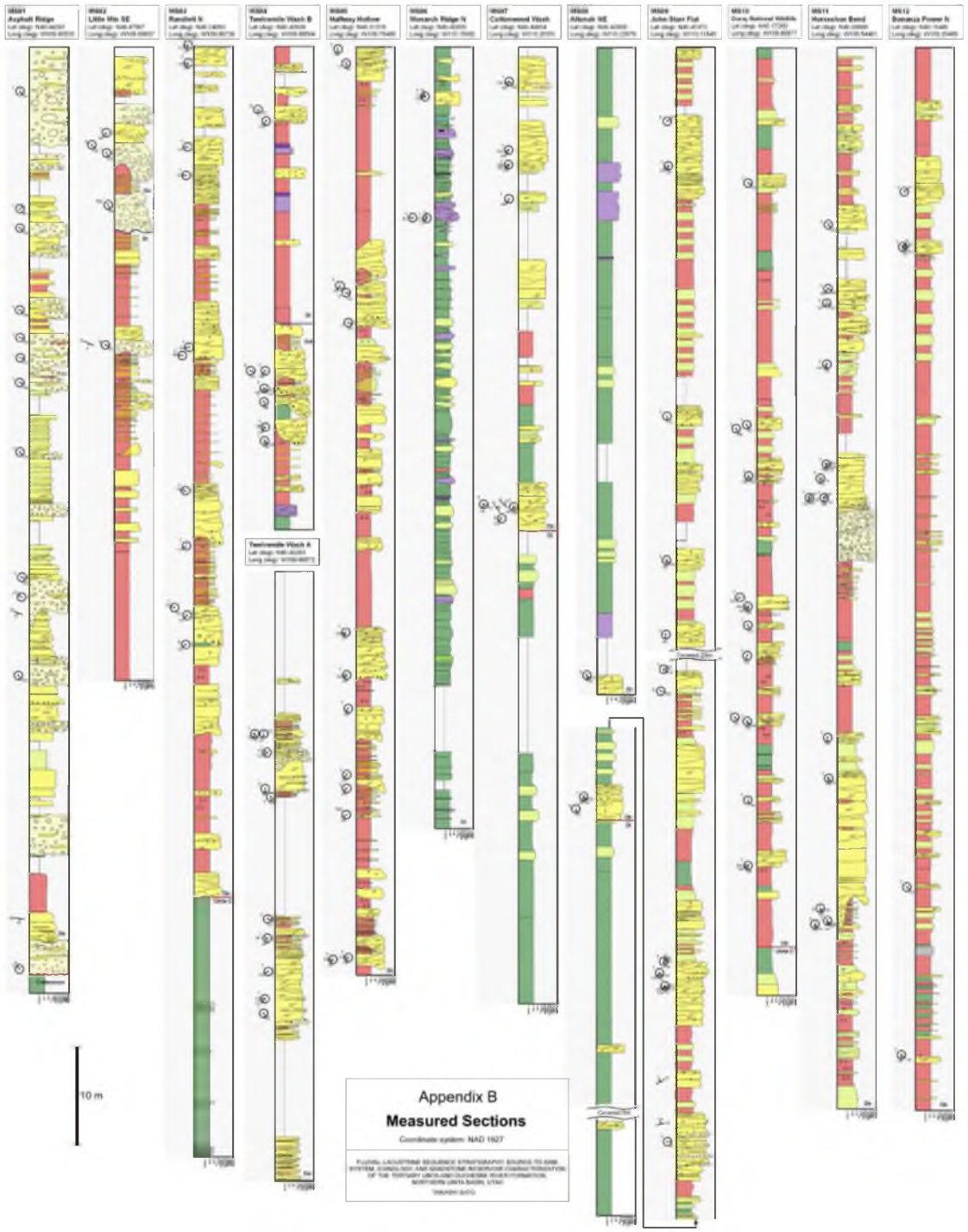

Figure B.1. Measured sections, MS01 to MS12 (high-resolution format in Appendix E of DVD), keyed to index map Figure 1.2.

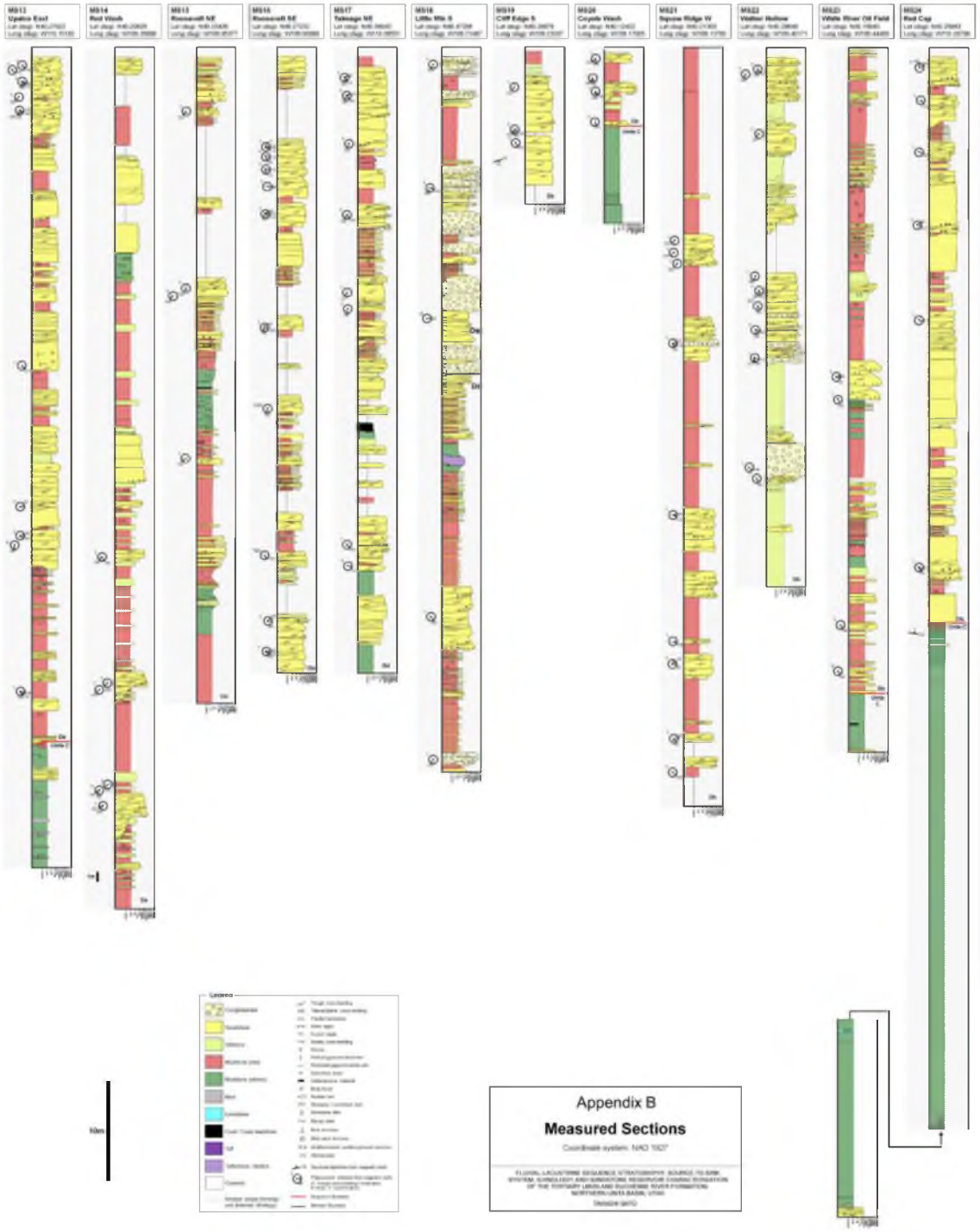

Figure B.2. Measured sections, MS13 to MS24 (high-resolution format in Appendix E of DVD), keyed to index map Figure 1.2.

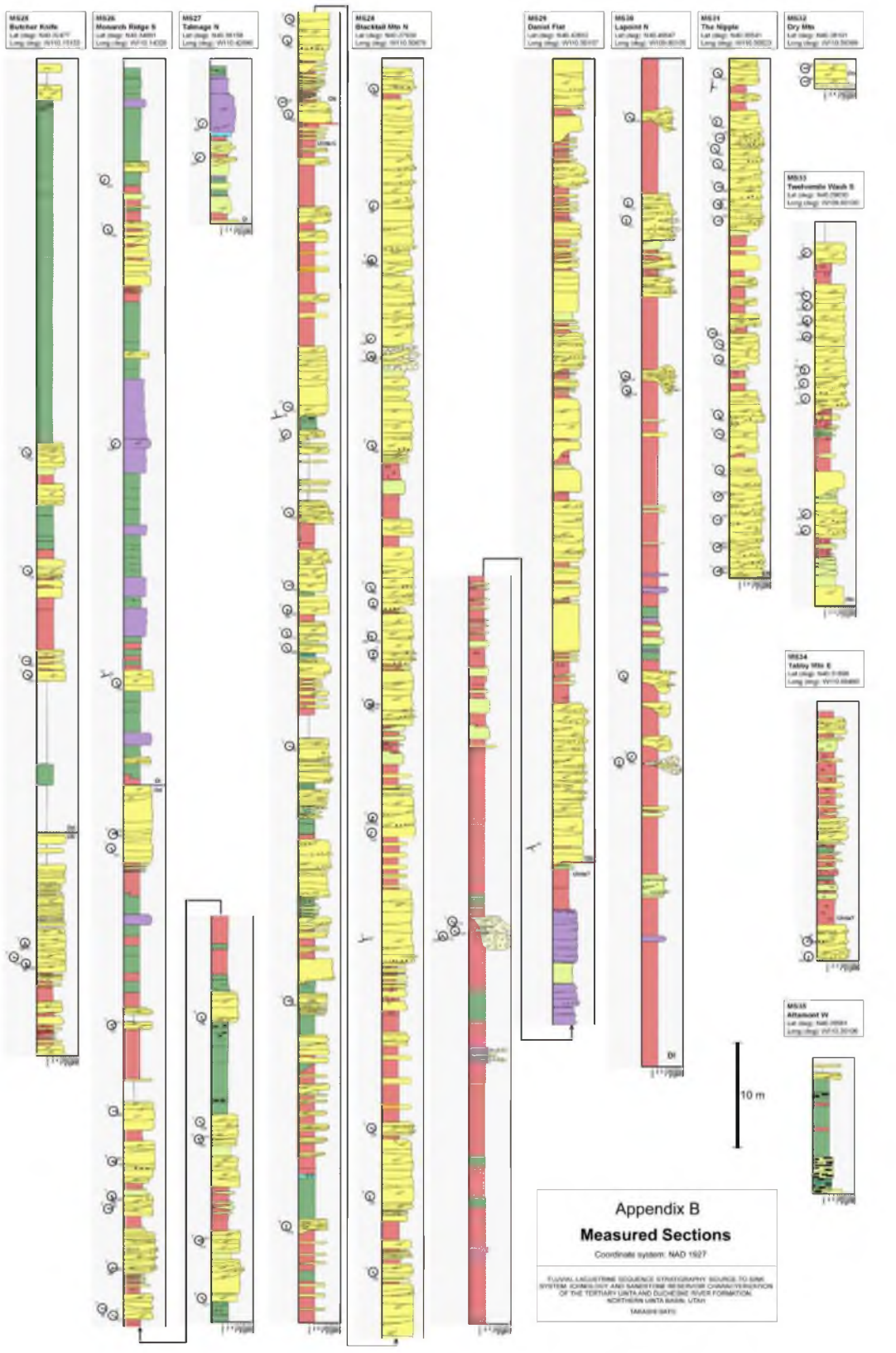

Figure B.3. Measured sections, MS25 to MS35 (high-resolution format in Appendix E of DVD), keyed to index map Figure 1.2.

APPENDIX C

LIST OF SANDSTONE SAMPLES AND RESULTS OF THIN SECTION AND QEMSCAN ANALYSIS

Table C.1 List of Sandstone Samples and Results of Thin Section and QEMScan Analysis

ID	Mbr	Locality	Coordinates (NAD1927)	Thin Section								QEMScan (Method 2)		
				Q%	K%	R%	R% (breakdown)			Cement /matrix %	Porosity %	Q%	K%	R (Ls+Dol) %
							Clastics	Carb	Chert					
#1	Db	MS28, Blacktail Mtn North	N40.27920, W110.50679	90.0	3.6	6.4	1.7	4.3	0.4	5.3	14.7	89.2	2.3	4.3
#2	Db	MS24, Red Cap	N40.25983, W110.28766	96.0	0.6	3.4	2.1	0.0	1.3	1.9	17.6	97.7	1.0	0.0
#3	Dd	MS26, Monarch Ridge South	N40.34881, W110.14320	97.4	0.2	2.4	2.2	0.2	0.0	6.7	19.0	97.9	0.7	0.0
#4	Db	MS13, Upalco East	N40.27922, W110.15182	97.2	0.6	2.2	2.2	0.0	0.0	4.2	17.4	97.8	1.0	0.0
#5	Db	MS16, Roosevelt SE	N40.27232, W109.90966	62.0	1.0	37.0	8.3	27.2	1.4	16.9	9.7	68.7	1.4	24.0
#6	Db	MS03, Randlett North	N40.24093, W109.80736	79.6	1.2	19.2	4.9	10.8	3.5	10.4	12.1	82.7	1.2	12.5
#7	Db	MS33, Twelvemiles Wash South	N40.29030, W109.60100	67.8	3.0	29.2	4.1	18.9	6.3	16.3	6.3	82.5	1.4	12.4
#8	Db	MS23, White River Oil Field	N40.15940, W109.44488	79.4	2.6	18.0	1.6	13.8	2.6	17.5	12.3	76.4	1.7	14.7
#9	Db	MS14, Red Wash	N40.20829, W109.28806	89.6	0.4	10.0	1.2	7.0	1.8	25.0	6.1	95.9	1.2	1.9
#10	Db	SP09, Blacktail Mtn West	N40.27206, W110.58815	n/a	n/a	n/a	n/a	n/a	n/a	n/a	n/a	95.5	2.9	0.0
#11	Db	SP07, Blacktail Mtn West	N40.27932, W110.54595	n/a	n/a	n/a	n/a	n/a	n/a	n/a	n/a	89.6	3.2	4.0
#12	Db	SP05, Duchesne North	N40.28607, W110.36244	n/a	n/a	n/a	n/a	n/a	n/a	n/a	n/a	96.8	1.7	0.0
#13	Dl	MS08, NE Altonah	N40.43758, W110.21249	n/a	n/a	n/a	n/a	n/a	n/a	n/a	n/a	90.8	3.4	2.6
#14	Db	SP02, Big Sand Wash	N40.29228, W110.21679	n/a	n/a	n/a	n/a	n/a	n/a	n/a	n/a	98.4	0.6	0.0
#15	Db	SP01, Roosevelt West along I-40	N40.28993, W109.99861	n/a	n/a	n/a	n/a	n/a	n/a	n/a	n/a	74.3	2.4	14.8
#16	Db	SP12, Fort Duchesne East	N40.28402, W109.84258	n/a	n/a	n/a	n/a	n/a	n/a	n/a	n/a	68.0	1.1	26.9
#17	Db	SP10, Pelican Lake North	N40.24449, W109.70727	n/a	n/a	n/a	n/a	n/a	n/a	n/a	n/a	91.0	0.6	6.4
#18	Db	SP11, Horseshoe Bend East	N40.28274, W109.53285	n/a	n/a	n/a	n/a	n/a	n/a	n/a	n/a	92.7	1.2	4.0
#19	Db	MS21, Squaw Ridge West	N40.21300, W109.13760	n/a	n/a	n/a	n/a	n/a	n/a	n/a	n/a	70.6	2.7	18.1
#20	Db	MS20, Coyote Wash	N40.12432, W109.17005	n/a	n/a	n/a	n/a	n/a	n/a	n/a	n/a	88.8	1.2	8.4

APPENDIX D

DETAILED PROCEDURE OF QEMSCAN AUTOMATED DISAGGREGATED COUNTS

QEMScan automated disaggregated counts (e.g., method described in Allen et al. 2012) for 20 samples were conducted to supplement the thin section data. Nine of the 20 samples were the same as those used for the conventional thin section analysis (Appendix C), which were included to ensure the consistency of the results between the two different methods. The pros and cons of the two methods are summarized in Table D.1. The biggest advantage of QEMScan automated disaggregated count is to shorten the analytical time, although the duration depends on the resolution and the number of particles to be counted.

In this study, 16 micron resolution (pixel size) and 1.5 h scanning duration were applied under the QEMScan particle counting mode. For all 20 samples, the effective numbers of particles (min 1344 to max 2118 grains, average: 1818 grains per sample) were acquired to compare with results from the Gazzi-Dickinson point counts (500 grain counts per section).

There are several different ways of postprocessing QEMScan automated disaggregated counts to obtain the number and type of grains. The following three methods were tested to obtain the most reasonable correlations with point counts from thin sections: Method 1 (M1) - filter by grain size (i.e., extract only 125-500 micron grains) and count the number of particles with a mineral area filter for each category (see details in Fig. D.1); Method 2 (M2) - apply no grain size filter and calculate the proportions of mineral areas; and Method 3 (M3) - filter by grain size and calculate the proportions of mineral areas. In all methods, major components such as quartz and carbonates exhibit good correlations and consistencies with the thin section data as shown in the crossplots of 9 calibration samples that have both thin section and

Table D.1 Comparison between Thin Section Point Counts and QEMScan Automated Disaggregated Counts

	Pros	Cons
Conventional thin section point counts	· Accurate and detailed information on grains if operator is skillful · Visible original texture (e.g., sorting, cementation, pore geometry, etc.)	· Possible human error (depending on operator's skill) · Possible inconsistent results between operators/researchers
QEMScan automated disaggregated counts	· Fast and easy · Automated · Repeatable · Consistency	· Losing information on texture (e.g., cementation and pore system) · No porosity data · Not differentiate some mineral (e.g., monocrystalline and polycrystalline quartz) · Variance between software programs

QEMScan data (Fig. D.2a and D.2b). Even though a minor component of K-feldspar tends to cause a deviation from the ideal correlation line, a reasonable trend is still seen in Figure D.2c. Thus, the use of QEMScan mineral composition data is appropriate to supplement the thin section data.

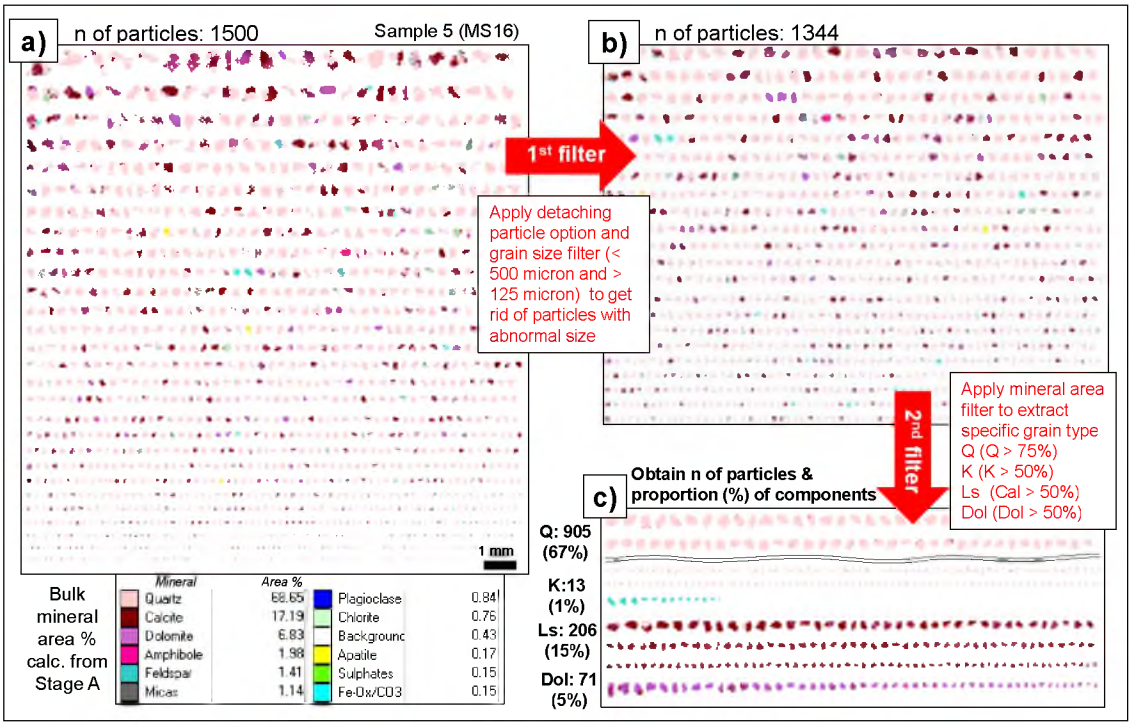

Figure D.1. An example (sample 5) of postprocessing (Method 1) with three stages (a, b, and c) of QEMScan automated disaggregated count. Stage a) shows all 1500 particles scanned for 1.5 h by QEMScan (bulk mineral areas (%) of Stage a) also tabulated). Stage b) set (1344 particles) is acquired using filters to detach compound particles and to get rid of particles with abnormally large and small sizes (over 500 micron and less than 125 micron). Stage c) sets are acquired through mineral area filters to extract specific grain types such as Q: quartz (if Q > 75%), K: k-feldspar (if K > 50%), Ls: limestone (if calcite > 50%) and Dol: dolomite (if dolomite > 50%). Finally, sandstone composition (proportion of component grains) is calculated by using the number of each grain type (e.g., Q: 905 particles) divided by filtered total grains (1344 particles).

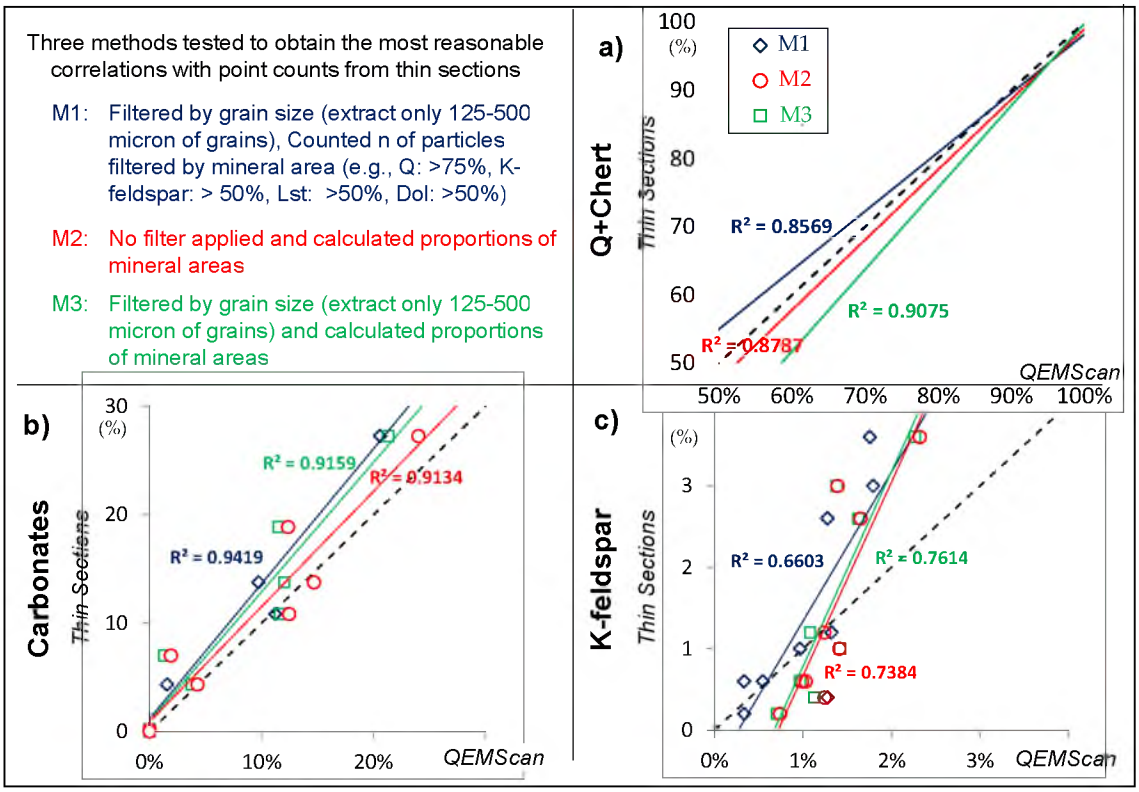

Figure D.2. Crossplots of grain type proportions from QEMSCan (X-axis) with three different processing methods (M1, M2, and M3) and proportions from thin section examination (Y-axis). Major components such as quartz (plot a) and carbonates (plot b) exhibit quite good correlations with the thin section data. A minor component of k-feldspar (plot c) shows some deviation from the ideal correlation line. Nevertheless, the overall trend is still reasonable.

APPENDIX E

DATA IN DIGITAL FORMAT (DVD)

List of Contents

ID	Name	Format
E.1	Measured sections (complied)	pdf
E.2	Measured sections (with raw descriptions)	pptx
E.3	E-W cross-section	pdf
E.4	N-S cross section	pdf
E.5	Paleocurrent data	xlsx
E.6	Basemap	cvx
E.7	GPS data (BaseCamp backup file)	backup
E.8	Thin section point count data	xlsx
E.9	QEMScan raw data	xlsx
E.10	Thin section vs QEMScan calibration	xlsx
E.11	QEMScan plan & procedure	pptx
E.12	BTM GigaPan photo (uninterpreted)	jpg
E.13	BTM GigaPan photo (interpreted)	jpg
E.14	Gamma Ray data (MS01)	xlsx
E.15	MS-1 to MS-4 correlations	pptx
E.16	Photo distortion correction factor calculation	xlsx
E.17	Channel width:depth statistics and aspect ratios	xlsx
E.18	Wellbore static connectivity analysis	xlsx

E.19	Petrel project backup files	folder
E.20	Presentation figures	folder